AGEDI
مبادرة أبوظبي العالمية للبيانات البيئية
Abu Dhabi Global Environmental Data Initiative

an initiative of

UNEP

هيئة البيئة - أبوظبي
Environment Agency - ABU DHABI

AGEDI | THE ABU DHABI GLOBAL ENVIRONMENTAL DATA INITIATIVE

CLIMATE CHANGE PROGRAMME

REGIONAL CLIMATE CHANGE ARABIAN GULF MODELLING

- Atmospheric Modelling
- Arabian Gulf Modelling
- Terrestrial Ecosystems
- Marine Ecosystems
- Transboundary Groundwater
- Water Resource Management
- Al Ain Water Resources
- Coastal Vulnerability Index
- Desalinated Water Supply
- Food Security
- Public Health Benefits of GHG Mitigation
- Sea Level Rise

Full Technical Report

agedi.org

AGEDI
مبادرة أبوظبي العالمية للبيانات البيئية
Abu Dhabi Global Environmental Data Initiative

Suggested Citation: AGEDI. 2015. Regional Ocean Modeling Arabian Gulf - Future Scenarios. LNRCCP. CCRG/USP

José Edson (Principal Investigator)

Ilana Wainer

Bruno Ferrero

Oceanography Institute

University of Sao Paulo in Brazil

AGEDI
مبادرة أبوظبي العالمية للبيانات البيئية
Abu Dhabi Global Environmental Data Initiative

Acknowledgments

Many individuals provided invaluable support, guidance, and input to the Modeling projects.

The authors would like to express their sincere and heartfelt expressions of gratitude for their review by providing comments, feedback, data and/or the opportunity to present multiple deliverables within the project process including:

- Dr. Abdulla Al Mandoos, National Centre of Meteorology and Seismology
- Dr. Bernhard Riegl, Nova University
- Dr. Fred Launay and the Environment Agency- Abu Dhabi team
- Dr. Holger Hoff, Stockholm Environment Institute
- Dr. Mansour Al Mazroui, Centre of Excellence for Climate Change Research (CECCR)
- Mr. Mufleh Alalaween, IUCN ROWA
- Ms. Naoko Kubo, UAE Ministry of Environment and Climate Change (MOCCAE) and team
- Dr. Omar Abdullah, National Centre of Meteorology and Seismology
- Dr. Paola Ferreira and the Emirates Wildlife Society (EWS) – WWF team
- Dr. Rachel Mcdonnell, International Centre for Biosaline Agriculture (ICBA)
- Dr. Robert Baldwin and Dr. Simon Wilson, Five Oceans
- Dr. Saeed Al Sarmi, Research Centre from Public Authority for Civil Aviation (PACA)
- Dr. Sultan Al Yahyai, Sultan Qaboos University
- Dr. Tarek Sadek, UNESCWA

A very special thank-you to the academic scientific research teams of Khalifa University (KU), MASDAR Institute of Science and Technology (MIST), New York University (NYU) for your data expertise and scientific feedback, support and opportunities for further research.

We are additionally thankful the participation, time and effort that multiple stakeholders across the region who participated in the multitude of meetings and dialogue.

About this Final Report

In October 2013, the Abu Dhabi Global Environmental Data Initiative (AGEDI) launched the "Local, National, and Regional Climate Change (LNRCC) Programme to build upon, expand, and deepen understanding of vulnerability to the impacts of climate change as well as to identify practical adaptive responses at local (Abu Dhabi), national (UAE), and regional (Arabian Peninsula) levels. The design of the Programme was stakeholder-driven, incorporating the perspectives of over 100 local, national, and regional stakeholders in shaping 12 research sub-projects across 5 strategic themes. The "Regional Atmospheric Modeling" sub-project within this Programme aims to develop high resolution, regional climate data that will serve the Climate Change Impacts, Vulnerability and Adaptation Assessment Activities locally as well as organizations across the broader Arabian Peninsula

This final technical report offers a summary of what has been learned in carrying out the research activities involved in the "Regional Ocean Modeling" sub-project. This report describes the methodological approach, data used to support the approach, and descriptions of specific and general findings. This report seeks to provide a useful technical synthesis of the work, offering partners and stakeholders having the requisite technical expertise in regional ocean modeling, the opportunity to understand what was done, and request additional information as needed. The resulting data archive is large and because of this large size, a tool called the "Climate Inspector" is under development to visually demonstrate the outputs, as well as provide access to download datasets that other researchers may find valuable for their studies.

Table of Contents

AGEDI
مبادرة أبوظبي العالمية للبيانات البيئية
Abu Dhabi Global Environmental Data Initiative

List of Figures

page

Climate Change Research Group

IO Instituto Oceanográfico

List of Acronyms

°C	Degrees Celsius
AG	Arabian Gulf
AR5	The 5th Assessment Report of the IPCC
AVHRR	Advanced Very High Resolution Radiometer
CCSM4	The NCAR Community Earth System Model Version 4
cm	centimeter
CMIP5	Climate Model Intercomparison Version 5
CO_2	Carbon dioxide
CTD	Conductivity-Temperature-Depth
DSL	Dynamic Sea Level
EAD	Environment Agency of Abu Dhabi
ECMWF	European Center for Medium Range Forecast
ESM	Earth System Model
GCM	Global Climate Model
GMSL	Global Mean Sea Level
GTE	Global-ocean Thermal Expansion
IPCC	Intergovernmental Panel on Climate Change
km	kilometer
LLJ	Low Level Jetstream
LNRCC	Local, National, and Regional Climate Change
LTR	Long-Term Run
m/s	meters per second
MPI	Max Planck Institute
MPIMR	Max Planck Institute Mixed Resolution model
NODC	National Oceanographic Data Center
OCL	Ocean Climate Laboratory
psu	practical salinity unit
RCM	Regional Climate Model
RCP	Representative Concentration Pathway
ROMS	Regional Ocean Model System
SSH	Sea Surface Height
SSS	Sea Surface Salinity
SST	Sea Surface Temperatures
TCS	Turbulent Closure Scheme
TS	Temperature-Salinity
UAE	United Arab Emirates

W/m^2	watts per square meter
WOA	World Ocean Atlas
WOD	World Ocean Database
WRF	Weather Research and Forecasting model

Executive Summary

The goal of this study was to develop projections of regional climate for the Arabian Gulf (AG) at fine spatial and temporal scales. To achieve this, a Regional Ocean Model System (ROMS) was deployed to dynamically downscale the climate of the AG using ground truth data to evaluate the model. It was also used a specific run, from an Earth System Model (ESM), to force ocean boundaries and Atmospheric fluxes (The Max Planck Institute ESM), hereafter MPIMR. The final results show what global climate change likely means for the AG waters regarding main ocean properties, like sea surface temperature, salinity, sea level height, and currents up through the year 2100, from a "business as usual" IPCC's scenario (RCP8.5). Pondering the natural limitations from the ESM results and the downscaling process, the results are expected to lighten the likely climate changes effect on the Gulf ocean dynamics. There is also confidence that these results have created a baseline to insight new experiments, concerning the gulf dynamics, to quantify and increase the accuracy of the carbon related warming effects as well as the local anthropogenic changes on the salinity generation processes. The results from the experiments will be available to be used in support of climate change impact research planning in the marine environment throughout the Gulf.

Final conclusions

Figure ES-1 highlights a subset of major results. The conclusions discussed in the main body of this report focus on the early and late 21st century periods (2000-2019; 2080-2099), under a high greenhouse gas emissions trajectory (i.e., Representative Concentration Pathway 8.5, RCP8.5) and corresponding to a 1 km resolution domain. In addition, final results for a mid 21st century period (2040-2049), under RCP8.5 for the same spatial resolution are discussed separately in the Annex to this report.

Overall conclusion: The overturning circulation in the AG changes from early to late 21st century trigs a dilution progression in the AG seawater. The long-term seawater freshening is connected mostly with the increase in the Arabian Sea inflow, and secondarily with the increase of precipitation in the area, projected by the RCP8.5 results.

Fundamentally, the Regional Climate Model (RCM) results show that: there is an overall increase in the average temperature together with an increasing small-scale vertical mixing processes (mostly at northern areas), which partially disrupts the overturning cycle, transferring the deep southward transport to the surface. This process decreases the associated deep density salinity gradients along the deep channel, increasing the entrainment of lighter less saline waters from the Arabian Sea.

The chain of climate change related patterns reproduced in the area by the RCM, early and late simulations, allows following the related physical mechanisms. The increase in the inflow starts from a break in the overturning equilibrium, caused by a significant warming in the seawater temperature that, at North, does cause a migration of the dense (saline and

cold) subsiding waters to the shallower Southwest AG coast. The northern mixing patterns have also changed, from the historically well behaved and stratified current system, to a fast vertically mixing system (increased vorticity). Part of this northern saline waters are advected southward by the Northerly wind and, by the anticlockwise residual current system that characterizes the overturning system in the gulf. In the southern areas, nearby UAE coast and Qatar, the saline surface waters from North join the local saline waters, rendering a salinity spatial asymmetry distribution along the gulf, by the end of 21st century. It has to be better investigated with further experiments; however, the early and late trends denote a likely salinity time asymmetry as well, mainly at shallow areas. From the current results stage, it is possible to infer an increasing salinity at coastal areas in the early 21st period and a more stationary behave at late 21st century.

Figure ES-1: Selected final results

Salinity	• Salinity rules the AG ocean dynamics during the historical and early 21st periods (up to 2020). The results for the late 21st experiments have shown the AG as a more mixed and diluted system. • By the end of the century, salinity is still the most important variable to define the internal circulation. But the balance between the cooling temperature zone at the northernmost gulf area and the high natural salinization balance has been broken. • It is also observed a spatial asymmetry in the salinity changes. The local salinity decreases in the eastern side of the Gulf (deeper zone) and increases along the western side.
Temperature	• Significant warming in all layers is an expected and very likely result for entire AG. • The increase on the temperature is part of the mechanism responsible for the changes in the salt circulation, by means of reduction of the winter cooling processes at northern areas.
Sea Level	• The Dynamic Sea Level (DSL) was used as the barotropic external forcing of the Regional Climate Model (RCM). • DSL does have small amplitude if compared with the Global Mean Sea Level (GMSL) projections to the 21st century. Nonetheless, it does contribute to the local dynamics, reinforcing the "residual current" structure observed in the area.
Currents	• The AG circulation is strongly defined by its baroclinic internal gradients (density gradients). Thus, the increased salinity asymmetric distribution causes acceleration in the internal recirculation system, which does appear in the mass transport along the Gulf. • Warmer temperature at North reduces dense (saline) groundwater subsidence, moving the system from advection to mostly turbulent mixed. • The Northernmost saline water (now on surface) is carried by advection towards south, by wind-generated currents and the permanent coastal current system. • The coastal jets, mainly along the Southwestern coast, are a good parameter to evaluate the long-term local salinity accumulation (by transport) along the UAE coastline.
Vorticity	• The summer pattern does change the larger scale eddies, directly connected with the Arabian Sea low salinity inflow waters. • At north, the early 21st low vorticity areas have been replaced by higher frequency eddies. This explains partially, how the warmer climate conditions have affected the northernmost dense water formation zone.

Background

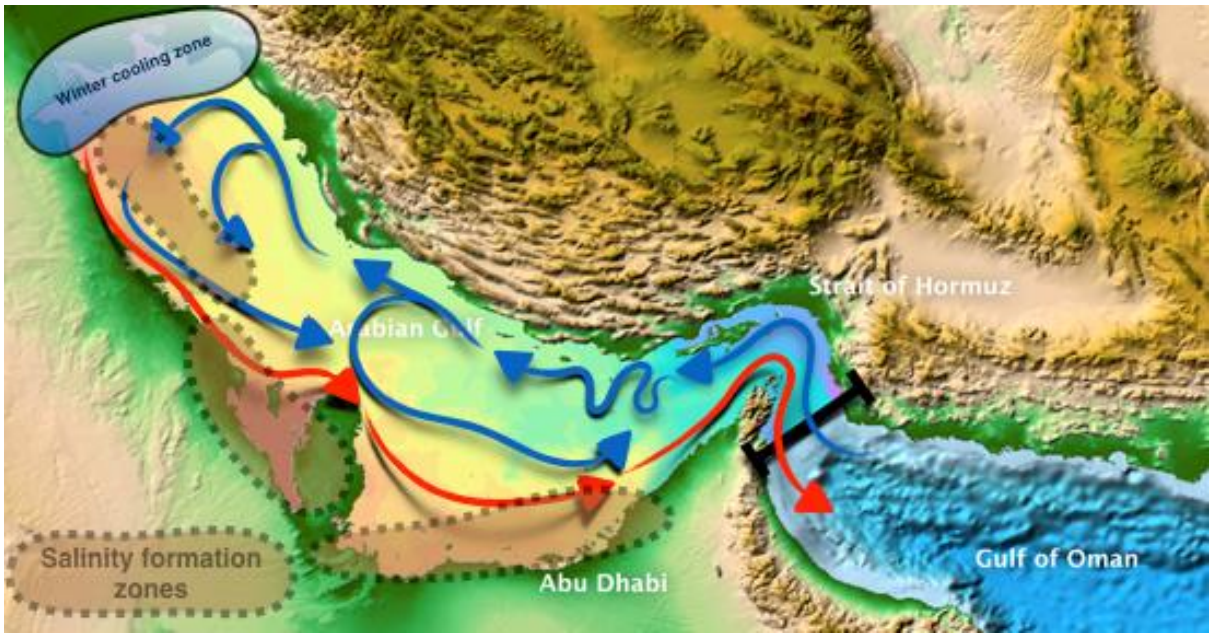

Figure ES-2: A regional model result, Sea Surface Salinity (SSS) snapshot composed with local topographic features (ETOPO source) and a schematic overturning circulation system. Shaded areas indicate the dense water formation zones.

Researchers at the Oceanography Institute at the University of Sao Paulo developed and validated to AG a Regional Ocean Model setup, to capture and downscale the projected climate changes to the Gulf. The RCM uses the ROMS model, which is a free surface, terrain-following, hydrostatic primitive equations ocean model. This model was used to dynamically downscale fields from the MPIMR, a coarse gridded Earth System Model that covers the entire globe.

The ocean model has been validated for the AG in a highly focused domain of (1.1 km resolution using available ground truth for validation. The validation uses Sea Surface Temperature (SST) from Satellite; reduced climatologies from the Word Ocean Atlas 2014 (WOA13); and previous compilations and analysis published for the area (e.g., Reynolds, 1993). Figure ES-2 shows the sea surface salinity (SSS) summer snapshot, overlain on a topographic map (Etopo, Amante, W, & Eakins, 2009) and illustrates the high salinity zones detected with the RCM.

The historical runs used to validate the model have used the same forces that have been considered in the long-term experiments (climate projections). This approach was deliberately used to evaluate if the model is able to retain its skill to reproduce the local ocean dynamics forced by the ESM (coarse resolution) fields. Figure ES-3 (right) illustrates these results where the formation of large summer stationary eddies is reproduced. The detail on

the right shows the regional model, satellite and the ESM for a specific area. Figure ES-3 summarizes the validation experiment assessment and shows the model skill in the area. The RCM results for temperature and salinity results (black lines) are plotted against the ESM (Blue lines), WOA13 climatology (repeated cycles, green lines) and satellite data.

Experiments	Periods	Available Datasets
Validation	**2002-2008**	**Figures and reports**
Sensibility	**2002-2008**	**Figures and reports**
Early *21st*	**2000-2020**	**• Pos-processed databas, resolution: 384 x 256 x 20 • Datasets: • daily, 1 file / variable • monthly mean data, 1 file /variable • climatologies, all variables 1 file**
Late *21st*	**2080-2100**	**• Pos-processed databas, resolution: 384 x 256 x 20 • Datasets: • daily, 1 file / variable • monthly mean data, 1 file /variable • climatologies, all variables 1 file**

The ocean climate change investigation periods are the 2000-2019 (Early 21st) and 2080-2099 (Late 21st). The finalized experiments are listed in Figure ES-4. These experiments have been carried out with MPIMR results, reported and discussed in the following sections.

Figure ES-3: Status of the RCM experiments

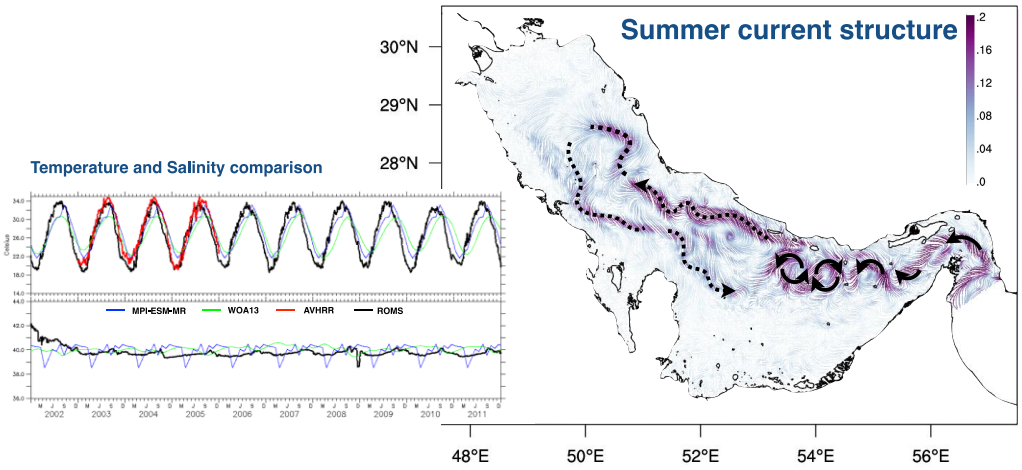

Figure ES-4: The climatological summer transport pattern reproduced by the regional model in the AG. The left side detail compares the SST from the regional model with the satellite and ESM (same box area). Temperature and salinity the ground-truth datasets are also plotted.

Future sea surface temperature

AG waters near the surface will be warmer in the future by about 1° to 2°C. The SST differences can reach 2.8°C in some areas (see Figure ES-5). The warming in slightly smaller at the bottom layers, but still significant. As further discussed, these temperature changes are one of the physical mechanisms to disrupt the vertical overturning circulation at AG.

Future ocean salinity

The ESMs atmospheric forces reveal a slight increase in the precipitation and humidity, mainly at South AG. It also shows a decrease in the Northerly winds over the area. These results are understood as a consequence of the changes in large scale monsoon patterns as described in Sandeep & Ajayamohan (2014). Such results suggest a decrease on the salinity at the southern gulf area, where precipitation increase has been observed in the ESM results. The RCM results show, on full area averaged, the same trends as the atmospheric fluxes changes have pointed out.

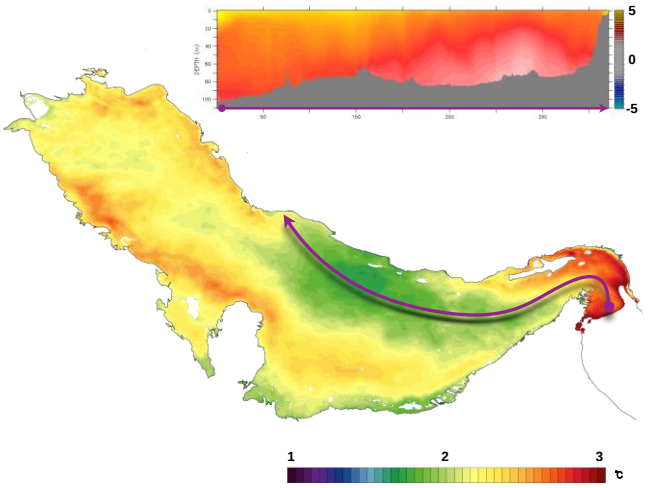

Figure ES-5: SST difference between Late and Early 21st century experiment. Purple arrow indicates the vertical section area (detail - top right)

However, the opposite spatial salinity pattern is reproduced. There is a significant increase in salinity at the southern gulf area and a decrease along the central channel. This can be clearly seen in Figure ES-6. These unexpected oceanic responses motivate an expanded assessment on the RCM results which outcomes in the main conclusion earlier presented. Despite the salinity importance to the area, the most significant climate change is the temperature. The warming process disrupts the vertical

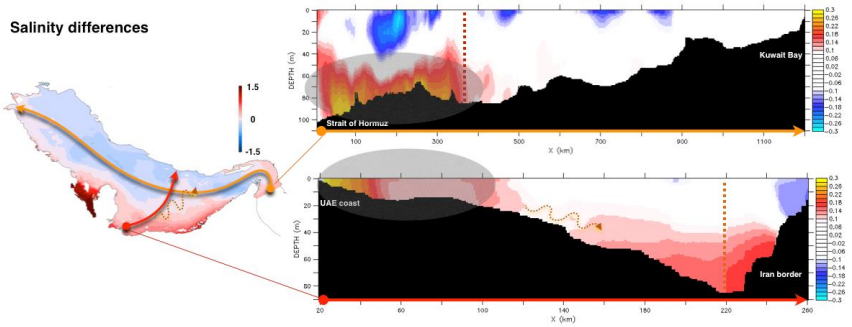

Figure ES-6: (Left) Sea surface salinity for the Late 21st century experiment and vertical profile references. (Right) the vertical profile salinity differences (late-early 21st)

pre-existent overturning system, increases the horizontal recirculation energy and creates the salinity observed in the RCM results. Along time precipitation trends may reduce this asymmetry as final trends from late 21st period suggest.

Future ocean currents

Gulf water currents will be altered by climate change. The regional model resolution was initially designed to allow an eddy-resolving model for all seasons in the AG. During the winter-spring season, the mixing scale eddies decay to 5-10 km. This kind of climate modeling approach has its price, basically it increases dramatically the time required to complete the experiments. However, the positive result of conducting high-resolution modeling is shown on Figure ES-7, where the velocity streamlines of the model results are plotted, focusing on the Abu Dhabi offshore area. The current fields in very shallow and coastal areas show a seesaw flow pattern, which is altered by climate change and could be important to help identify conservation priorities in the area.

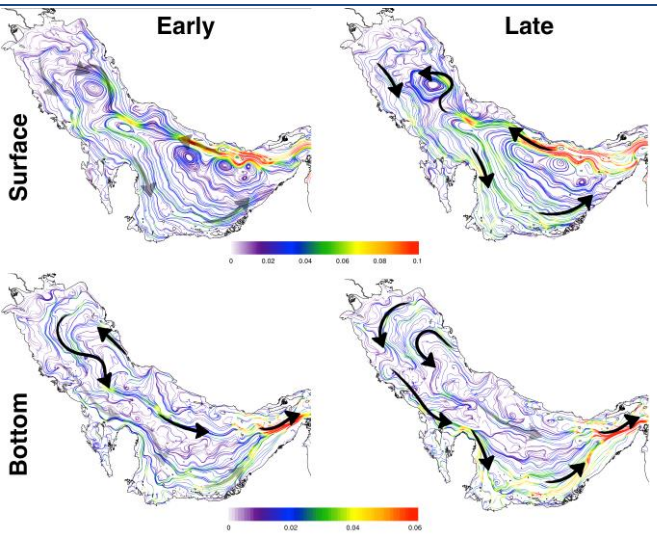

Figure ES-7: Sea surface and bottom currents change

Future sea level height

Dynamic Sea Level (DSL) was used to define large-scale barotropic changes. It was considered only dynamically modeled variables to force the RCM in the projected scenarios.

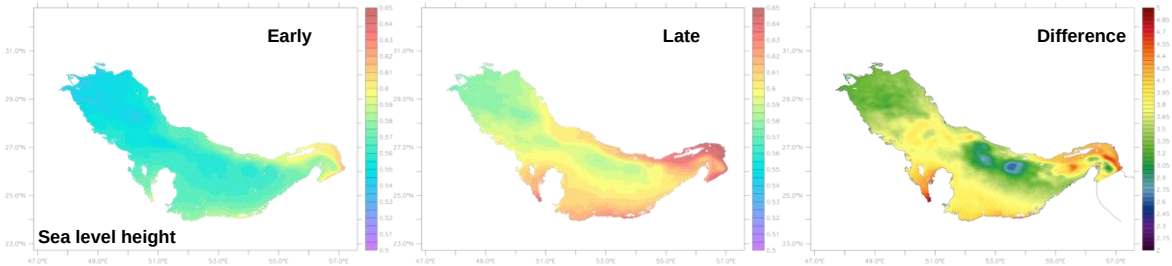

Figure ES-8: Sea level height for Early 21st climatology (left), for Late 21st century (center) and the difference between Late – Early 21st periods (right).

The Global Mean Sea Level (GMSL) is an averaged variable and has not been consider in the RCM simulations. The DSL results are mostly connected with the changes in the internal dynamics, and it will rise in 4 cm maximum (Figure ES-8). These numbers directly reflect the various ESM trends for the area, up to 3 cm for the same periods, Early and Late 21st century.

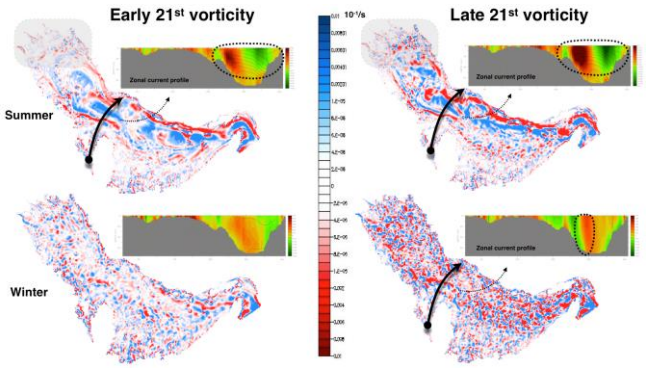

Figure ES-9: AG vorticity to Early (left) and Late (right) 21st century climate runs. Results were based on climatology. Details show the corresponding current zonal current profile. The scale (1/s) is the same for all the vorticity plots.

Future vorticity

Small-scale eddies increases in intensity and frequency with climate changes. Vorticity is a very important variable to the AG. It defines how and at what rate the mixing processes will occur. The late 21st warmer scenario, imposes an increase in the small scale eddies to the area, including in summer, when historically larger scale eddies used to prevail, along the deep channel (Figure ES-9). Therefore, there is a direct connection between small-scale vorticity (intensity and frequency) and warmer climate conditions. It allows and contributes to all kind of theoretical inferences about the climate effects in the area.

Parting thoughts

The MPIMR ensemble used has shown good accuracy in reproducing the localized ocean-atmosphere balance. The regional climate model (RCM) combines a traditional and long tested formulation with a very particular morphology, with a narrow and relatively shallow connection with the adjacent ocean (i.e., the Arabian Sea). The combination of all the characteristics mentioned above allows the regional model to achieve high standards on its skill in reproducing local ocean dynamics, despite the highly baroclinic unstable physics for the area.

The results assessments were based on IPCC's methodology and show expected outcomes for main AG variables and phenomena. Salinity shows a quite surprising response, an asymmetrical equilibrium structure. Such behavior motivates digging deeper on the RCM's results final analysis. Those analyses have shown a break in the vertical overturning system equilibrium, caused by warmer winters and longer summers at the north gulf area. The disrupted balance decreases the gulf impedance to light waters inflow, which causes the fast increase in the Arabian Sea entrainment "fresher" waters.

It is important to note that these conclusions are based on model experiments. The modeling process implies in a cumulative knowledge, which needs to be layered with field

observations and other approaches, to increase its statistical meaning. There are also limitations and uncertainties associated with the modeling process. These errors can be estimated, or even reduced, by replication of these experiments (changing the source of the forcing fields for other ESMs or high resolution atmospheric models) and/or by diagnostic experiments, explicitly following the IPCC's methodology (Mastrandrea et al., 2011).

An inter-connection analysis between the ocean and atmospheric findings could also present new causal insights that could better explain those surprising results. These connections could include into the ocean high frequency atmospheric changes (periods up to 1 day) and more precise orographic wind patterns. That combination certainly will increase the ocean model physical accuracy, which has been proven to be essential to understand the climate change effects in the area.

In terms of future research directions, it would be valuable to explore the connectivity of the AG and Arabian Sea. The AG, despite its relatively small size when compared with ocean circulation scales, may be a real player in the general ocean circulation. Its contribution to specific water mass in the Arabian Sea has already been recognized as a significant process (Kumar et al. (1999); Wang et al. (2013) and others).

Finally, the quite astonishing dynamic behavior under warmer seawater should be considered as a basis on which to explore related effects. That is, the results call attention to the need for studies that could include not only the anthropogenic Carbon Cycle effects (i.e. global warming) in the regional model dynamics, but also the direct changes in the environment due to desalination plants (Mohamed, 2009; Smith, Purnama, & Al-Barwani, 2007), since the AG has also a very important role as a water reservoir for human uses.

1. Introduction

Covering about 70 percent of the Earth's surface, the world's oceans have a two-way relationship with the Earth's climate. It influences climate on local to global scales, which in its turn can fundamentally alter many properties of the oceans. As greenhouse gases trap more energy from the sun, the oceans are absorbing more heat, resulting in an increase in sea surface temperatures, salinity and sea level[1].

Changes in ocean physical and chemical properties brought about by climate change lead to alterations in climate patterns around the world e.g. warmer waters are related to stronger storms in the tropics, which can cause property damage and loss of life.

One of the tools for understanding how the global climate may change in the future (**climate projections**) are the Earth System Models (ESM), which are the next generation of the coupled **general circulation models (GCMs)**. However none of these global scale complex models can currently provide information on scales small enough for understanding the regional-to-local processes that directly affect society.

The **global warming effects** future projections also require risk assessment analysis for specific matters, statistics and human science diagnoses tools that, together, will define the parameters to the modeling process. There are massive efforts to sustain a permanently evolving methodology to couple all the science fields that compose the climate system. The current stage on climate prospection is represented by the **Fifth Assessment Report** (IPCC, 2013), provided by the Intergovernmental Panel for Climate Change **(IPCC)**.

Under IPCC's methodology, there are up to 42 models number of model ensembles (e.g. KNUTSON et al., 2013). There was a long process to choose the right model for the area (Arabian Gulf). The Max Planck Institute ESM – Mixed Resolution (hereafter MPIMR; Marsland et al. 2003), was selected as the most suitable ESM to be used.

In order to translate the climate information obtained from the IPCC class models (CMIP5) into the local scale of our region of interest, the Arabian Gulf (AG), a numerical **downscaling** approach is used. It is based on **domain adjustments**, which uses the natural ocean basin morphology to capture the local scale dynamics

The **Arabian Gulf (AG)** ocean circulation and water masses properties have unique characteristics, which involve complex dynamical factors acting on different temporal and spatial scales. We address in this report the ocean downscaling process of the AG, using the climate information originated from the Global Earth System Models (ESMs) to develop,

[1] In this context, it's a general term that includes, the sea ice, ice sheet and land Ice melt. It also includes the global-ocean thermal expansion (GTE) and the dynamic sea level (DSL), the last two diagnosed by general circulation models (Griffies et al., 2012).

setup, validate and to be used as a tool to examine time-slices in the future.. For short, we named this regional system as a **Regional Climate Model (RCM).**

1.1. Objectives

To produce high-resolution simulations from the early and late 21th Century based on the most realistic ocean regional model possible, and focusing on the AG. The climate change projected scenario (RCP8.5 [2]) derives from the IPCC's 5th Assessment Report – AR5 (2013) models.

1.2. Project framework

In order to understand the changes in the AG driven by Climate Change we consider differences in the physical behavior of the ocean between 2000 and 2020 (that allows assessing the Gulf's present and near future status) and; from 2080 to 2100, (which makes it possible to glance at the long term future of the AG).

Therefore, our *Regional Ocean Climate Sub-Project* is divided into three phases: 1) model development by itself including validation against historical data; 2) the model use as a tool to investigate the main phenomena in the area aiming to explore the model skills and its limitations and 3) the model use to downscale the ESM results.

There are also many other activities that go hand in hand in support of the 3 phases outlined above. These include data pre-processing, investigation of the local dynamics and a delicate interactive post-processing method to adjust the numerical domain in order to successfully accomplish the downscaling procedure.

[2] RCP 8.5 - Representative Concentration Pathways (RCPs) are the greenhouse gas concentration trajectories adopted by the IPCC for its AR5. It supersedes the Special Report on Emissions Scenarios (SRES), from AR4. The Index 8.5 identifies the "*business as usual*" scenario, with a likely range of radiated forcing values from the year 2100 relative to pre-industrial values (+8.5 W/m^2)

The procedure to successfully obtain the downscaling of the climate information from the ESM into the AG downscale is summarized in the flowchart diagram below Figure 1-1. This Flowchart outlines the methodological steps.

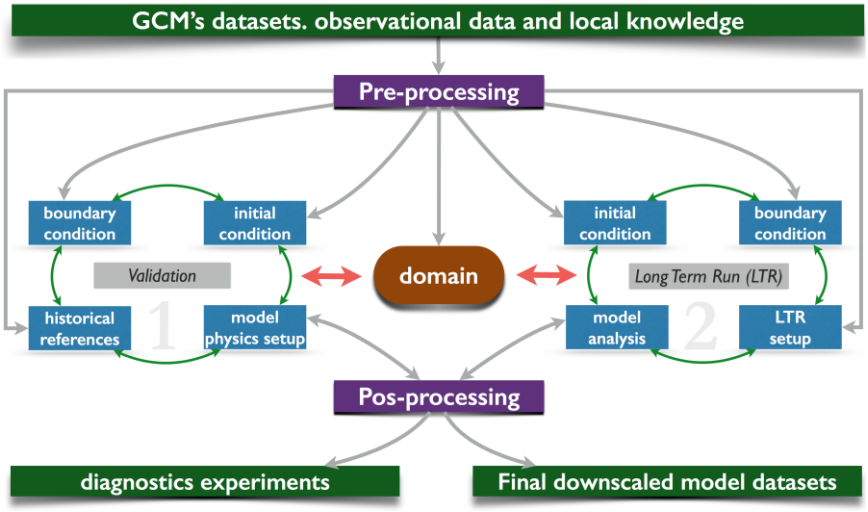

Figure 1-1: Flowchart presenting the two sub-project internal phases.

The Flowchart structure presented in Figure 1-1 is used to organize this report. First the scientific background and understanding of the region of study is presented together with the observed and available data and the ESMs related datasets (*The scientific background*). The first loop (**1**) in Figure 1-1 comprises the model validation processes, i.e. the *Arabian Gulf Downscaling*. It is here that the domain definition and the diagnostic experiments are discussed.

The *Ocean Climate Projections* (second Loop), described in Figure 1-1 are related with the final domain and setup adjustments to support the time sliced runs, the metrics to evaluate local climate ocean impacts and the final analysis and possible future steps to refine this project conclusions.

2. The scientific background

The first approach in any modeling procedure, including climate studies, is to define a background of local dynamics and establish ground-truth databases that represent the main features for the region. The method used here combines references from previous studies (Johns et al., 2003; R M Reynolds, 1993), satellite data, climatological datasets derived from a collection of observed data (Johnson, Garcia, & Boyer, 2013), numerical inferences from previous local modeling in the area (Kampf & Sadrinasab, 2006; Yao & Johns, 2010), and also the background datasets provided by global climate models, the ESMs (IPCC, 2013; Marsland et al., 2003; Roeckner et al., 2003).

2.1 The Arabian Gulf characteristics

The AG is a semi-enclosed sea located between latitudes 24–30N subject to arid climate since it is surrounded many deserts (Figure 2-1, left). The most significant atmospheric phenomenon that impacts the AG is a northwesterly wind known as *Shamal* (Perrone, 1979). Although it occurs year round, there is some well defined seasonal differences: wintertime is characterized by intermittent occurrences related to the passage of synoptic weather systems never exceeding 10 m/s, while summertime that wind shows a more continuous regime (Emery, 1956). The summer Shamal is associated with the relative strengths of the Indian and Arabian thermal lows. The winds, in the area ahead of an approaching cold front, blow from the southeast. These winds, "*called Kaus in Arabic or Shakki in Arabian, slowly increase in intensity as the front approaches*" (Reynolds, 1993).

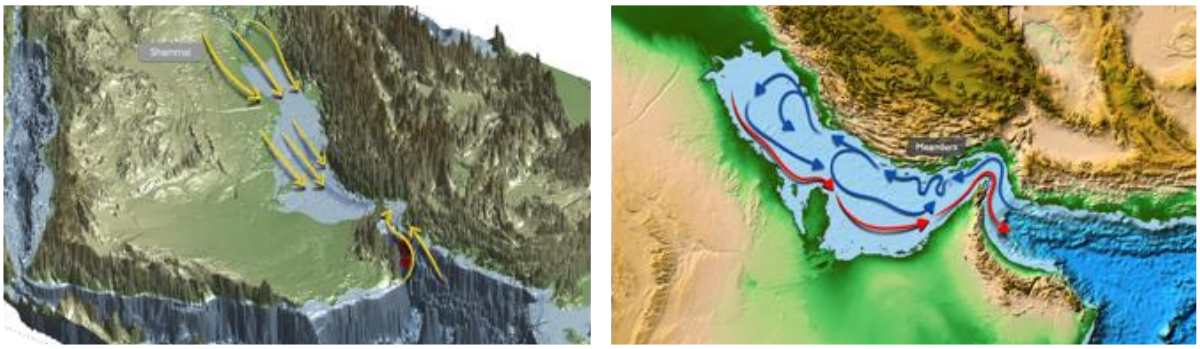

Figure 2-1: Arabian Gulf topography showing some schematic wind patterns (left) and a schematic ocean circulation (right).

The topographical feature associated with the Northwesterly trough orientation is the Zagros orography – the Zagros Mountains. As part of the Alpine-Himalayan mountain chain, it extends for about 2000 km in a NW-SE direction from the East Anatolian Fault of eastern Turkey to the Oman Line (DERCOURT et al., 1986).

Figure 2-1 (right) shows the circulation pattern based, on the winds described earlier, the seasonally stratified waters (Arabian Sea entrainments) and the highly unstable baroclinic dynamics in the area. A classical transient circulation feature (Summer to Fall) observed in the area is presented in Figure 2-2. It connects all the complex dynamical processes acting in the AG and typifies a good metrics to evaluate any model in the area.

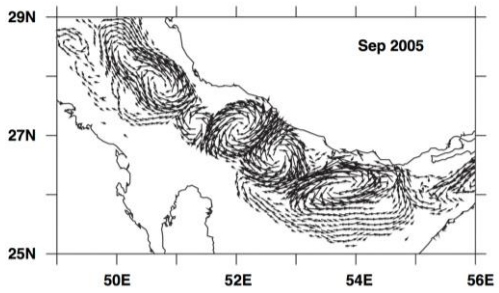

Figure 2-2: Large scale eddies formation during fall. Extracted from (Thoppil & Hogan, 2010c)

Another particular characteristic of the region is the dense water formation during winter in shallow waters along the West coast and at Northwest ocean areas. This area is characterized by an intense evaporation accompanied by a sinking of the leftover dense water mass.

As reported by Thoppil & Hogan (2010a) the water vertical structure at the AG presents very strong seasonal oscillations, characterized by a strong stratification during summer (Figure 2-3) and a fairly mixed vertical profile during the Winter months. The packed contours around 10 m seen on the temperature section (Figure 2-3) indicate a temperature inversion that defines the summer pattern. These are important features that we must seek to represent throughout the modeling process of the AG.

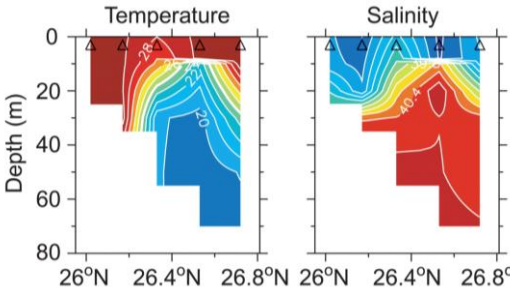

Figure 2-3: Vertical sections of observed temperature (left), salinity (right, contour interval is 0.2 psu) during 7 Jul 1968. (Extracted from Thoppil & Hogan, 2010b).

2.2 Datasets

2.2.1 *Earth System Models - IPCC AR5*

The Earth System Models (ESMs) are characterized by fully coupled equations of the ocean, atmosphere, cryosphere, biosphere and land areas. These equations are the basis for complex computer programs that simulates Earth's climate.

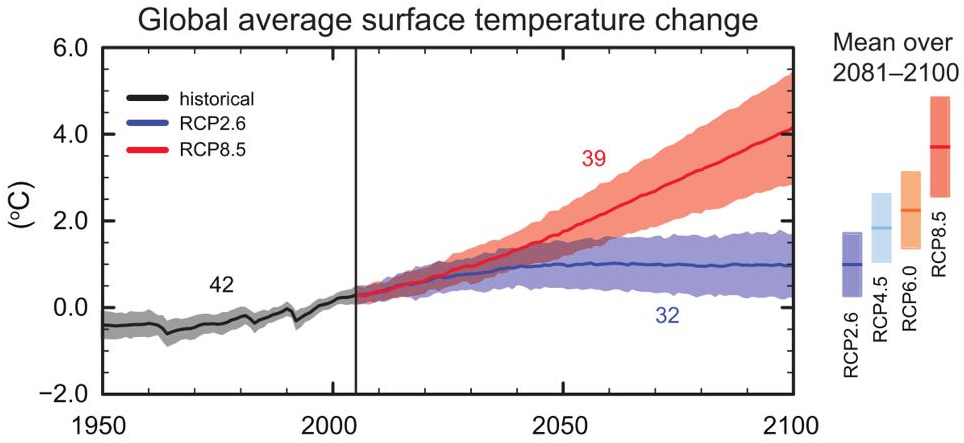

Figure 2-4: (Extracted from IPCC AR5). It shows the extremes and consequently, the projected temperature range till 2100

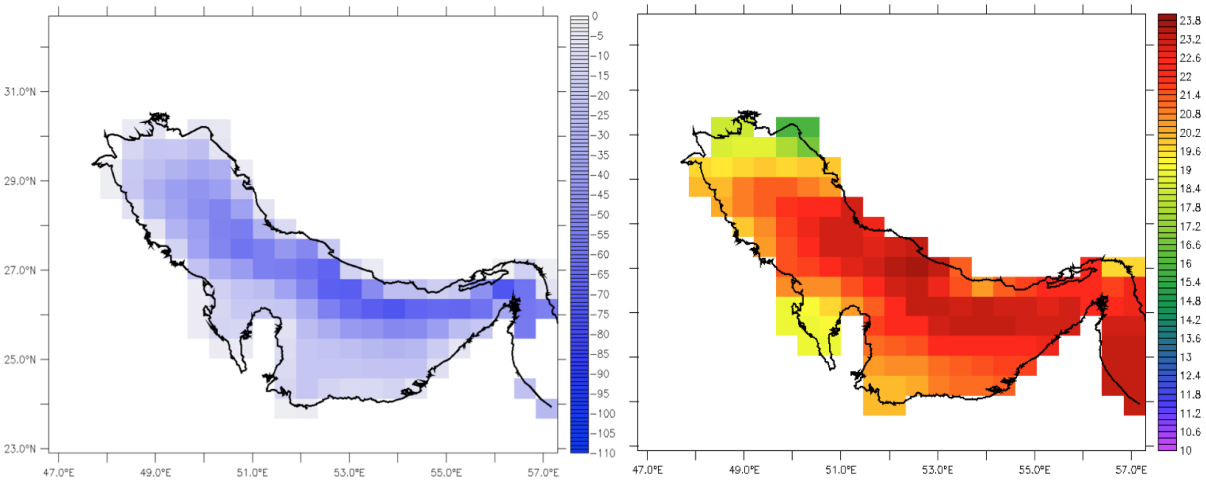

Figure 2-5: Example of a medium resolu tion GCM for the Arabian Gulf area. Left panel is the bathymetry (m) and the right is the sea surface temperature (Celsius).

In this project we are interested in the simulation results for the 20th (*historical*) and the 21st centuries (future scenario). The future scenarios are known as *Representative Concentration Pathways* (**RCP**). RCP scenarios describe pathways for social and economic development, which will determine different radiation forcing scenarios. Figure 2-4 summarizes the idea of RCP in terms of global temperature changes.

The AG is inadequately incorporated in global models mostly because of the lack of spatial resolution required to represent the morphological characteristic in that area, i.e. the sharp bathymetric structure that partially isolates AG from Oman Gulf and consequently open Arabian Sea (Figure 2-5).

Based on the requirement of local ocean-atmosphere flux equilibrium, we've tested several ESMs among the CMIP5 models and chosen a specific simulation from the Max-Planck (MPIMR) ensemble. The *historical* and the RCP8.5 scenario are used.

2.2.2 *The MPIMR*

The MPI-ESM-MR couples the atmosphere, ocean and land surface through the exchange of energy, momentum, water and important trace gases such as carbon dioxide. Compared to the previous version ECHAM5/MPIOM, the MPIMR was extended by numerous developments. It is based on the components of ECHAM6 for atmosphere and MPIOM for ocean as well as JSBACH for terrestrial biosphere and HAMOCC for the ocean's biogeochemistry. The coupling of atmosphere and land on the one hand and ocean and biogeochemistry on the other hand is made possible by the separate coupling program OASIS3. Energy, momentum, water and CO_2 are exchanged with the help of this coupling (Zanchettin et al., 2012).

MPIMR oceanic and atmospheric variables are used for the initial conditions, boundary layers and external fluxes for the downscaling methodology. The regional ocean model will respond for these forcing fields, so it's critical to analyze and evaluate these results for the area.

The variables used to compose de energy fluxes that will force the ocean surface are: Air Temperature at 2 meters (tair), Specific Humidity at 2 meters (huss), Pressure at Sea Level (psl), Net Shortwave Down Radiation at surface (rsds), Net Longwave Down Radiation at Surface (rlds) and Zonal/Meridional wind components at 10 meters (uas, vas). The ocean variables (border conditions) are: potential at temperature (temp), seawater salinity (salt), sea surface height (ssh), and Zonal/Meridional velocity components. Figure 2-6 shows an MPIMR's original grid resolution fields of an oceanic salinity field with surface currents (left) and a wind distribution with the humidity field (right).

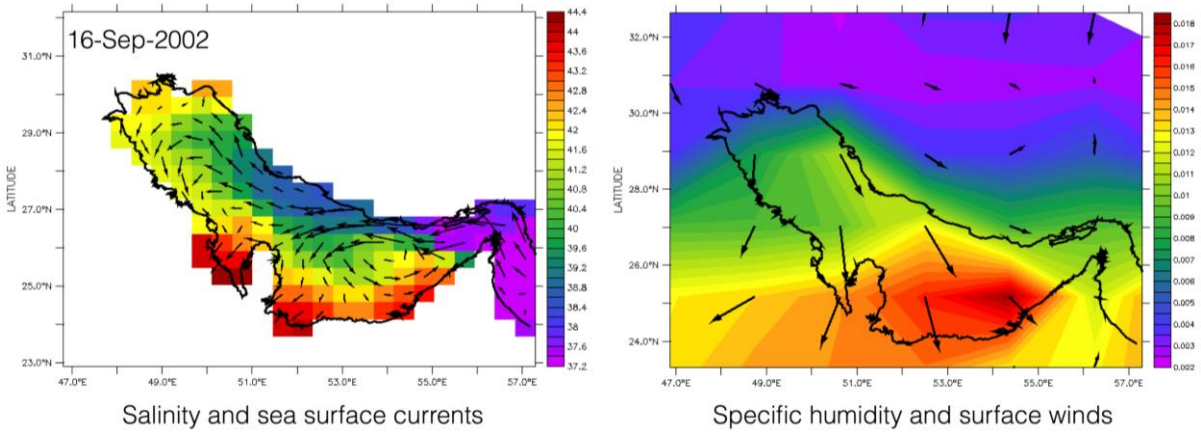

Figure 2-6: MPIMR's oceanic and atmospheric variable in its original resolution.

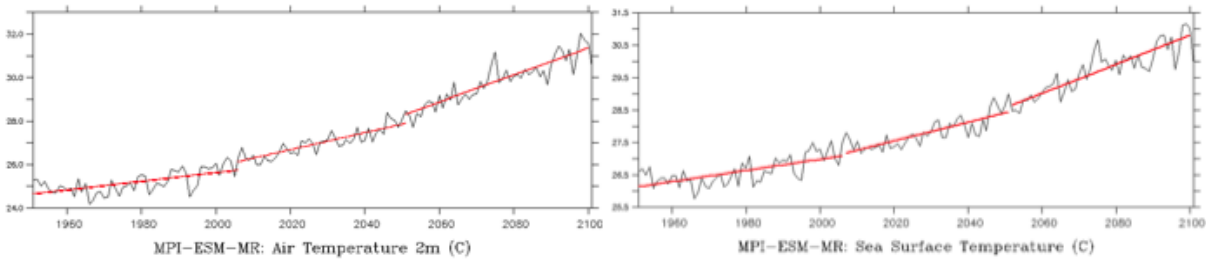

Figure 2-7: Trends for Arabian Gulf Region for the period from 1950-2100 – RCP8.5 scenario. Air surface temperature (left side panel) and sea surface temperature (right side panel).

It is important to assess the behavior of MPIMR trends (Figure 2-7), for both ocean and atmosphere fields in order to trace these changes in the downscaled model results but also - and mainly - to anticipate extreme events that might cause severe changes in the ocean response.

Figure 2-7 shows the air and sea surface temperature linear trends averaged for the AG area. Both time series show a temperature increase during the 21th century and with higher trends after 2060.

2.3 Local observations

2.3.1 *Published data*

To validate this regional model, understanding the physical characteristics of the region is of significant importance. Since ocean datasets with enough temporal resolution to be reliably used are quite rare, examine the local ocean dynamics already described in the literature, centered on Reynolds (1993, op. cit.) and updated by: Bashitialshaaer, Persson, & Aljaradin, 2011; Elshorbagy, 2008; Lattemann & Höpner, 2008; Thoppil & Hogan, 2010; Yao & Johns, 2010 among others. Some oceanographic characteristics presented in previous section will be used as a dynamical reference and part of the metrics used to validate the current model.

Figure 2-8 shows winter temperature and salinity fields based on observed data. These are literature reference results extracted from Reynolds (1993, op. cit.), and are the main salinity environmental reference used in this work. The river discharges were not considered in this work, since the dams and the agricultural uses mostly drain the fresh water sources, which are already historically low (Issa, Sherwany, & Knutsson, 2014).

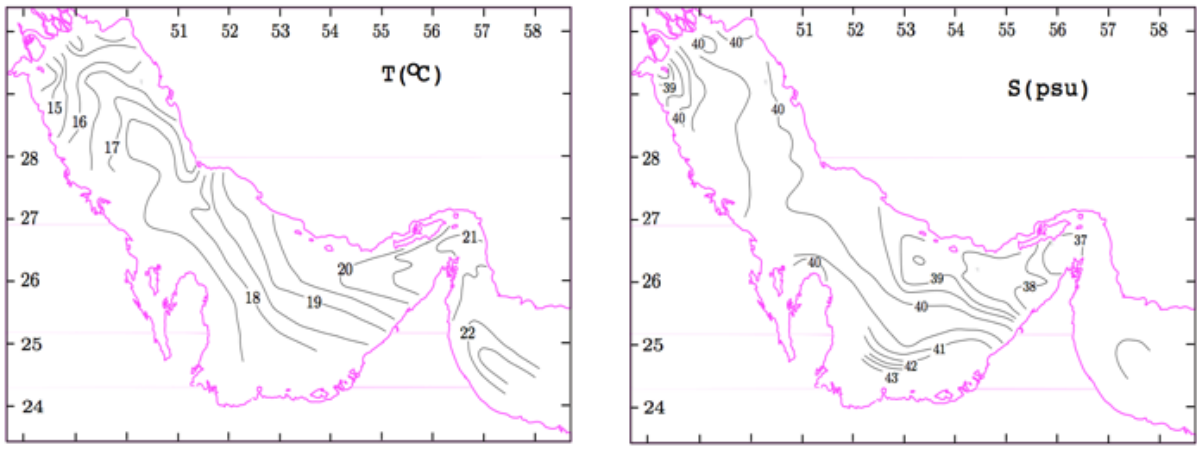

Figure 2-8: Observed winter sea surface temperature and salinity extracted from R M Reynolds, 1993)

The MPIMR humidity wavelet spectrum, averaged at AG, is presented in Figure 2-9. This kind of signal amplification, which will change the regional model responses in the AG, are connected with large-to-global climate changes in the ocean and atmosphere, as the very likely pole-ward shift of the Low Level Jetstream (LLJ) associated with the Summer Monsoons (Sandeep & Ajayamohan, 2014), and the SST ocean dipole changes already observed and with large consequences to ocean surface temperature waters (Weller & Cai, 2013).

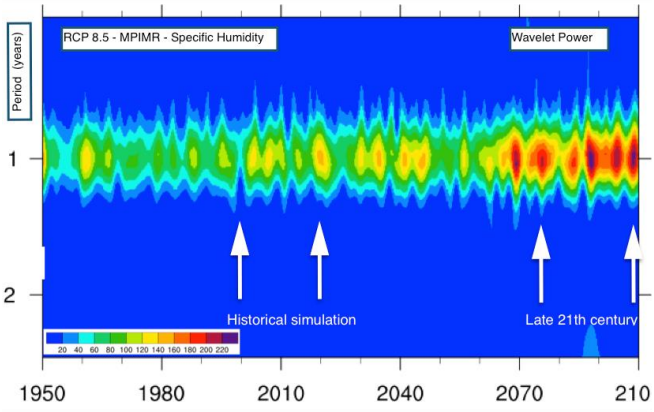

Figure 2-9: MPIMR-RCP8.5 wavelet analysis (area averaged). The arrows show the humidity increase in amplitude and average signals.

2.3.2 *Satellite data*

Beside the published data, another data source to be used during the model validation process is the remotely sensed sea surface temperature. Satellite SST data used in this study derives from the Advanced Very High Resolution Radiometer (AVHRR) from 2003 to 2012. This data has global coverage and spatial resolution around 1.1 km in a daily frequency. Figure 2-10 shows winter AVHRR sea surface temperature map with its original 1.1 km horizontal resolution. This data will be used as a ground truth result for validation purposes.

2.3.3 *World Ocean Database 2013*

Another source of observational data used is the World Ocean Database 2013 (WOD13). WOA13 is a collection of scientifically quality-controlled ocean profile data, maintained by the

National Oceanographic Data Center (NODC) and Ocean Climate Laboratory (OCL). The WOD13 includes data from all sorts of instruments, such as CTD (conductivity-temperature-depth) and high-resolution XBT (expendable bathythermograph). Figure 2-11 (left) shows the distribution of CTD stations and XBT devices from the WOD13 for the region of the AG (data available at http://www.nodc.noaa.gov/OC5/WOD13/data13geo.html). Averaged temperature and salinity distributions are shown in Figure 2-11.

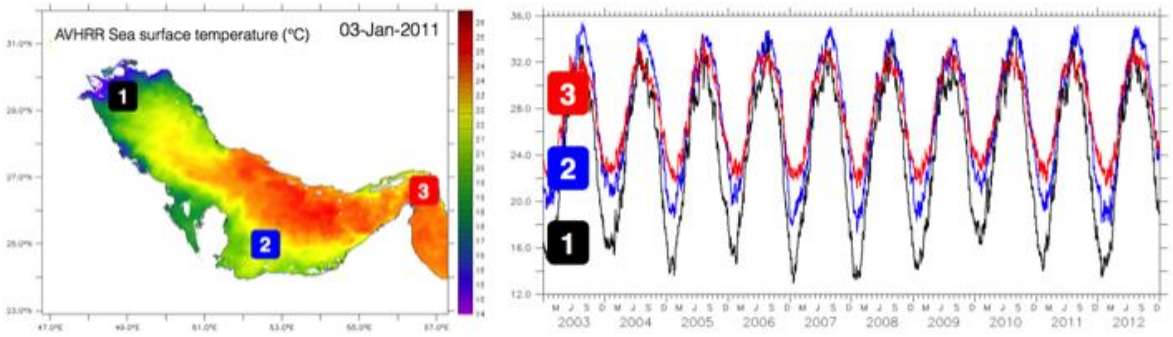

Figure 2-11: Satellite sea surface temperature for 2011. Upper panel shows the annual mean temperature. Lower panel shows the annual temperature oscillation at three regions: 1 - the head of the Gulf; 2 – the UAE region; and 3 – the Strait of Hormuz.

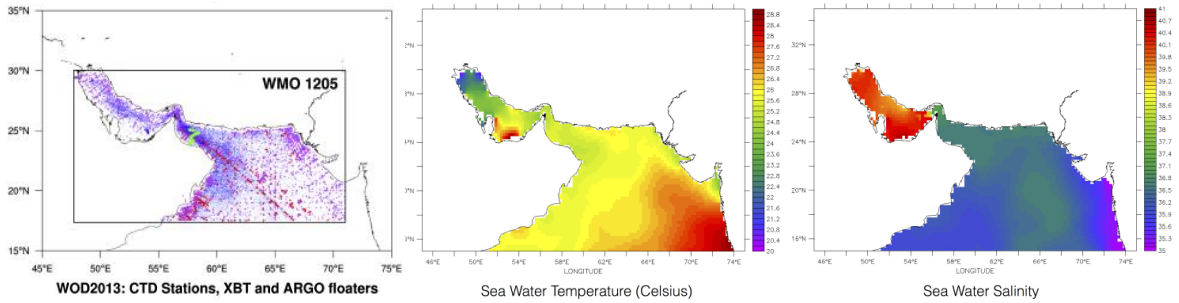

Figure 2-10: Left: XBT (blue), high-resolution CTD stations (red), CTD stations (purple) and ARGO floaters (green) from the World Ocean Database project, used for the World Ocean Atlas 2013 climatology. Center: Sea surface temperature based on gridded data composed from WOD13; Right: salinity based on gridded data composed from WOD13.

3. The Arabian Gulf Downscaling

This section includes the activities described in the center and left of the flowchart's presented in Figure 1-1. The domain definition is a critical path for the downscaling process. The domain does change the requirements for initial and boundary conditions.

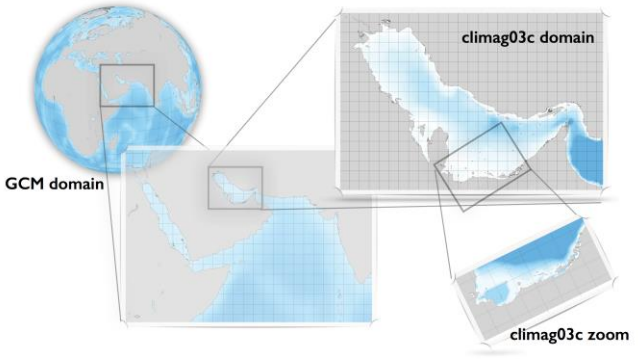

Figure 3-1: Scales transitions until required focus in the Arabian Gulf and Abu Dhabi seashore.

It is also crucial to choose the ESM's with proper skills to reproduce the meso to large-scale dynamics, where the domain is included. And, the most important aspect is: the search for a coverage area, which allows the local physics to be self-contained. A validated RCM, based on the above criteria is a pre condition to successfully achieve the project goals, the climate projections downscaling at AG.

3.2 Downscaling Methodology

The purpose of this project is to translate the climate information generated by the complex IPCC-class ESM to a very constricted area, i.e. the AG. To provide good quality downscaled climate projections from the CMIP5 models the regional domain has to be able represent local dynamic features, which are not represented by ESMs, because of their coarse resolution which combines unsolved smaller scale dynamics and bathymetric misrepresentation into sub-grid dissipation effects and, consequently disrupted the variables and fluxes equilibrium.

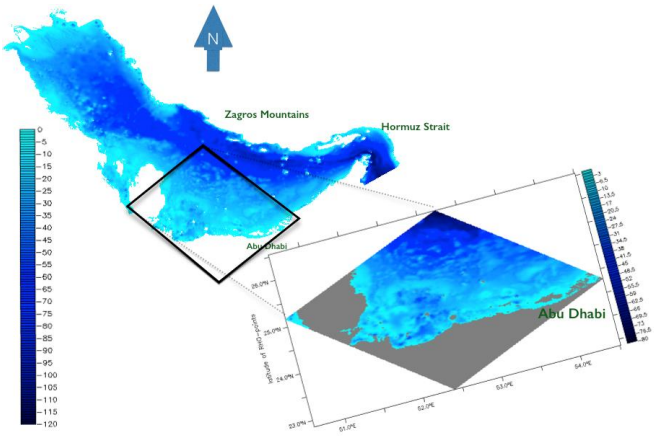

Figure 3-2: Bathymetric data projected on climag03c and the costal tailored adjustment along coastline of the Arabian Gulf. Plot detail nearby Abu Dhabi shoreline, depths in meters.

3.2.1 *Domain definition*

This domain cascade is illustrated in Figure 3-1. It shows the different resolution perspectives from the coarse grid ESM to our final modeling domain, until reaches the requirements for maximized resolution, simultaneously affordable to climate projections experiments.

The working domain developed is named ***climag03c*** – "*Climate Modeling at Arabian Gulf*" in its third horizontal configuration version; "*c*" stands for the type of adjustment with the computational resources (*b*=coarse test grids, *c*=best fitted grid, *d*=short term integration, computational expensive resolution). This grid (***climag03c)*** has 1.15 km averaged horizontal resolution and vertical resolutions varying from 0.1 cm till 4 meters. It uses ETOPO bathymetric data (Amante, W, & Eakins, 2009). The coastlines are tailored based on satellite data and the model numerical requirements. The final grid configuration is presented on Figure 3-2.

The ocean downscaling implemented here aims to transfer the ESM's coarse grid signals directly to just one local domain with the highest resolution possible (and numerically affordable). The main paradigm or this approach relies on the water high viscosity (if compared with air) and the natural basin physics usually captured by enclosed systems. If well accomplished, the final model configuration acts as a "numerical ground-truth filter", i.e., it is able to retain the most significant signals (realism), naturally expelling spurious forces. On the other hand, the price for that is to find an adequate domain adjustment, since it became an internal coupled variable for the methodological problem, as the flowchart (Figure 1-1) indicates.

3.2.2 *Model setup - ROMS*

The model used in this study is the Regional Ocean Model System - ROMS, which is a free surface, terrain-following, hydrostatic primitive equations ocean model (Mcwilliams, n.d.; Penven, Debreu, Marchesiello, & McWilliams, 2006; Shchepetkin & Mcwilliams, 2005). All 2D and 3D equations are time-discretized using a third-order accurate predictor (Leap-Frog) and sigma dispersion corrector time-stepping algorithm. In the horizontal, the primitive equations are evaluated using boundary-fitted, orthogonal curvilinear coordinates on a staggered Arakawa-C grid. In the vertical, the primitive equations are discretized over variable topography using stretched terrain-following coordinates.

3.2.3 *Ocean open boundaries*

The regional model setup process is focused both on the ability of the regional model (ROMS) to capture low-resolution ESM (MPIMR) results, transfer it to the internal domain. However it also ought to allow the regional model open boundaries formulation to radiate out of the system signals that are not physically sustainable by the Arabian Gulf Dynamics.

The input forces from the ESM model along the southern AG ocean boundary (Hormuz Strait) is illustrated in Figure 3-3 for the salinity fields, already pre-processed and stretched to the model mathematical domain.

Based on a relaxation and anti-relaxation principles, several number of modeling sensitivity experiments were performed, to achieve the right balance between the external climate forces (Figure 3-3) and the natural physical responses from the inner domain. The final tuning result is presented in Figure 3-4, where the regional model output and the ESM results are compared exactly at the open boundary, in the case for the temperature field. The best fit here is expected not only with satellite data (the ground truth reference) but also mostly between the regional model and the ESM.

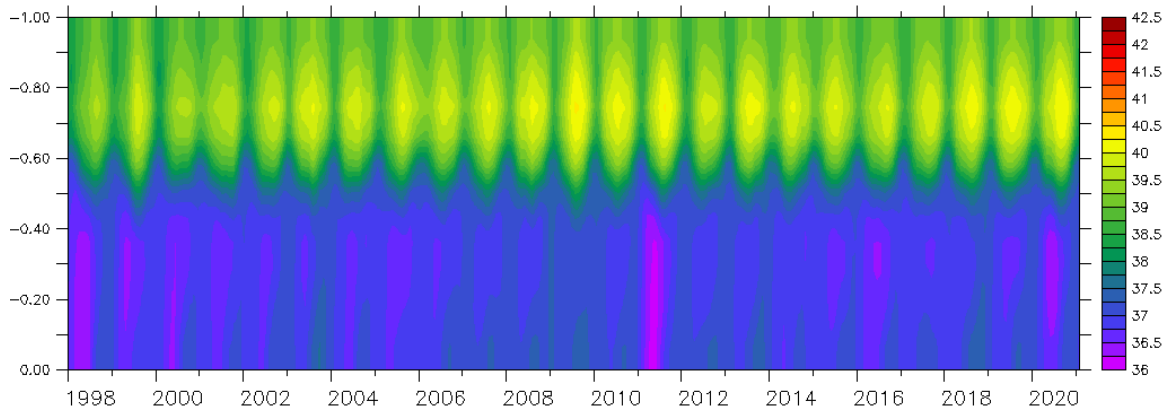

Figure 3-3: Early 21th century salinity time evolution at the regional model southern boundary.

3.2.4 *Initialization*

With open boundaries, the initial conditions are part of the natural theoretical problem solution and require especial considerations. Two main aspects to be evaluate: the pre-

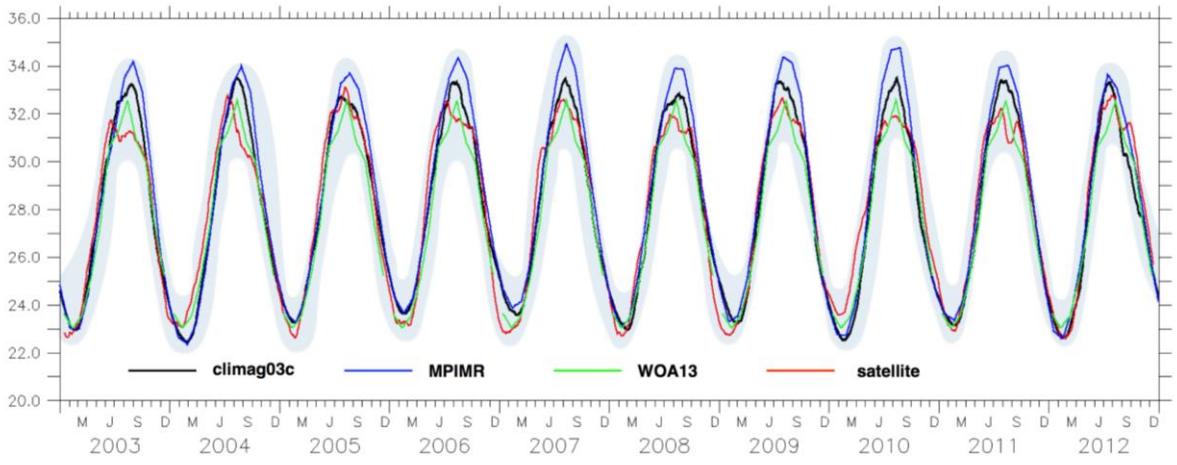

Figure 3-4: Temperature time series combining the regional model and GCM results in the same position at Southern ocean open boundary.

processing original ESM forces which will initialize the model and the Regional Model uses to smoothly induce the geostrophic balance in the initialization fields.

Most of the initialization fields are basically extrapolations and filters in the dated ESM results. Specifically salinity has an especial treatment between Qatar and Bahrain shallow embayment. The regional model cannot eject the extremely high salinity induced by the ESM in this area, which remains trapped along time. There is a natural salt accumulation in that area, but it has to be induced directly by the regional model and not by extrapolated fields. Figure 3-5 shows the final salinity initial configuration used by the early 21st century simulation.

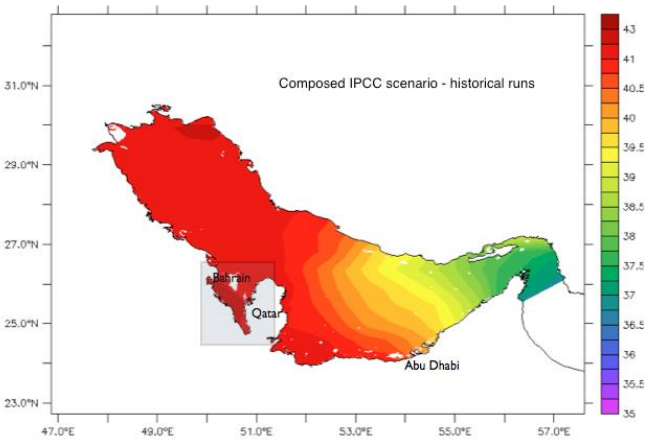

Figure 3-5: Remapped salinity initial condition (early 21st century). The shaded area points out the area where salinity has been changed.

To obtain a physically consistent initialization spreading field, it has been used climate ensembles were used, instead of using only MPIMR (Zanchettin et al., 2012) results. In the present case we also used ECMWF (Danabasoglu et al., 2012) and CSIRO (Jeffrey et al., 2013) results for the same time stamp. The spin up process starts from the condition shown in Figure 3-5 results and consists of the use of the regional numerical model to equalize the geostrophic balance from the original extrapolated ESM results. Usually it is an implicit methodological modeling process. However, because the further time slices projections, it requires a very accurate procedure, which is illustrated and summarized in Figure 3-6.

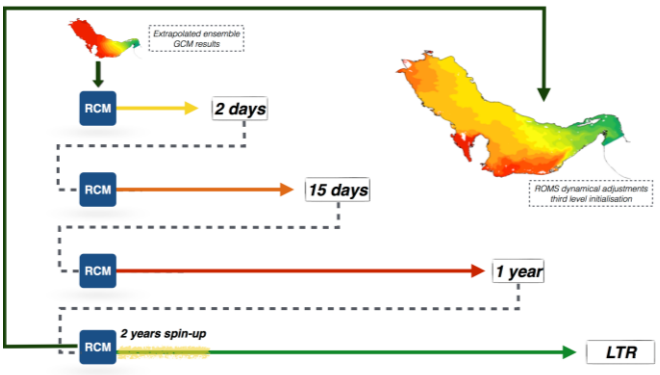

Figure 3-6: Pre-processing and the 3 warm up stages to initialize the model. The forth level refers to a safety spin up before defining the time slice analysis period.

3.2.5 *Validation*

The validation procedures were performed along various stages of the project aiming the best adjustment to a proper local circulation relative to hydrodynamic fields. The Long Term Runs do motivate changes in the validation parameters, including domain definitions, resolution and coastline adjustments that will be described in

further topic. The actual result does include the warm up processes, to illustrate the model behavior in the initialization process.

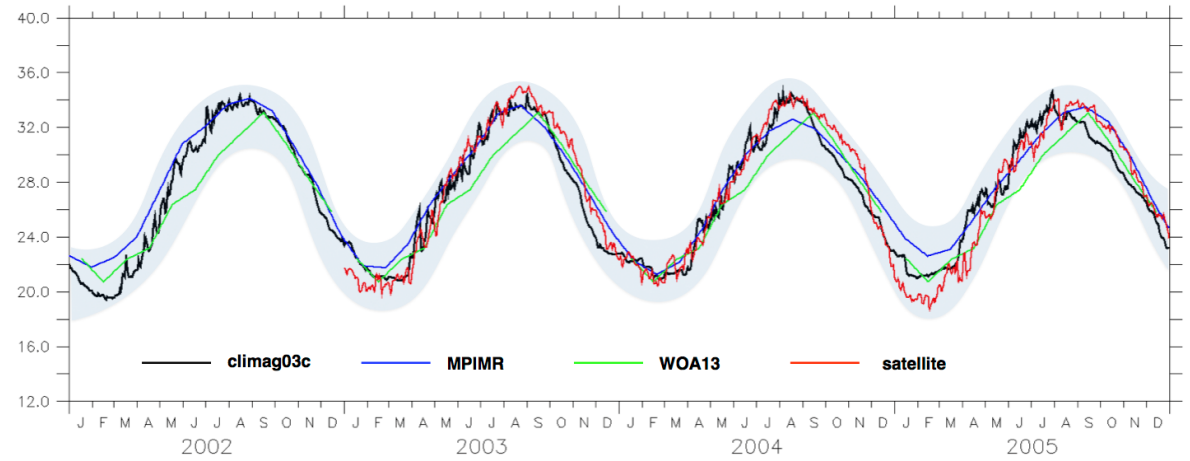

Figure 3-7: SST local averaged time evolution. The model results in black, satellite in red, extrapolated GCM in green and climatological cycle based on WOA13 in blue.

Figure 3-7 shows Abu Dhabi region averaged sea surface temperatures (SST) comparing the regional model results, satellite data, WOA13 (Johnson et al., 2013) climatological dataset and the MPIMR ESM. From these results, it is clear the downscaled models skills to represent the area.

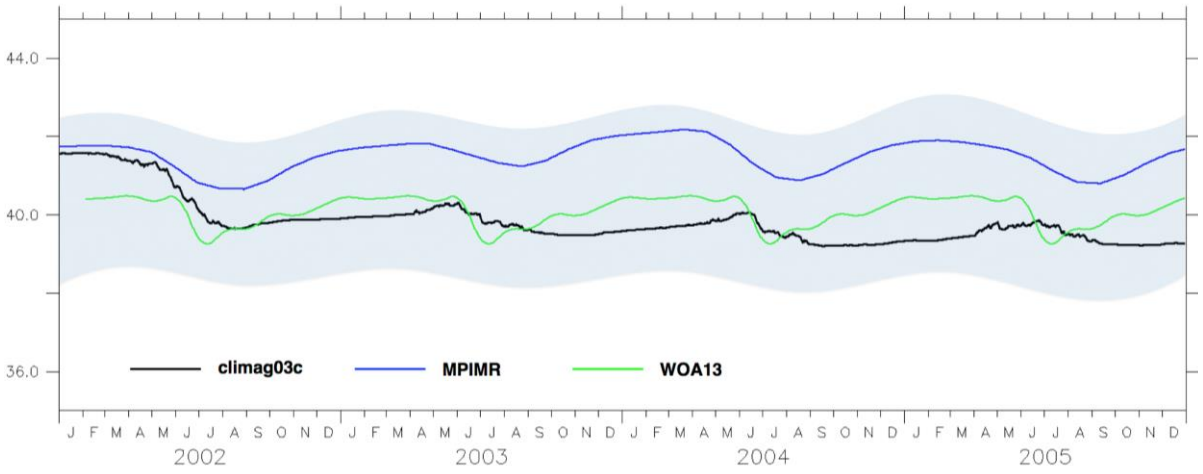

Figure 3-8: SSS averaged for the southern Arabian Gulf area The model results in black, WOA in green and extrapolated GCM in blue.

The salinity validation results (Figure 3-8) have a much slower warm up profile due to the differences between the real patterns and the ESM initial conditions, clearly seen when

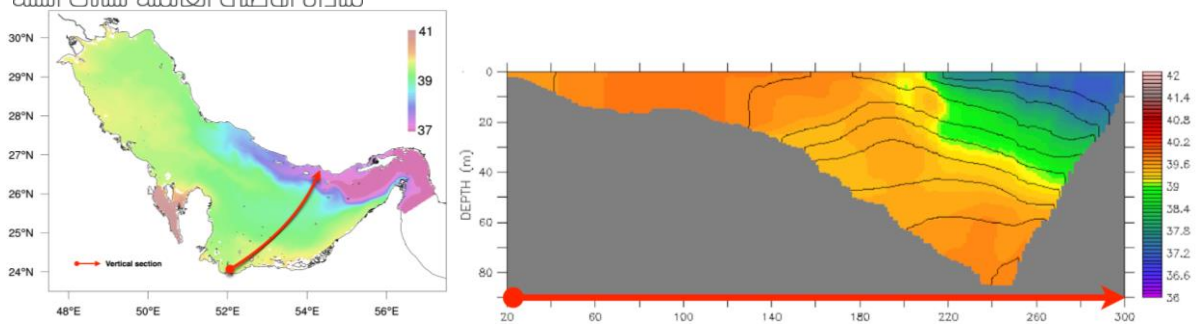

Figure 3-10: Left: Snapshot of salinity fields with arrow shows the vertical profile position; Right: Salinity profile along the red line - summer to fall condition.

compared against the climatological WOA13 (Johnson et al., 2013). The current climag03c setup is able to correct the erroneous signal from ESMs initial conditions.

The local circulation dynamics (Figure 3-9) is also validated because of its very distinctive structure, well known to the area. It is characterizes by the maximum "fresh water" flow that enters the Gulf from the Arabian Sea (Summer to Fall period).

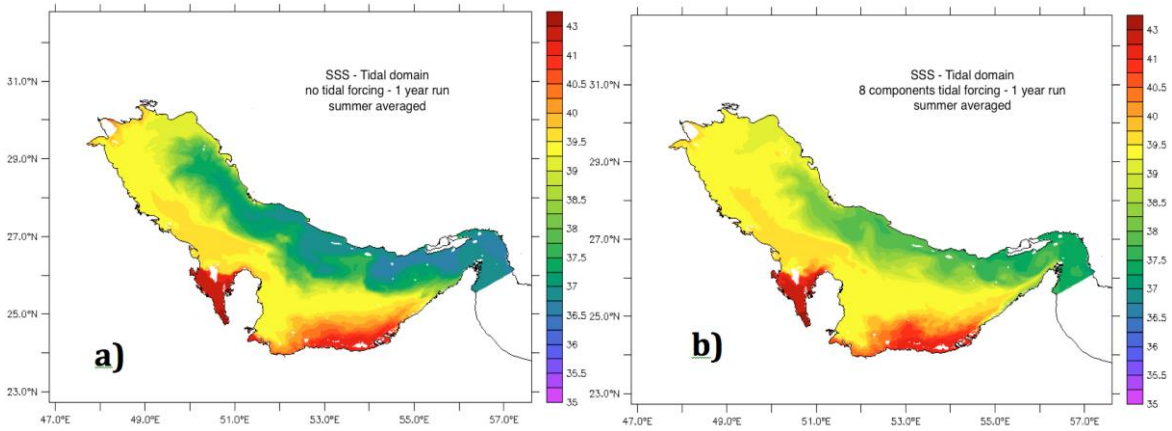

Figure 3-9: Summer SSS based on no-tidal forcing (a) and on full tidal forcing (b), using the same model formulation.

The high-density differences between these waters increases the mixing eddies scales and also produces the maximum stratifications observed in the area, as represented in Figure 3-10.

This final setup was able to capture and reproduce the stratification reported by available observational studies. This result indicates that the regional model setup is not only providing good quality numerical results of local oceanographic processes, but also improving the representation of such processes.

3.3 Diagnostic experiments

This section refers to the transition between both flowcharts' sides presented in Figure 1-1 and shows the effort to stabilize and validate the regional model to the domain of interest.

3.3.1 *Tides*

The tidal structure at the AG has a very particular dynamical behavior, with most of the components forming at least two Amphidromic circulation systems, some tests were performed to asses its impact on the modeling runs. To evaluate the tidal influence in the area, the regional model grid (**climag03c**) has been reformed to sustain the tidal forcing. However, this increases the execution time by an order of 10^2. This value does not make any climate projection computationally affordable at present. Thus, to evaluate the tidal effects in the thermodynamic fields, the model was run for 2 years, with hourly output.

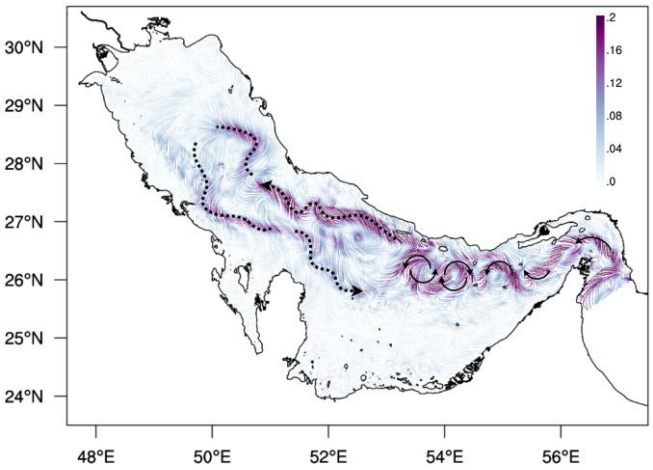

Figure 3-11: Summer to Fall Arabian Sea water entrainment in the Gulf, shade is speed (m/s).

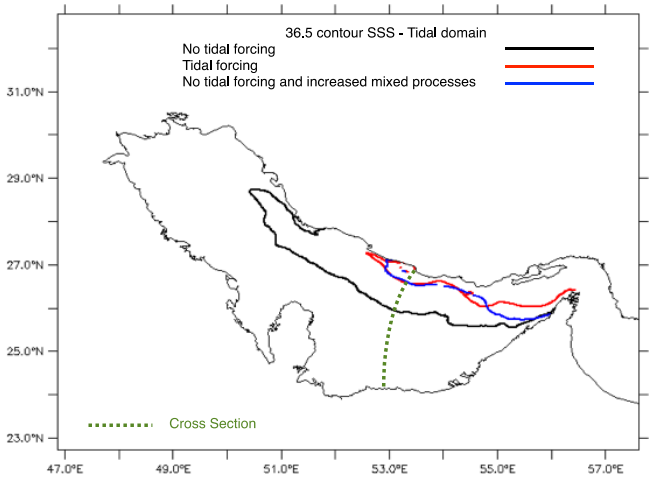

Figure 3-12: 37.5 psu SSS contour lines. Comparison between no-tidal forcing, full-tidal forcing and the original climag03c setup with higher initial mixing coefficients.

Usually, because of its barotropic characteristics, tide does not impact the general circulation significantly. However, in the AG, the experiments have pointed out an important role for tides in the general mixing process (horizontal and vertical). The AG admittance for Arabian Sea fresher waters is reduced by this mixing process, which is shown in Figure 3-11.

These results clearly show the Arabian Sea "fresh water" entrainment differences. Since our goal is to downscale the ocean circulation aiming at climate projections time scales, there are no computational resources to sustain such expensive runs. Based on that, we have chosen to use the *Turbulent Closure Scheme* (**TCS**) from the ocean model to increase the mixing

processes. Thus, we can reproduce the impact from tides, without substantively increasing the model execution time. The comparison between previous results (i.e., Figure 3-11) and the non-tidal highly mixed simulation (using TCS) are presented in Figure 3-12.

3.3.2 *Humidity corrections*

Specific Humidity is an important parameter to define the ocean fresh water flux balance with the Atmosphere. Figure 3-13 shows the spatially averaged fields between 2002-2006 for three different MPIMR compositions and one for a regional atmospheric model based on a ground-truth simulation (*WRF-Interim*).

The correction used shows minor differences to WRF-Interim results, however slightly but important coastal changes will be observed in the regional model simulation in the salinity fields, which required fine-tuning of the humidity input into the regional model.

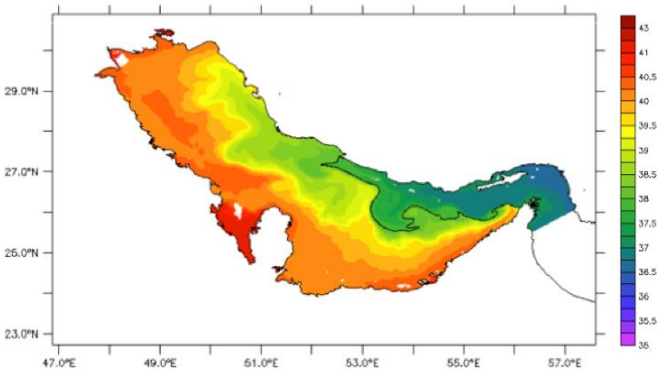

Figure 3-14: Final configuration for LTR. SSS summer condition. For further references, the salinity 38 is the black contour line.

3.3.3 *Shallow water salt production*

Since the humidity correction has been only replaced from an analytical expression to a bias correction, the heat flux has not been meaningfully changed, thus there is no changes on temperatures fields adjustments. However, considering all kind of observations related with salinity in the area (literature reviews, datasets and personal information), the regional model bulk formula sensibility to shallow waters fresh water balances has been increased.

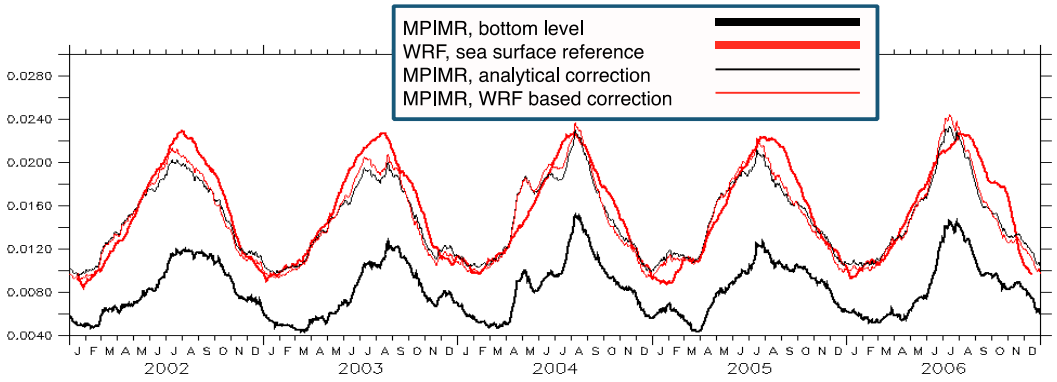

Figure 3-13: Humidity corrections based on WRF ERA-INTERIM atmospheric simulation.

The combination of this with the increase in the mixing processes resulted in a slightly different balance along the gulf's Northwestern coast. There was a reduction in the seasonally mixing processes along Kuwait and Iran coastline. Figure 3-14 presents the new configuration observed in salinity fields, considering all the fine-tuning that have been made. In general, these changes resulted in a less stratified environment and a general salinity increase along the AG's Southwest coastline.

3.4 Downscaling conclusions

The regional model system - RMS (C) is comprised by: the established numerical domain with its horizontal and vertical resolutions; the ROMS hydrodynamic equations configured to solve the system; the formulation of the boundary conditions; the initialization of the internal parameters and the exchanges of fluxes with the atmosphere. These combined, stable, internally conservative and validated components acting together were the target and the main contribution of the first part of the project.

This RCM has proven also to be accurate enough to be used as phenomena diagnose tool or to overlook regional climate changes in the area. The use of this system to time-slice the ESM results is the next stage of this project. As phenomena diagnosing tool, it contributes to better understanding the local dynamics. The model also does contribute how the baroclinic and barotropic[3] ocean components are combined. To diagnose the AG main characteristics, the results from the climatologically reduced historical integration are presented here.

The sea temperature and salinity gradients sustain most of the observed overturning circulation in the AG, because of their extreme gradient patterns. The temperature shows a clear seasonal cycle everywhere in the Gulf (see previous Figure 3-7), which does not necessarily happen with salinity, when considered in the full area averaged. The vertically averaged density structure (Figure 3-15, plot (A) at top) shows salinity predominance all over the Gulf, except for the northern area, where temperature also plays an important role (blue area). The vertical profiles alternate from a very defined summer stratification to fully mixed (winter and spring seasons), as presented also by the density profiles on Figure 3-15, plots (B) and (C) at bottom).

[3] Generally, a **barotropic** fluid is a fluid whose density is a function of only pressure. **Baroclinic** fluids are those where density gradients are not parallel to the pressure gradients. This is a very important concept to understand the Arabian Gulf Circulation, since the temperature and salinity gradients (density) strongly define the dynamics.

The salinity field obtained with the historical forcing (early 21st Century) is presented again in Figure 30, to reinforce the role of this variable in the general baroclinic dynamics and to signal the salinity formation zones. Figure 3-16 (plot (A), at top) is used to reference the vertical profiles (B) and (C). The overlain contour lines are now the meridional current component to

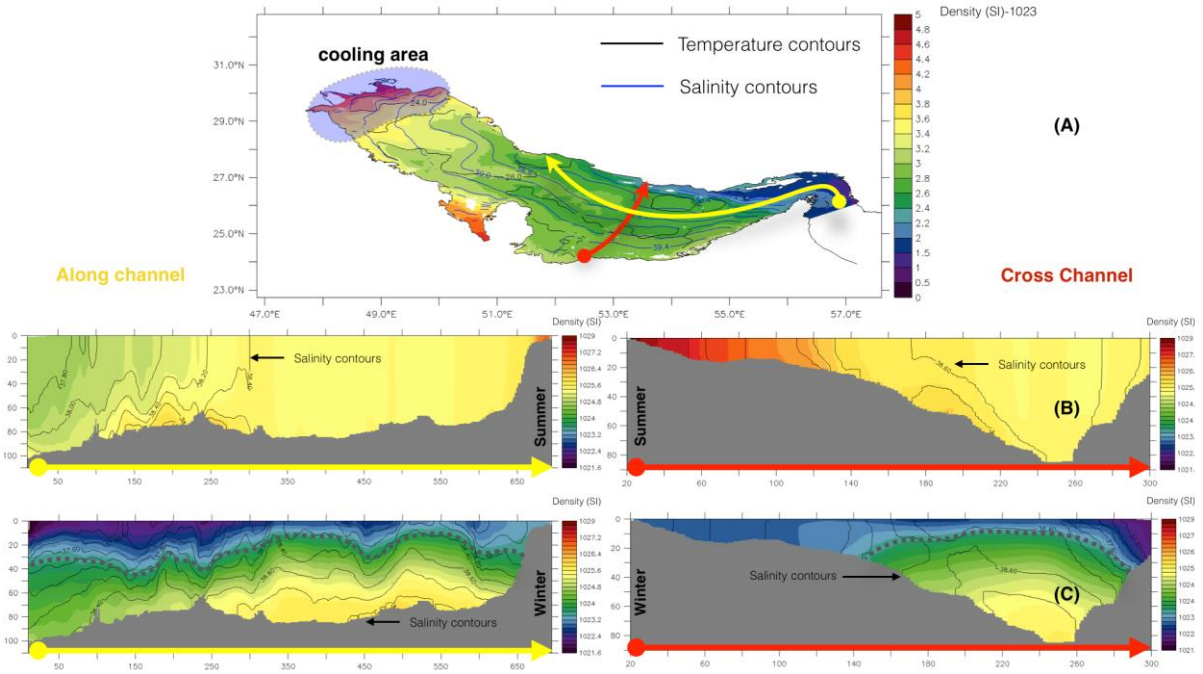

Figure 3-15: (A): Historical climatological density structure reproduced by the RCM in the AG showing temperature and salinity contours. Red and yellow lines are the reference to the vertical sections (B, C plots), for summer and winter condition. At winter (C) historical climatology, the grey lines point out the stratification structure.

the same period. As shown in Figure 3-16 (plots (B) and (C), at bottom) not only the salinity horizontal structure defines the circulation, but its vertical distribution and leakage from shallow to the deep channel also defines the mixing processes.

The mixing process driven by seasonality reproduced in the AG justifies the choice of the domain definition, since it ought to resolve these small-scale processes. To reinforce these very local dynamic characteristics, Figure 3-17 connects the time dependence of the vorticity horizontal and vertical scales, which are key elements to define the general overturning in the gulf and the main physical mechanisms that are able to sustain that system.

This explains why the ESMs, although including the AG on its domain, overestimates variables like salinity and temperature in the area, they simply cannot solve such a complex baroclinic structure and the eddies scales.

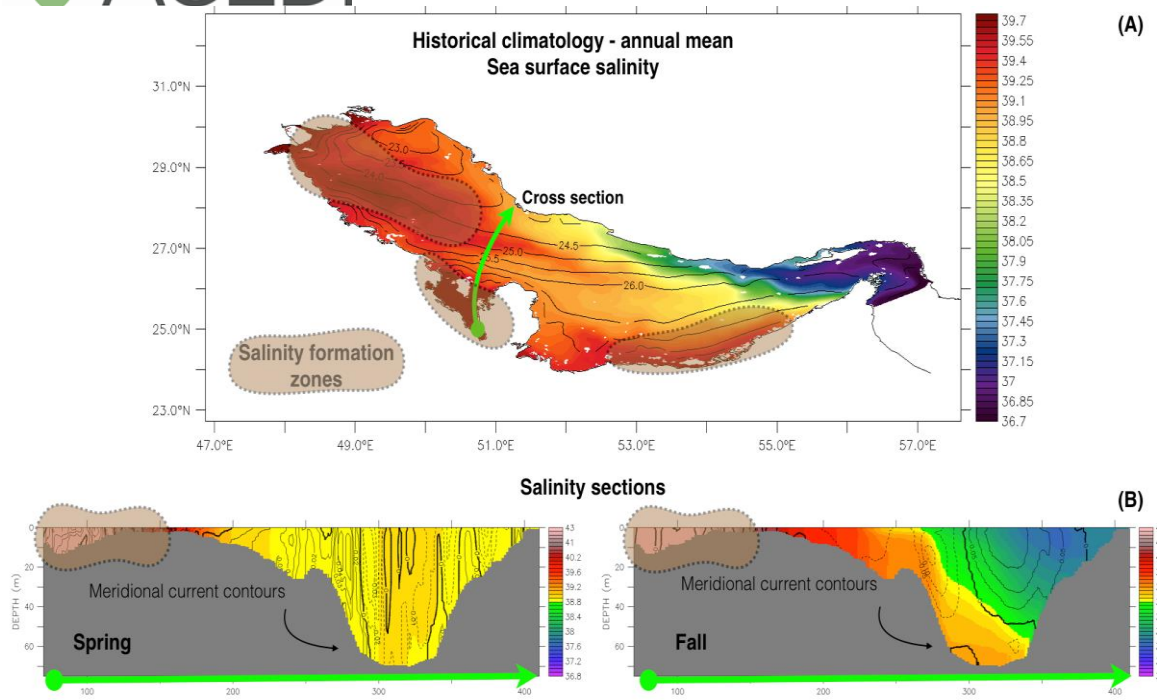

Figure 3-16: (A): Sea Surface Salinity averaged climatology reproduced by the historical simulation. B: Salinity seasonal (spring and fall) cross sections and meridional current contours (m/s).

The RCM horizontal resolution has to be maintained in high resolution (eddy resolving) to actually solve the vorticity processes. Therefore, it is also possible to use this very same tool to evaluate more localized dynamic processes in the area, as the current parallel to the coast, already observed and described in the area (W Elshorbagy, 2008; R M Reynolds, 1993).

The assessment of the actual results does show a residual flow (daily data, averaged over 5 years integration period), directly connected with the baroclinic gradients in the area,

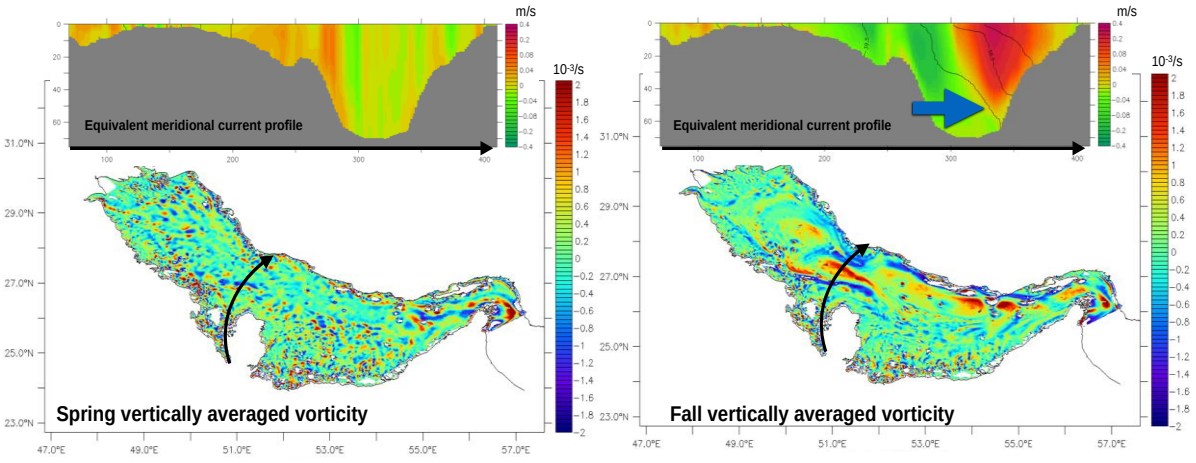

Figure 3-17: Vorticity (10^{-3}/s) from historical simulation (reduced by season). It shows the spatial and temporal scale of the mixing processes. Details above (meridional current profiles) show the vertical characteristics and maximum mixing depth (blue arrow).

disturbed or intensified by the wind field, as presented in Figure 3-18. This "residual" or equilibrium current field shows a remarkable pattern and clarifies the expected barotropic and baroclinic current system in the area, sustained by the density and sea level gradients balanced by the morphological characteristics in the area (Figure 3-18).

This horizontal recirculation is mostly affected by the frontal systems caused by the salinity gradients (time dependent mixing scale) and wind fields. However, the predominant Northwesterly wind is also important and plays different roles along the recirculation anticlockwise path.

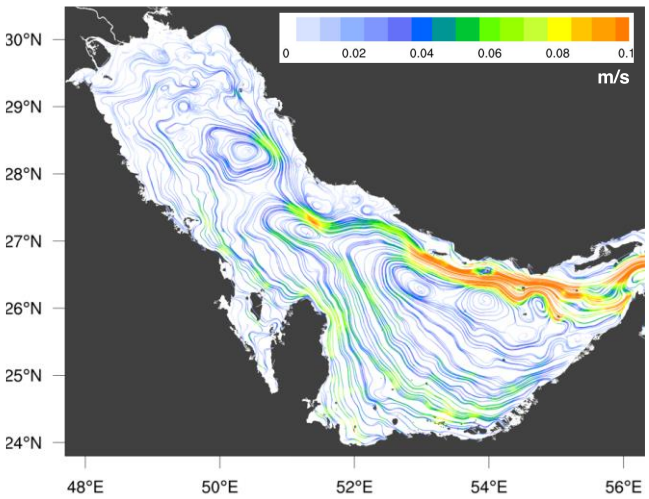

Figure 3-18: The historical residual current structure reproduced by the RCM at the Arabian Gulf.

Along Iran coast the wind reduces the AG water inflow. Offshore Qatar, the current jets observed by Reynolds (op. cit.) is fully explained by the combination of this system with the most frequent wind blowing in the same direction, southeastward. When the morphology forces the equilibrium current to east-west alignment (along Abu-Dhabi and Dubai coast), the Westerly wind component, although smaller, reinforces or revert the current system, creating the seesaw statistical systems reproduced by Figure 3-19.

Combining the information from Figure 3-18 and Figure 3-19, it is possible to disclose a general circulation system that comprises the entire AG, forming a recirculation low frequency system. On top of that: all the seasonal related mixing processes (periods from hours to days) and its related salinity frontal system and the wind fields that will locally intensify or reduce the averaged current system. The northernmost AG area also contributes to form a vertical recirculation, by increasing salinity (formation zone) and reducing the ocean temperature, mostly at wintertime.

4. Ocean Climate Projections

4.1 Long Term Run (LTR)

These experiments have used the combined historical and climate projection (RCP8.5 MPIMR - r1i1p1) experiments to create a unique and continuous dataset to force the RCM, at the ocean boundaries and surface, using bulk formulation to the atmospheric fluxes. No discontinuity is observed between historical and projected climate results, when those fields are jointed. Thus, the RCM setup experiments use the ESM forcing continuously.

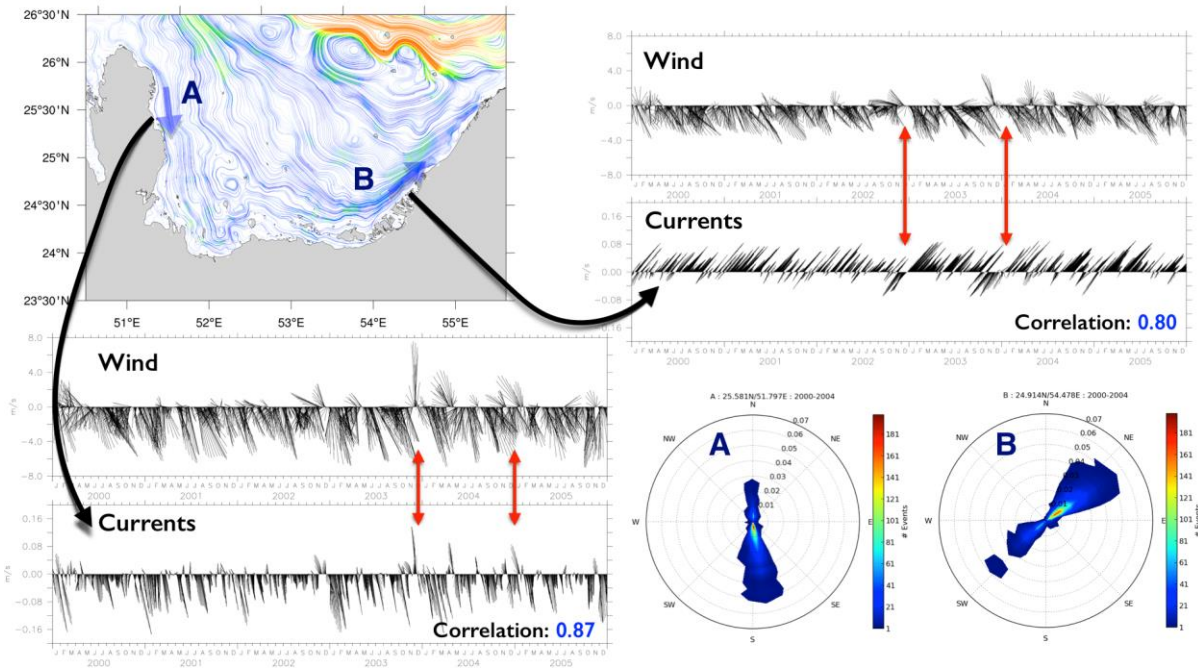

Figure 4-2: Coastal current jets and its spreading correlation with the GCM wind field.

It is important to notice that there are conceptual differences between the historical and the climate projections ESM setup. The first considers volcanoes activities, but the latter does not. Carbon dioxide (CO_2) affects precipitation, thus the fresh water fluxes could be also slightly affected because of the theoretical carbon cycle pathways used (RCP8.5). And finally, the climate projection's spectral radiation data used in the projected climate scenario are based on repeated cycles based on observation until 2008 (Giorgetta et al., 2013). Those are good approximation to the ESM model, but it is inevitable to infer that the ESM physics has been changed. Therefore, small local unbalances in the ESMs fluxes will be felt by the RCM in such small resolution. It implies the existence of short transients within the regional model, as further discussed.

4.1.1 *Time slices experiments*

This report presents the time slices periods from 2000 till 2020 and from 2080 till 2100, hereafter called *early 21st* and *late 21st* Century. Other experiments have been executed and are summarized in Figure 4-1. In addition, a mid-century experiment was undertaken after the long-term results were completed. A discussion of the mid-century results in provided in Annex 1 only.

The climate projection final data results reduced from the climag03c domain will be available to download and visualize in NetCDF format on a regular grid (*x*, *y*, *z, t*). The 1.1 km horizontal model resolution was reduced to approximately 2.8 km. The vertical resolution has been fixed

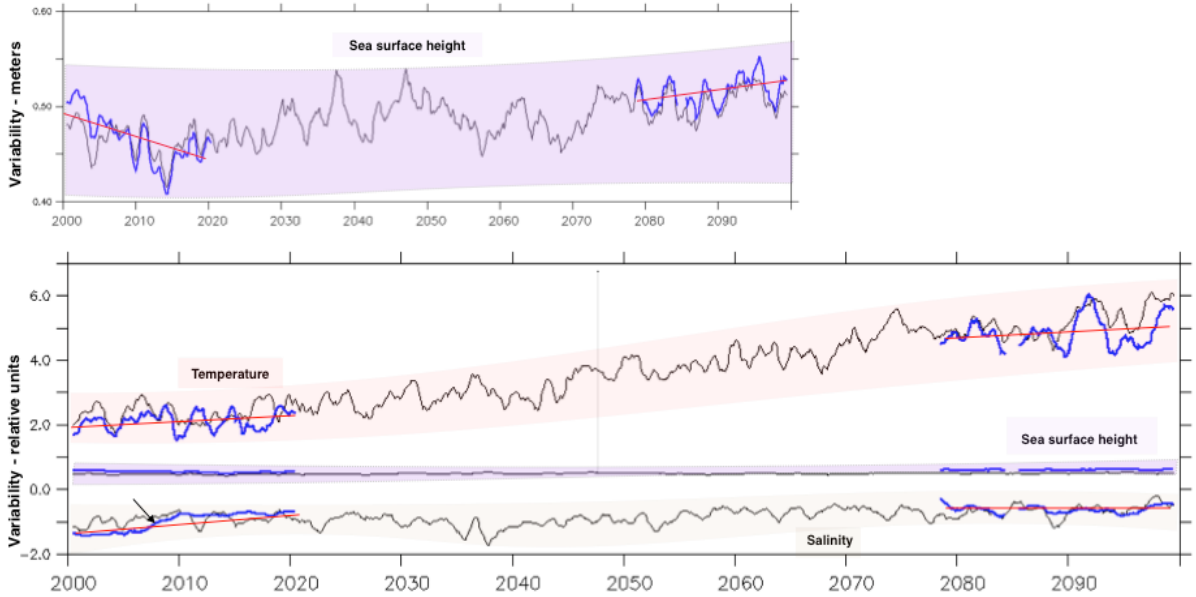

Figure 4-3: Normalized trends for surface temperature, salintiy and sea level. GCM in black, RCM results in blue and linear trends in red. Detail (up left) expands the SSH trends. Black continuous arrow point out salinity transition from historical to RCP differences.

at 5 meters, which means 20 levels, to maximum depth of 101 meters at the Hormuz Channel limits. The reduced spatial and temporal resolutions aims to easily make available to further analysis the RCM result.

4.2 RCM trends

To illustrate the simulations results and start to present the RCM we can examine in Figure 4-2 the area-averaged[4] trends for the time-slices. The data used in the trends analysis were monthly averaged (SST, SSS and SSH) and filtered to remove seasonal cycles (blue lines). In the same plots and considering approximated equivalent area and filters, the MPIMR average trends are also presented (black lines).

All the variables have been referenced to an initial averaged sample to evidence the trends and their relative proportions. The variability units were kept as the original dataset (^{0}C, PSU and meters, respectively). The detail (top left) expands the SSH trends for better visualization. The sea level is a large-scale barotropic variable imposed by the ESM on the ocean open boundary. That signal is combined with the RCM high-resolution internal dynamics that will basically search the equilibrium gradients. However, it is clear from Figure 4-2 that the low frequencies (periods above seasonal) are precisely trapped with the external forces.

Time fixed differences between ESM and RCM results have been arbitrarily removed to clear the plots. To further references, the real fixed differences values are (mostly related with the

[4] A centered area at Arabian Gulf, where the main contributions to the local dynamics rules, basically combines the shallow areas along Abu-Dhabi-Dubai coast and the adjacent channel, closer to the Iran coastline.

ESM salinity bias): 2.5 psu for salinity (less saline RCM), 1.5^{0}C for temperature (cooler RCM) and -0.1 meters (RCM oscillates in a higher level). Those results show both models in a general agreement in the trends, which is an obvious but important quantitative result, since the ESM provides the forces to the RCM.

The ocean temperature will be warmer by the end of the 21st century in both models (ESM and RCM), but the RCM shows a slightly less warm result. The salinity will be also smaller (on average) in the RCM, explaining the smaller temperature (these are thermodynamically coupled variables). The smaller salinity (2.5 bias from ESM) is also expected as the historical results (validation period) have shown. The net shortwave imposed by the ESM has not changed. There is also a bias observed in the RCM trends (black arrow on lower left of Figure 4-2), which is coincident with the ESM historical and projected transient. Because of that, we will focus as much as possible more sensitive analysis on the historical period, since it was fully validated.

4.3 Ocean Climate changes

4.3.1 *Thermodynamics changes in the RCM experiments*

It has been clear since the first validation experiments that the baroclinic patterns are predominant in the area, at least in the historical period assessed. Previous studies in the area, also evaluate these density gradient based on observation and modeling the area (W Elshorbagy, 2008; Kampf & Sadrinasab, 2006; Sultan & Ahmad, 1993; Swift & Bower, 2003) and the dense AG exchange with Oman Gulf and the Arabian Sea (Johns et al., 2003; S. P. Kumar & Prasad, 1999; S. Kumar & Prasad, 1999).

The temperature and salinity trends have been shown in Figure 4-2 normalized. The absolute differences observed between the early and late RCM scenarios provide knowledge about the local alterations due to global climate change. These variations can be perceived in static averages and difference maps between the early and late 21st experiments which are presented on Figure 4-3 for SST, SSS and SSH. The maximum differences will occur between the historical climatology and the last 5 years climatology, for the late 21st experiment, when all the atmospheric changes have settled down.

These results show an increase in three variables, which agrees with the trends observed in Figure 4-2. Temperature and sea level will increase everywhere, excepted for the central gulf area. This area concentrate the largest scale eddies (at summer) which implies in smaller local climate changes, since the dominant water mass is connected with the Arabian Sea. For the same reasons, the salinity decreases in the late 21st century along the deep channel. The salinity increase along UAE coast is most likely connected with the climate change in the local gulf dynamics, as further discussed. The gulf water's dilution process that appears in these

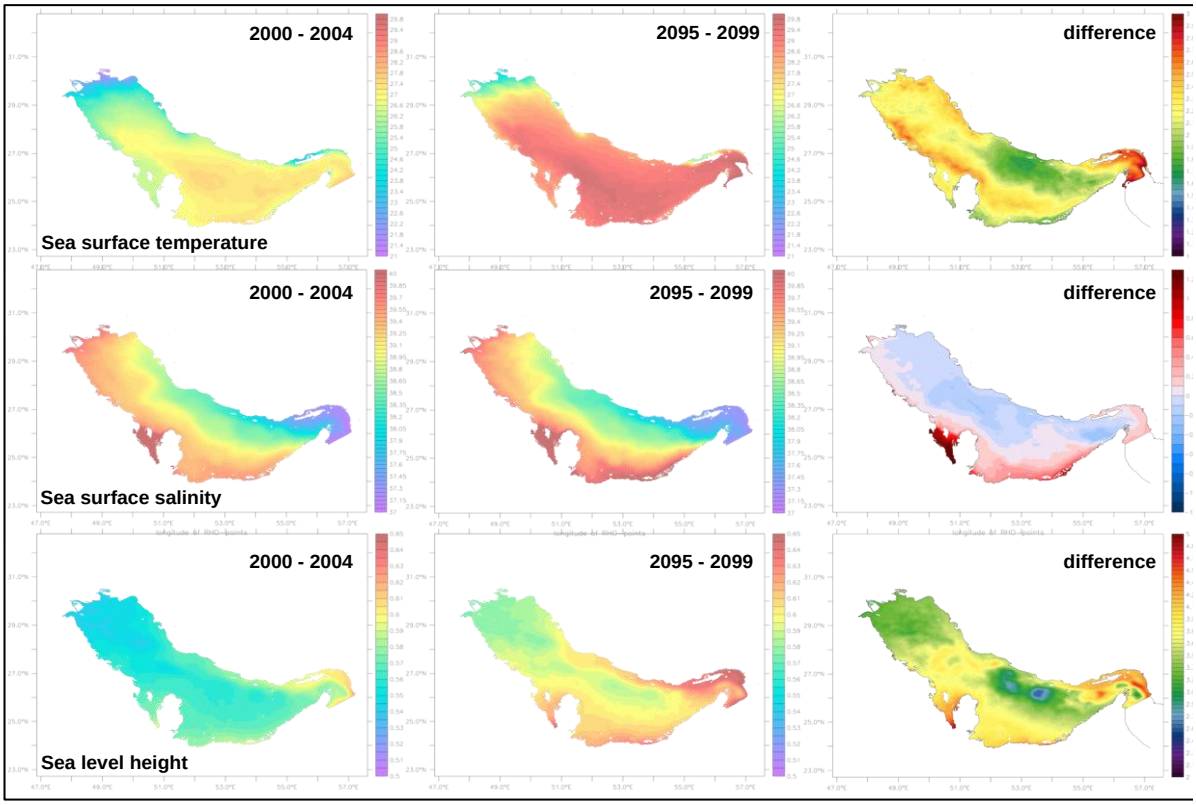

Figure 4-4: The first line show results for time averaged SST; the second line SSS; and the third line SSH. The first column is the average results for the early 21st experiment (2000-2005 climatology); the second column is the average for the late 21st experiment (2095-2099); and the third column is the difference between both experiments (Late 21st - Early historical 21st).

results does increase along the late 21st experiment, denoting a long term predominance of the RCP8.5 scenario conditions, warmer and wetter then early century conditions. By the end of 21st century, the salinity differences reveal a very likely progressive flushing of the high-density waters out of the system

The salinity profiles, from the difference between late minus early 21st century, do confirm the previous observed changes in the thermodynamic structures (Figures 4-4). The higher

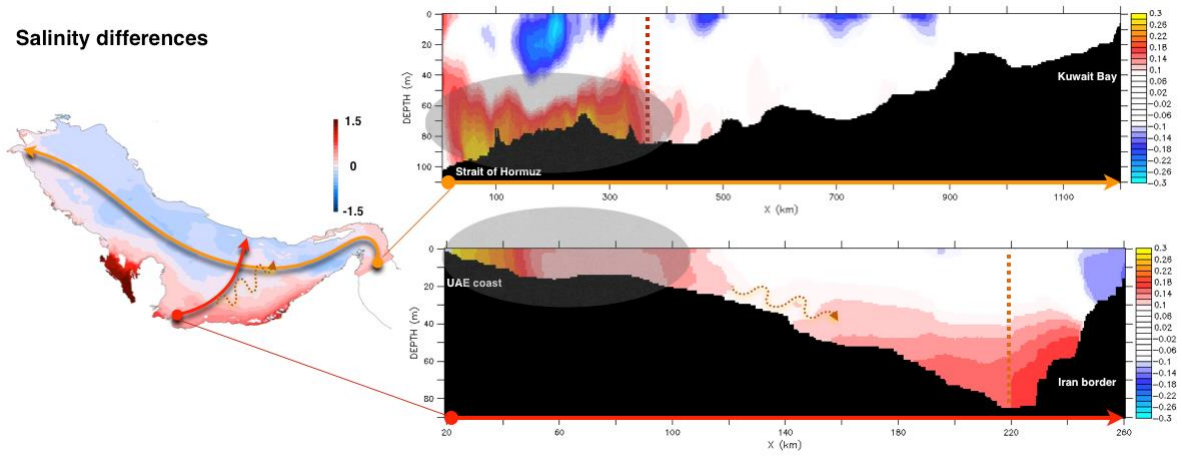

Figure 4-5: The vertical profiles for salinity differences between early and late 21st century climatologies. The dashed lines point out approximately the crossing point between the sections.

saline and warmer waters from late 21st will prevail at southern gulf zone, sinking to the deep channel in this area.

The question at this point is: what happens with the dense water formation zones? There is a very likely unbalance in the basic thermodynamic variables gradients in the area, as previously pointed out, bringing warmer waters to north and pulling salt to south. Aiming at first tracking on that changes the combined plots in Figure 4-5 (A and B) show the maxima and minima temperature (A) and salinity (B) spatial distribution with the previous cooling and salt water formation zones, for both experiments.

The northernmost saline area was clearly diluted by the increase of the open seawater inflow, which seems to have opposite effect on the coastal formation zones, e.g. UAE coast line. Temperature increases everywhere, but from the differences plot (Figure 4-3) mostly along the coast. The northernmost warming by the end of 21st century (Figure 4-5A) does have a potential to change and explain the dynamic changes. To clarify that point, Figure 4-5C shows the annually averaged density in the historical cooling zone as presented in the downscaling section. It shows that, the late 21st scenario general characteristics (sea water warming and dilution) directly change the density structure spatially and along time, reducing the natural descending high salinity flux to the deep channel.

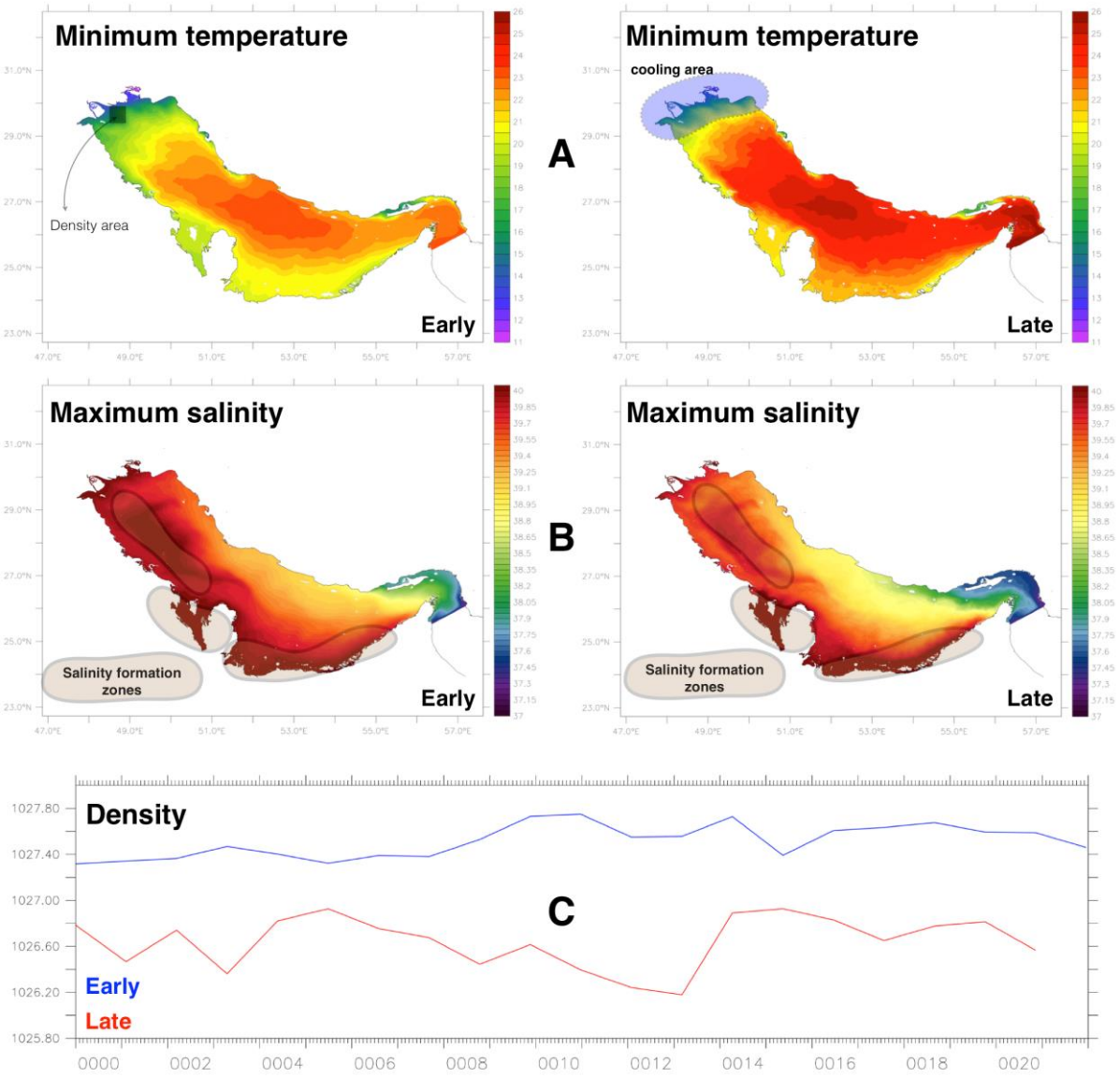

Figure 4-6: A complementary view for the scenario differences earlyer presented. The anual maxima and minima, averaged to the whole experiments. It shows the spatial changes in the main patterns observed to the area (A and B). The C sub-plot shows the anually density averaged, reduced to a generic time axis. The area is refered in the A line, left plot.

Another local climate changes effect in the AG thermodynamics is highlighted in Figure 4-6. There are expected changes in the overturning pattern, since all the equilibrium between the external flux entrainment in the area, the dense water subsidence at north and the northernmost dense water formation zone have been affected. The assessment of these results clearly point out to a substantial mass transport change and redistribution in the

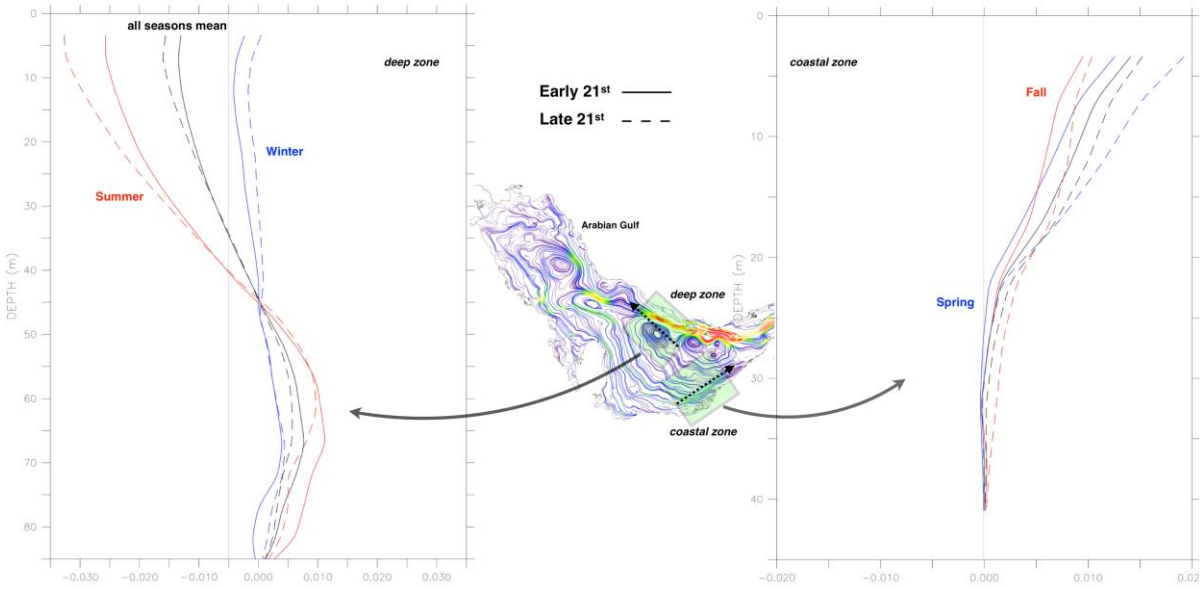

Figure 4-7: Early (up) and Late (down) climatological seasonal net transport. The map shows the reference areas (legends). The red arrows point to the largest changes observed between the periods.

balance between the internal and atmospheric forces acting in the area, as we start do discuss in the next topic.

4.3.2 *Ocean dynamic changes*

The results up to this point indicate a very likely freshening of the AG system, despite the general increase of the ocean temperature. It suggests changes in the internal dynamical overturning process and very local specific changes, which we investigate, using as baseline, the dynamics obtained with the current model setup.

Changes in the circulation dynamics are related to the salinity changes discussed, since it drives most of the internal baroclinic balances and mixing processes in the AG. There is an evident increase in the overturning and mixing process. It is observed by the net transport in specific areas, where the circulation is known (Figure 4-6). The reference axis in Figure 4-6 (center) was rotated to align with the local preferential direction. These changes in the overturning speed happen unevenly in time, depending on season.

Also observed is a systematic increase in the mass transport in the late 21st experiment (black continuous and dashed lines, Figure 4-6) is sustained yearlong. Intriguingly, the transport extremes happen in different seasons in the channel (deep zone, left side) and in the shallow areas (coastal zone, right side). This behavior suggests that, in the channel prevails the offshore seasonal cycle. On the other hand, in the coastal zones, the combination of the advection by wind and density gradients are likely more significant. Figure 4-6 also shows that

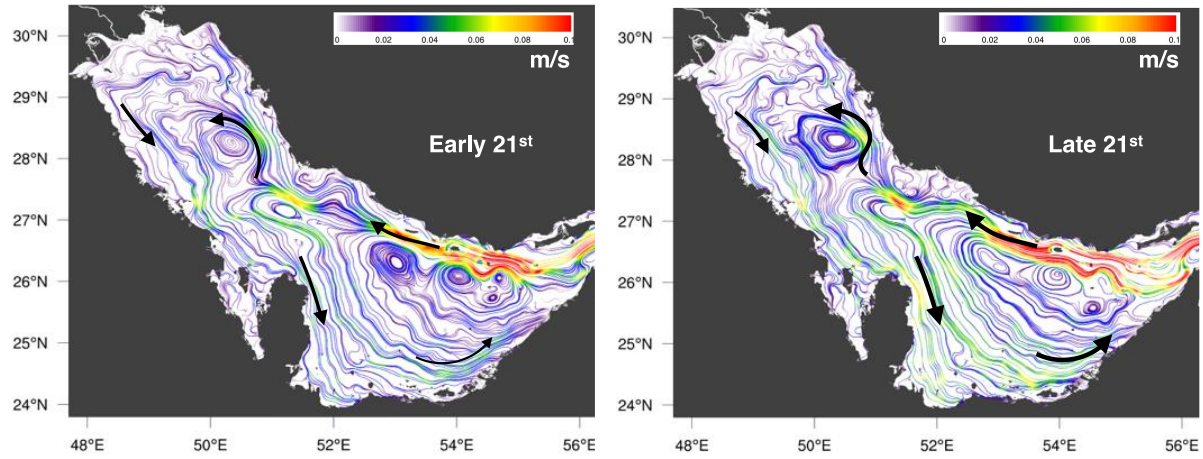

Figure 4-8: Residual current streamlines at surface layer, early and late 21st century.

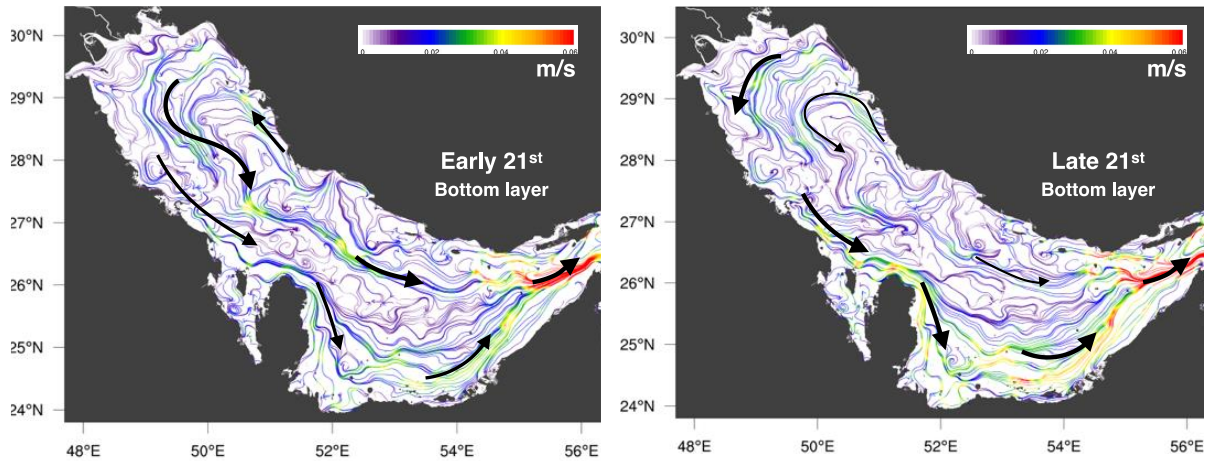

Figure 4-9: Residual current streamlines at bottom layer, early and late 21st century.

the bottom transport (southeastward) the late 21st century is smaller, when compared with results of the beginning of the century. It can be better understood observing the time averaged (hereafter, residual current) in Figure 4-7 and Figure 4-8.

The dynamics underneath the baroclinic structure previously presented can now be better understood. Left side panels from Figure 4-7 and Figure 4-8 respectively reveals that averaged flux for the early 21st century is less intense. The dense water flux out of the AG is balanced between shallow waters and the deep center channel.

On the right side panels there is a change in the dense water fluxes. It is increased at surface over all the Southern Gulf area. At the bottom, the deep channel dense water flux is reduced, moving towards the shallow southern zones.

Combining the information from thermodynamic variables and last results above, we are able to list the following conclusions about the changes in the ocean circulation pattern:

- The salinity by the end of the century still is the most important variable that defines the internal circulation. The balance between the cooler temperatures zone at the northernmost gulf area and the high natural salinity is not sustained.
- The high saline waters from the northern areas are partially redirected to south at upper layers, reaching the shallow zones below Qatar. It will result in an increase in the mass flux intensity and, of course, in the salinity local balance.
- It is also possible to observe the strengthen in the Arabian Sea inflow, that will reach the gulf northern areas and contributes to a long term freshening of the average salinity, as observed in the late 21st trends, presented in Figure 3-14. The freshening is related to an increasing the precipitation, imposed in the RCM from the MPIMR dataset. The increase of the precipitation is a very likely climate change outcome for the area, as described in Sandeep & Ajayamohan (2014).
- A reduction in the overturning periodicity is a very likely consequence from these dynamic changes. It is also expected that the freshening process will increase the AG intake to the external less dense flows (lighter waters).

4.4 Others climate changes in the Arabian Gulf

Another important aspect to assess the AG dynamics and consequently the possible changes with a regionalization for global warming effects is the mixing process.

4.4.1 *Turbulent changes*

The mixing processes in the AG, identified by the current RCM setup, mostly happen by means of fingering and turbulent mixing. The small-scale fingering does couple the barotropic and baroclinic dynamic patterns, and had directly effects on the modeling performance. For example, this coupling reduces dramatically the model time step, especially for the late 21st experiments, when the energy of the ocean system rises internally. This type of mixing is solved internally by the configured model turbulent closure scheme (Large, Mcwilliams, & Doney, 1994) and includes all the forces that will create instabilities in the water column.

The sinking of dense (saline) waters is captured by the model when the surface high salinity waters gets unstable and progressively sink directly to the channel, forming fingering type of structures, that will flow to Hormuz strait.

To evaluate the local climate change impacts, the comparison between the early and late climatology rotational fields are presented on Figure 4-9 for the two most significant seasons. The zonal current profiles to the same period are also presented in Figure 4-9. Eddies are

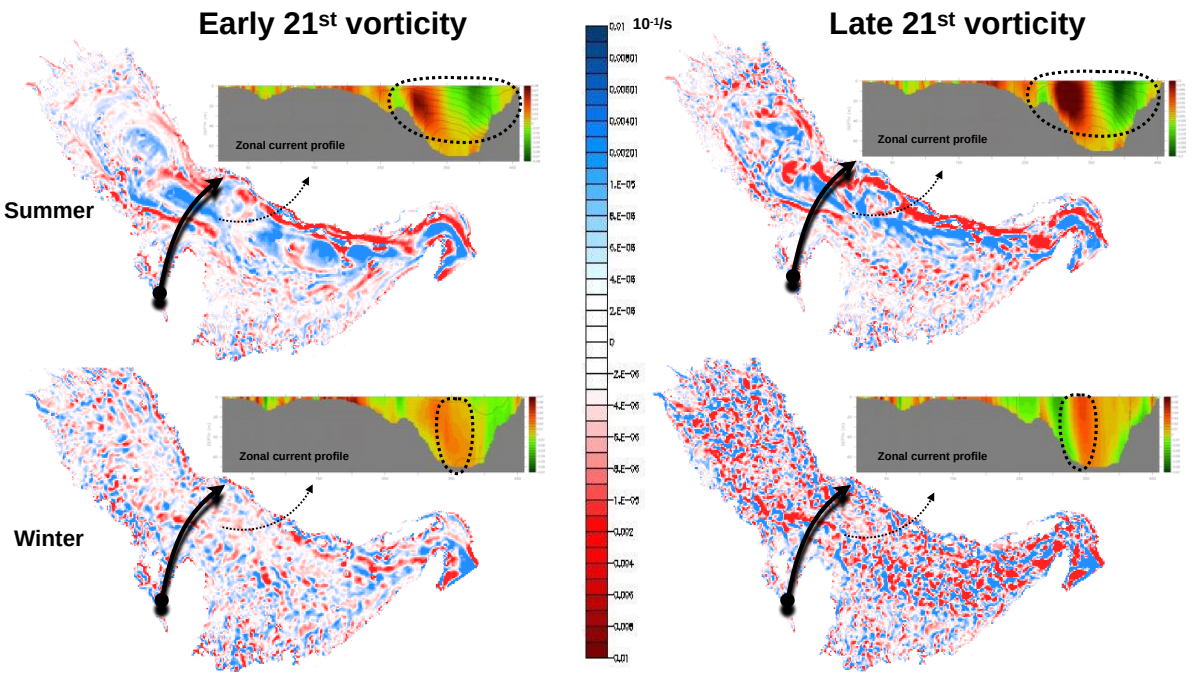

Figure 4-10: Arabian Gulf vorticity to early and late 21st century climate runs. Results were based on climatology. Details show the corresponding current zonal current profile. The scale (1/s) is the same for all the vorticity plots.

directly connected with the water column stratification and stability. Figure 4-9 dashed contours shows the summer eddies are still trapped by the bottom salinity structure.

These results reveal and connect the increase of the overturning kinetic energy with a decrease in the small scale eddies average periods (order of minutes, shade center scale). The summer pattern does change the larger scale eddies, directly connected with the Arabian Sea low salinity inflow waters (shadow -white areas - between higher frequency eddies). In the north, in the late 21st summer vorticity map, it is also possible to observe that the previous (early) white areas (low vorticity) have been replaced by high frequency eddies. This explains partially, how the warmer late 21st conditions have affected the northernmost dense water formation zone.

4.4.2 *Wind driven changes*

Historically in the area, the wind effects on the ocean dynamics are significant (W Elshorbagy, 2008; Thoppil & Hogan, 2010c). The wind advection is noticed along shallow areas, where the seawater has little or no stratification and also along the Gulf's Channel, where it dumps the fresh water entrainments.

However, the MPIMR wind slightly decreases its average magnitude along the century (Figure 4-10) for the RCP8.5 scenario. The wind keeps the predominant signal alight with the

Northwest-Southeast direction, but the averaged intensity reduces along the century because the Northwesterly winds and Southwesterly frontals systems. It is time to remember that, these results are originated from an ESM model that does not have resolution enough to fully perceive regional morphology, as the Zagros Mountains. IPCC's models do have a common sense climate change to the area where are expected changes in the Indian Ocean dipole (Weller & Cai, 2013) and in a Northward migration of the monsoon related signals (Sandeep & Ajayamohan, 2014).

The AG waters is a low frequency gyre system (the overturning) and the historical winds have a Southeastward predominant direction (Elshorbagy et al., 2006; Perrone, 1979; Reynolds, 1993). The combination of both systems will increase the shallow and high saline coastal flow southward and reduce the northward low saline waters from Arabian Sea. Despite the different dynamics, these effects on the advection are clearly seen on Figure 4-6 where the northward averaged vertical transport is damped at surface and the southward increases.

A conclusion from above analysis is that, despite the decrease in the wind-averaged intensity along the century, the wind does play an import, although smaller, role in the general AG circulation system, as previously described.

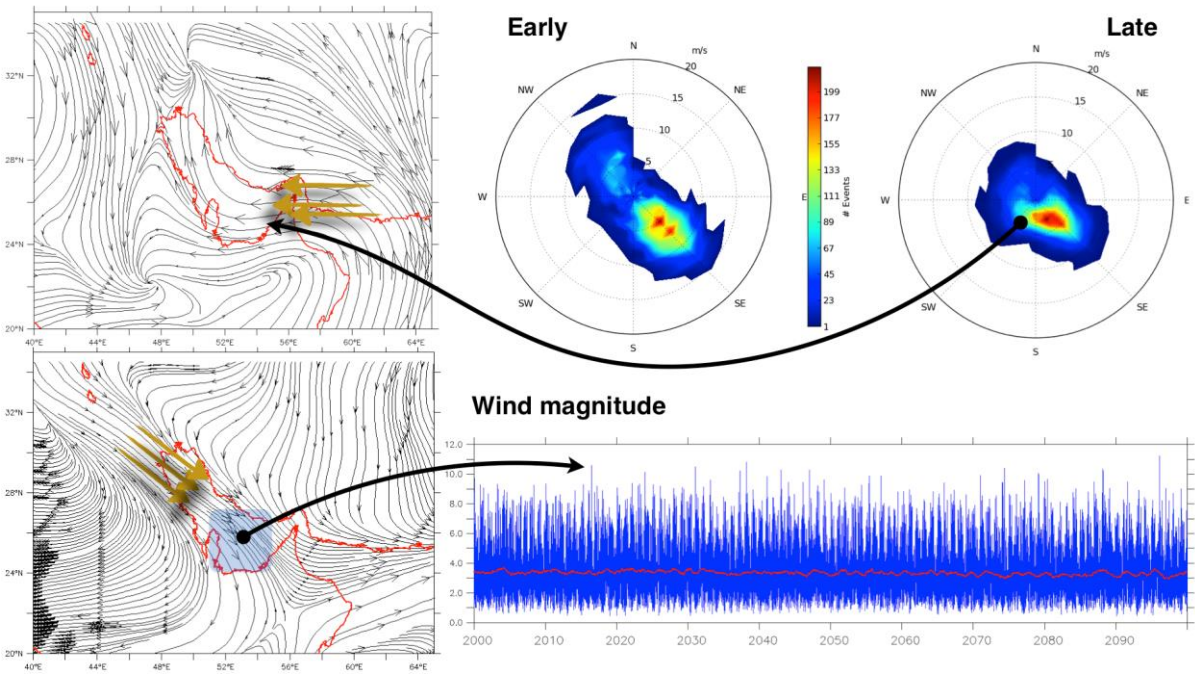

Figure 4-11: The ESM wind pattern changes reproduced by the MPIMR in the area. The left is the wind streamline snapshot, to exemplify the changes observed in the wind field. The right top plot presents the wind intensity (averaged in the box area) and the 2 right left polar histograms shows the cumulative early and late events (wind directions follows vectorial convention.

The localized effects of the wind changes are more evident at the shallow areas, where the coastal jets are well defined as described by Reynolds (1993) along Qatar coast. These events are very constrained in space. Even so, the RCM model reproduces these coastal currents, based on a combination of density gradients and wind forces. Those "jets" were previously analyzed, showing a good correlation with the wind, especially with reversions in the wind system (Northward winds).

The global climate change effects in these local patterns can be observed in Figure 4-11, where two points are analyzed, the Qatar jet and the Coastal UAE to assess the wind changes effects on the local circulation.

The reduced Northwesterly wind intensity and the increase on the Southwesterly wind components are evident on the late 21st results to points A and B. The point A, there is a general decreasing on current intensity (the Southerly direction). Point B shows amplification on both preferential current directions, which evidence the changes carried out by the Southwesterly wind by the end of the 21st century.

Although very concentrated at the coastal zones, the changes (amplification and spreading) of this current system are important, because it will contribute to the salt transport balance in the UAE zone. It implies that the RPC8.5 scenario has created conditions to a new dynamic balance, including on local scale. The present consideration is a hypothesis, but explains how the dilution process, would spread out south, or the opposite, increasing the dilution time to the area.

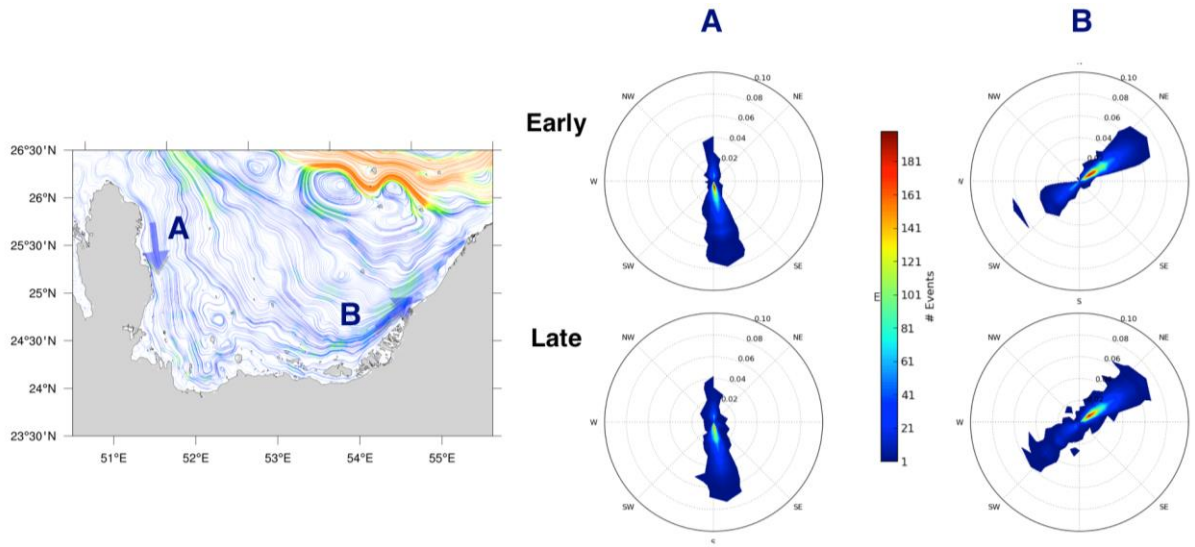

Figure 4-12: Qatar (A) and UAE (B) coastal jets. The left shows the residual current and the reference areas. The polar histograms on the right show the cumulative frequency of the current at the A and B positions, for the early and late 21st cases.

4.4.3 *Sea level changes*

Dynamic Sea Level (DSL)[5] variable from the MPIMR ESM was used to force the RCM ocean open boundary. The approach used is described at IPCC's sub-section 13SM (J.A. Church & Clark, 2013). Results from MPIMR were used to evaluate DSL globally. The DSL global averaged results (Yin, 2012) are reproduced in Figure 4-12. The global sea level changes are composed by modeled variables and parametric assessment projections, which includes, for example, melting of glaciers, ice sheets (Greenland and Antarctic), land water storage, tectonic movements, etc. (J.A. Church & Clark, 2013; Griffies & Greatbatch, 2012).

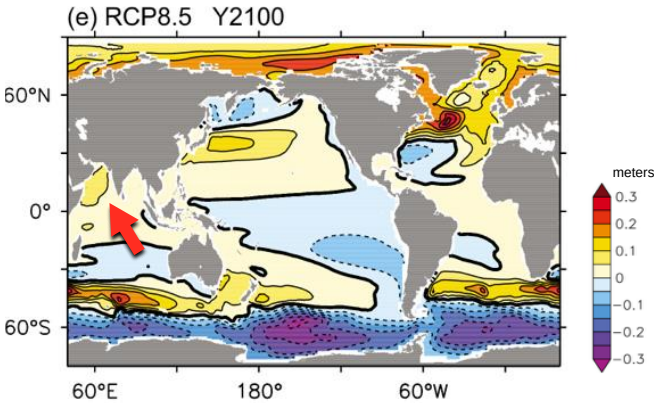

Figure 4-13: Ensemble Global averaged Dynamic Sea Level (DSL), for the year 2100, based on RPC8.5, extracted from Yin (2012).

The Global Mean Sea Level (GMSL) is composed by the DSL, the thermosteric sea level, and the land-ice sea level contributions, as shown by the red line in Figure 4-13 (J. A Church & Clark, 2013). As noted by Church & Clark (2013): "…Ocean thermal expansion and glacier melting have been the dominant contributors to 20th century global mean sea level rise. Observations since 1971 indicate that thermal expansion and glaciers (excluding Antarctic glaciers peripheral to the ice sheet) explain 75% of the observed rise (high confidence)…" (J.

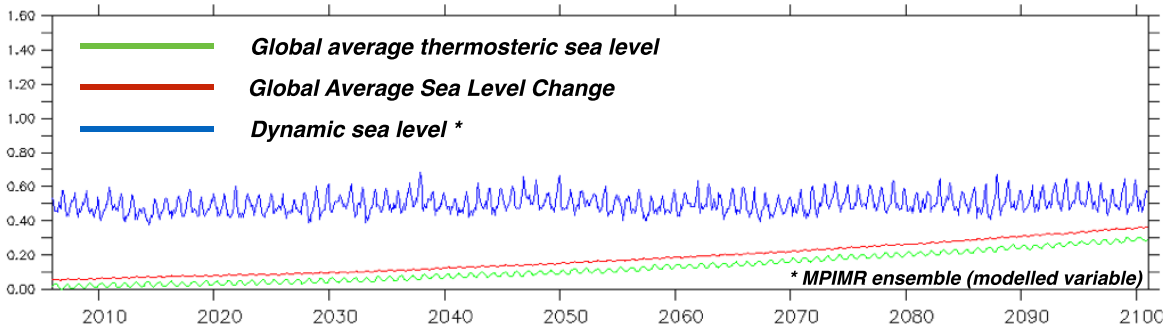

Figure 4-14: Dynamic sea level (DSL) and the AR5 global averaged Sea Level components (meters)

[5] Dynamic sea level (DSL) refers to the sea level related with the dynamic of the ocean and modeled based on ocean physics formulation, i.e. ocean currents, density, and boundary fluxes of mass."…There is presently no global numerical model that incorporates all of these effects impacting sea level. In particular, climate models presently provide an estimate just of dynamic sea level…" (Griffies & Greatbatch, 2012)

A Church & Clark, 2013). Those variables are available in any IPCC ensemble member as global mean time series as presented in Figure 4-13 and will be available to access, as the post-processed RCM results.

The DSL, which includes the local sea level reference from the geoid, is usually the modeled variable. And as so, used to force the RCM along Hormuz open boundary. The DSL, combined with the atmospheric forces and the density gradients forms a stable structure during summer and fall seasons, that is presented on Figure 4-14, averaged along the 21st experiment results.

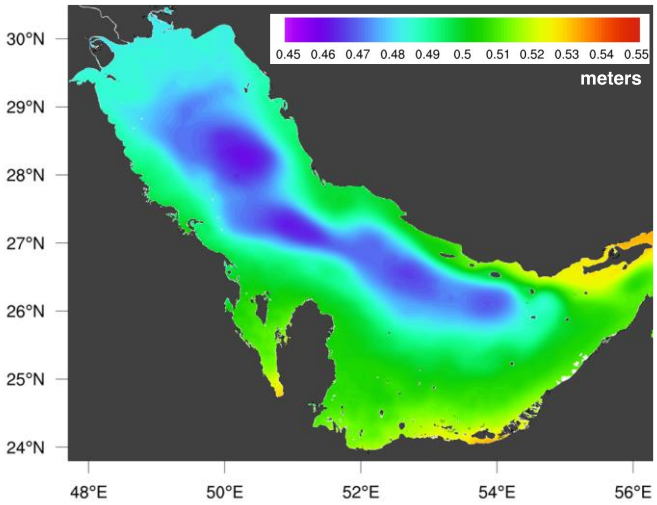

Figure 4-15: It shows the seasonal averaged (summer centered) distribution of the sea level height for the early 21st period.

The composed 10 cm gradient observed between the AG center and its borders and the 4 cm averaged due to 21st late climate change (Figure 4-3) is not the most important mean sea level variability if compared with the expected (projected) changes related to glaciers, ice sheet melting and ocean thermal expansion (Figure 4-13).

However, this 4 cm change is the AG barotropic natural response to the DSL and global warming changes, that will reduce the overturning cycle period and the fresh water intrusion from Arabian Sea, as previously evaluated.

The average centered in summer period is presented here because it represents the maximum large-scale (to the AG) structure observed. Because it is an AG barotropic natural response, minimum sea level along the AG center, that structure is quite similar to the Amphidromic circulation formed by the tidal forces in the area, therefore composing both signals.

4.4.4 *Water masses changes*

The fully reduced climatology presented in Figure 4-15 aims to illustrate another local effect of the climate change, reproduced by the RCM. The areas 1 and 2 are the surface averaged reference (right plot). There is a very likely expectation that the RCP8.5 warming changes does increase the ocean summer period, as the winter water temperatures rise. It is probably connected to the enhancing of the barotropic mixed processes or it could be directly related to the equivalent extended summer in the atmospheric fluxes. It does require specific experiments and analysis to better track its causes.

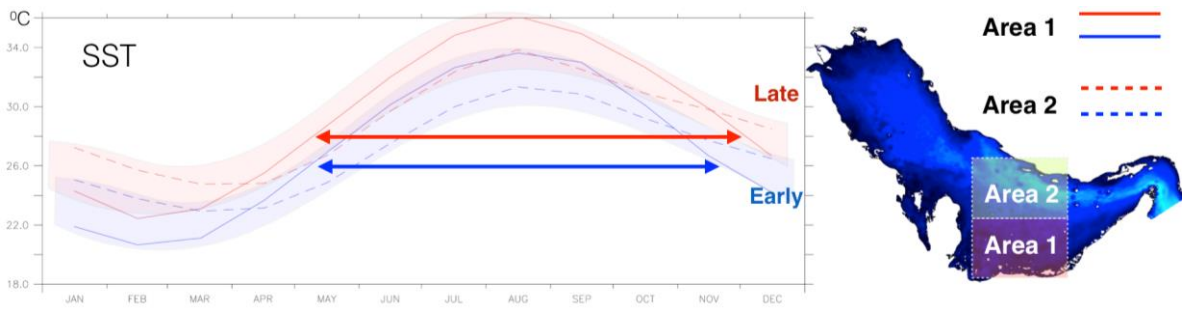

Figure 4-17: SST climatology to shallow & deep zones (areas 1 and 2, respectively). The red (blue) color indicates late (early) 21st experiment. Arrows shows the mid height time duration of the summer season.

Another useful analysis to assess the climate change effects in the AG is the Temperature-Salinity Diagrams (TS Diagrams). They were focused on a central area at AG, where both shallow and deep-water dynamics are noticeable. Figure 4-16 shows the RCM results for early and late experiments, reduced to a monthly averaged data. This analysis exposes the water masses movements and characteristics. It captures the seasonal cycle, the spreading for each season and also indicates the climate change effects by the end of 21st century (RCP8.5). The arrows (Figure 4-16, right) emphasize the displacement observed. The salinity spreading on the right side plot (Figure 4-16) also corroborates and shows the effects of the small-scale vorticity mixing processes over whole the gulf area.

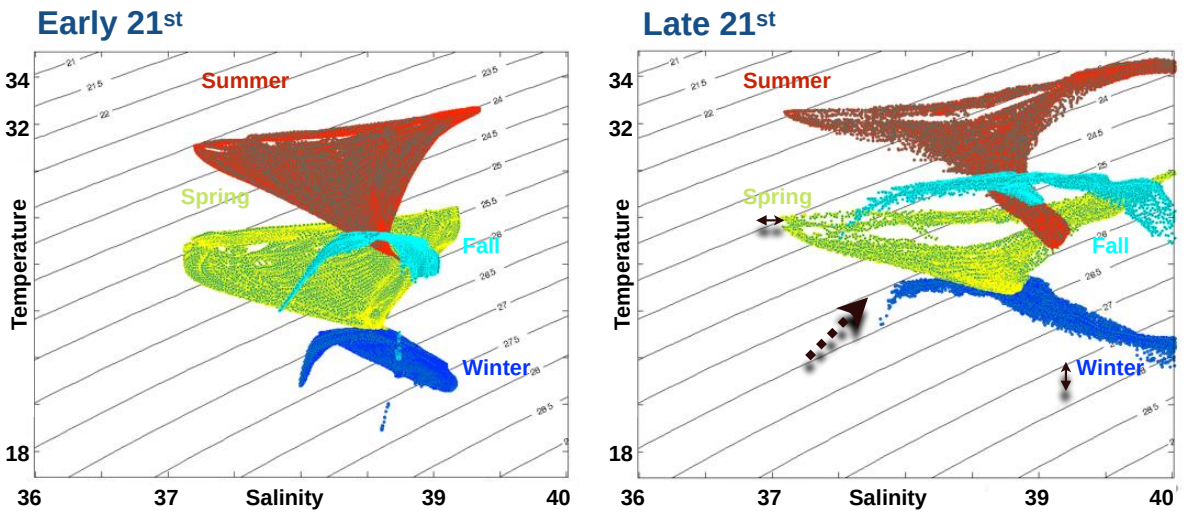

Figure 4-16: TS diagrams for early and late 21st century, monthly averaged data. The dashed arrows indicate the expected averaged warming in the water column.

The temperature and salinity ground truth data is relatively small to evaluate localized water mass. But, broadening the sample area (Figure 4-17, the dataset (WOA13) are statistically

significant and relatively recent (last update in 2013) to delineate the expected observed water mass structure in the gulf area.

The respective TS diagram is presented on Figure 4-17. There are of course a lot of spreading and noise results, since the data do not have an even and synchronized sampling over the gulf. The seasonal cycle and temperature scales are comparable with the early 21st results (Figure 4-16, left). The salinity field makes clear the initial assumption made on the project. The RCM is initialized and forced by the ESM that will provide the global climate changes fields based exclusively on carbon related warming, including the anthropogenic sources of the greenhouse gases. However, it does not include any land use related activity important in the area. The desalination plants (Barwani et al. , 2008; Bashitialshaaer et al., 2011; Lattemann et al., 2008; Mohamed, 2009), which are a really important source of salinity to the AG, or, negative fresh water fluxes on the point of view of the ocean modeling.

The dashed arrow on Figure 4-17 emphasizes the expected differences between the baseline climate results from the RCM and the real salinity fields observed in the area till 2013 (notice the axis does not have the same salinity scale).

As a final conclusion on this analysis, the likely freshening process reproduced by the RCM and discussed here, pends on the increase of precipitation, increase of sea water temperature, a relatively stable wind field and a increase in the small scale turbulent mixing processes. All those changes combined have reduced the salinity strengthen in the local dynamics, which, as consequence, reduces the natural system impedance to the open ocean

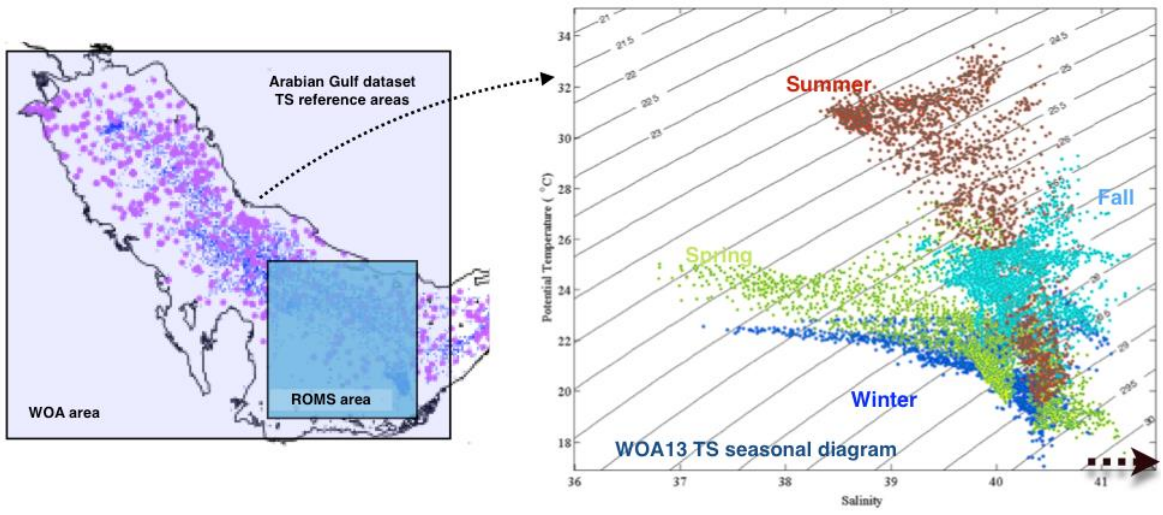

Figure 4-18: Left: WOA13 dataset positions and the reference area to TS analysis. It also includes the RCM dataset area, TS presented in Figure 4-10. Right: TS for the WOA13 dataset at Arabian Gulf.

freshwater inflow. Because of the scale of the human activity in the area, the desalination plants will very likely change the imbalance reproduced here, based only on natural sources.

5. Conclusions and recommendations

The Max Planck Institute mixed resolution ESM (MPIMR) was chosen to force our regional climate model (RCM). This choice was made after testing and selecting among several CMIP5 models, the one that best fits for our region of study.

5.1 Major findings

The RCM has shown high accuracy and skills to reproduce the local dynamics, even compensating the salinity bias observed in the MPIMR results, which gave us confidence to investigate the impact of the 21st Century climate projections.

The ESM atmospheric forces show by the end of 21st century, a high increase on temperature, small increase on precipitation and humidity, slightly decrease on the Northwesterly winds intensity (Shamal) and a small intensification on the Easterly wind component.

To look at the variations due to climate changes, two specific periods are investigated through time-slices: Early 21st and Late 21st Century. The final analysis of these results yields the following conclusions:

The overturning circulation in the Arabian Gulf changes from one period to the next. This change indicates a long-term freshening, rendering an asymmetric salinity distribution along the Gulf. There is an increase in the average temperature together with an increasing small-scale vertical mixing processes (mostly at northern areas), which partially disrupts the overturning cycle, transferring the deep southward transport to the surface. This process decreases the associated deep density salinity gradients along the deep channel, increasing the entrainment of lighter less saline waters from the Arabian Sea.

On the other hand, the entrainment of fresher from the Arabian Sea increases the larger central eddies. To the North, where the fast mixing processes have enhanced intensity, the less saline waters enter directly into the circulation system contributing towards further freshening.

The physical mechanism associated with the freshening is linked to the increase in the overturning mass transport. This fresh northward mass transport increase is partially damped by Northerly winds, which present weakening trends because of the displacement of the large-scale Indian Ocean monsoon systems.

5.2 Further research directions

Numerical modeling is a complementary tool to field observations and theoretical knowledge for an area. A specific modeling approach does not disclose all the possibilities to evolve the scientific knowledge in a specific problem. The present yearlong research study about the downscaled climate changes at the AG has left some insights about very interesting research themes, which remain still to be explored in the area.

The improvement in the spatial and temporal atmospheric fields forcing fields does always improve the ocean model skills to reproduce local phenomena. During the present project execution, some of the results from the parallel Atmospheric Downscaling project have been used, mostly to fine-tuning the MPIMR coarse resolution atmospheric fluxes.

The currents experiments outline a very likely dynamical change in the Arabian Gulf due to global warming. These dynamical aspects require permanent updates regarding the future ESMs next generation. Reviews from the present results based on the current CMIP5 climate change scenarios will also enlightening the knowledge about this area and, for sure, increasing the statistical meaning from the present results.

From the conclusions and findings presented here, it is quite clear the need to include salinity sources from the desalinization plants in the model dynamics. These plants, on first approximation, may have a significant impact on the AG circulation, if considered as salt sources. There are complex topics to address before any effort to a proper modeling of this magnitude, but definitely it is a very important research focus for further climate change prospections in the area.

Large-scale phenomena could also be considered as a relevant scientific topic to evaluate. The Indian Ocean Dipole effects in the AG area, for example. Because the spatial and temporal scale, this is a research topic that could be directly investigated within the CMIP5 models.

6. Bibliography

Amante, C., W, E. B., & Eakins, B. W. (2009). *ETOPO1 1 Arc-Minute Global Relief Model: Procedures, Data Sources and Analysis*. *Vasa* (Vol. 4506, p. 25).

Barwani, H. H. Al, & Purnama, A. (2008). Evaluating the Effect of Producing Desalinated Seawater on Hypersaline Arabian Gulf. *European Journal of Scientific Research*, *22*(2), 279–285.

Bashitialshaaer, R. A. I., Persson, K. M., & Aljaradin, M. (2011). ESTIMATED FUTURE SALINITY IN THE ARABIAN GULF , THE MEDITERRANEAN SEA AND THE RED SEA CONSEQUENCES OF BRINE DISCHARGE FROM DESALINATION. *International Journal of Academic Research*, *3*(1), 133–140.

Church, J. A., & Clark, P. U. (2013). *Sea Level Change* (pp. 1–8). IPCC-AR5 - Suplementary Material Sea Level Change. Retrieved from www.climatechange2013.org

Church, J. A., & Clark, P. U. (2013). *Sea Level Change*.

Danabasoglu, G., Bates, S. C., Briegleb, B. P., Jayne, S. R., Jochum, M., Large, W. G., … Yeager, S. G. (2012). The CCSM4 Ocean Component. *Journal of Climate*, *25*(5), 1361–1389. doi:10.1175/JCLI-D-11-00091.1

DERCOURT, J., ZONENSHAIN, L. P., RICOU, L.-E., KAZMIN, V. G., PICHON, X. LE, KNIPPER, A. L., … BIJU-DUVAL, B. (1986). GEOLOGICAL EVOLUTION OF THE TETHYS BELT FROM THE ATLANTIC TO THE PAMIRS SINCE THE LIAS, *123*, 241–315.

Elshorbagy, W. (2008). OVERVIEW OF ARABIAN GULF HYDRODYNAMICS AND ITS CIRCULATION CONDITIONS. In *COPEDEC VII* (pp. 1–16). Dubai, UAE.

Elshorbagy, W., Azam, M. H., & Taguchi, K. (2006). Hydrodynamic Characterization and Modeling. *Journal of Waterway, Port, Coastal and Engineering*, (February), 47–57.

Emery, K. O. (1956). Sediments and Water of Persian Gulf. *AAPG Bulletin*, *40*. doi:10.1306/5CEAE595-16BB-11D7-8645000102C1865D

Giorgetta, M. a., Jungclaus, J., Reick, C. H., Legutke, S., Bader, J., Böttinger, M., … Stevens, B. (2013). Climate and carbon cycle changes from 1850 to 2100 in MPI-ESM simulations for the Coupled Model Intercomparison Project phase 5. *Journal of Advances in Modeling Earth Systems*, *5*(3), 572–597. doi:10.1002/jame.20038

Griffies, S. M., & Greatbatch, R. J. (2012). Physical processes that impact the evolution of global mean sea level in ocean climate models. *Ocean Modelling*, *51*, 37–72. doi:10.1016/j.ocemod.2012.04.003

IPCC, I. P. on C. C. (2013). *CLIMATE CHANGE 2013 The Physical Science Basis* (p. 27). Retrieved from http://www.climatechange2013.org/images/uploads/WGI_AR5_SPM_brochure.pdf

Issa, I. E., Sherwany, G., & Knutsson, S. (2014). Expected Future of Water Resources within Tigris-Euphrates Rivers Basin , Iraq. *Journal of Water Resources and Protection*, *6*(April), 421–432.

Jeffrey, S., Rotstayn, L., Collier, M., Dravitzki, S., Hamalainen, C., Moeseneder, C., … Syktus, J. (2013). Australia's CMIP5 submission using the CSIRO-Mk3.6 model. *Australian Meteorological and Oceanographic Journal*, *63*, 1–13.

Johns, W., Yao, E. F., Olson, D. B., Josey, S. A., Grist, J. P., & Smeed, D. A. J. (2003). Observations of seasonal exchange through the Straits of Hormuz and the inferred heat and freshwater budgets of the Persian Gulf. *Journal of Geophysical Research*, *108*(C12), 3391. doi:10.1029/2003JC001881

Johnson, D. R., Garcia, H. E., & Boyer, T. P. (2013). *WORLD OCEAN DATABASE 2013 TUTORIAL*.

Kampf, J., & Sadrinasab, M. (2006). The circulation of the Persian Gulf : a numerical study. *Ocean Science*, *2*, 27–41.

KNUTSON, T. R., SIRUTIS, J. J., Vecchi, A., Garner, S., Zhao, M., Kim, H.-S., … Villarini, G. (2013). Dynamical Downscaling Projections of Twenty-First-Century Atlantic Hurricane Activity : CMIP3 and CMIP5 Model-Based Scenarios. *Journal of Climate*, *26*. doi:10.1175/JCLI-D-12-00539.1

Kumar, S. P., & Prasad, T. G. (1999). Formation and spreading of Arabian Sea high-salinity water mass. *Journal of Geophysical Research*, *104*(1998), 1455–1464.

Kumar, S., & Prasad, T. (1999). Formation and spreading of Arabian Sea high-salinity water mass. *Journal of Geophysical Research: …*, *104*(C1), 1455–1464. Retrieved from http://onlinelibrary.wiley.com/doi/10.1029/1998JC900022/full

Large, W. G., Mcwilliams, J. C., & Doney, S. C. (1994). OCEANIC WITH VERTICAL MIXING : A REVIEW LAYER AND A MODEL A NONLOCAL BOUNDARY. *Reviews of Geophysics*, *34*(94), 363–403.

Lattemann, S., & Höpner, T. (2008). Environmental impact and impact assessment of seawater desalination. In *Desalination* (Vol. 220, pp. 1–15). doi:10.1016/j.desal.0000.00.000

Marsland, S. J., Haak, H., Jungclaus, J. H., Latif, M., & Röske, F. (2003). The Max-Planck-Institute global ocean/sea ice model with orthogonal curvilinear coordinates. *Ocean Modelling*, *5*(2), 91–127. doi:10.1016/S1463-5003(02)00015-X

Mcwilliams, J. C. (n.d.). *Development and Utilization of Regional Oceanic Modeling System (ROMS) Delicacy , Imprecision , and Uncertainty of Oceanic Simulations : An Investigation with ROMS*. *Distribution*.

Mohamed, K. A. (2009). ENVIRONMENTAL IMPACT OF DESALINATION PLANTS. In *Thirteenth International Water Technology Conference, IWTC* (pp. 951–964). Hurghada, Egypt.

Penven, P., Debreu, L., Marchesiello, P., & McWilliams, J. C. (2006). Evaluation and application of the ROMS 1-way embedding procedure to the central california upwelling system. *Ocean Modelling*, *12*(1-2), 157–187. doi:10.1016/j.ocemod.2005.05.002

Perrone, T. I. (1979). *Winter shamal in the persian gulf*. Monterey. CA.

Reynolds, R. M. (1993). Physical oceanography of the Gulf, Strait of Hormuz, and the Gulf of Oman—Results from the Mt Mitchell expedition. *Marine Pollution Bulletin*, *27*, 35–59. doi:10.1016/0025-326X(93)90007-7

Reynolds, R. M. (1993). Physical Oceanography of the Persian Gulf , Strait of Hormuz , and the Gulf of Oman — Results from the Mt . Mitchell Expedition, (August), 1–49.

Roeckner, E., Bäuml, G., L, B., R, B., M, E., M, G., … U, S. (2003). *Report No . 349 Model description* (p. 140). HAMBURG, GERMANY.

Sandeep, S., & Ajayamohan, R. S. (2014). Poleward shift in Indian summer monsoon low level jetstream under global warming. *Climate Dynamics*. doi:10.1007/s00382-014-2261-y

Shchepetkin, A., & Mcwilliams, J. (2005). The regional oceanic modeling system (ROMS): a split-explicit, free-surface, topography-following-coordinate oceanic model. *Ocean Modelling*, *9*(4), 347–404. doi:10.1016/j.ocemod.2004.08.002

Sultan, S. A. R., & Ahmad, F. (1993). Surface a n d oceanic heat fluxes in the Gulf of Oman. *Continental Shelf Research*, *13*(10), 1103–1110.

Swift, S. A., & Bower, A. M. (2003). Formation and circulation of dense water in the Persian/Arabian Gulf. *Journal of Geophysical Research*, *108*(C1), 3004. doi:10.1029/2002JC001360

Taylor, K. E., Stouffer, R. J., & Meehl, G. A. (2012). An Overview of CMIP5 and the Experiment Design. *Bulletin of the American Meteorological Society*, *93*(4), 485–498. doi:10.1175/BAMS-D-11-00094.1

Thompson, Sir Willian - Lord Kelvin (1879). On Gravitational Oscillations of Rotating Water (Kelvin Waves). *Proceedings of the Royal Society*.

Thoppil, P. G., & Hogan, P. J. (2010a). A Modeling Study of Circulation and Eddies in the Persian Gulf. *Journal of Physical Oceanography*, *40*(9), 2122–2134. doi:10.1175/2010JPO4227.1

Thoppil, P. G., & Hogan, P. J. (2010b). A Modeling Study of Circulation and Eddies in the Persian Gulf. *Journal of Physical Oceanography*, *40*(9), 2122–2134. doi:10.1175/2010JPO4227.1

Thoppil, P. G., & Hogan, P. J. (2010c). Persian Gulf response to a wintertime shamal wind event. *Deep Sea Research Part I: Oceanographic Research Papers*, *57*(8), 946–955. doi:10.1016/j.dsr.2010.03.002

Weller, E., & Cai, W. (2013). Realism of the Indian Ocean Dipole in CMIP5 Models: The Implications for Climate Projections. *Journal of Climate*, *26*(17), 6649–6659. doi:10.1175/JCLI-D-12-00807.1

Yao, F., & Johns, W. E. (2010). A HYCOM modeling study of the Persian Gulf: 2. Formation and export of Persian Gulf Water. *Journal of Geophysical Research*, *115*(C11), C11018. doi:10.1029/2009JC005788

Yin, J. (2012). Century to multi-century sea level rise projections from CMIP5 models. *Geophysical Research Letters*, *39*(17), n/a–n/a. doi:10.1029/2012GL052947

Zanchettin, D., Rubino, a., Matei, D., Bothe, O., & Jungclaus, J. H. (2012). Multidecadal-to-centennial SST variability in the MPI-ESM simulation ensemble for the last millennium. *Climate Dynamics*, *40*(5-6), 1301–1318. doi:10.1007/s00382-012-1361-9

7. Annex 1 - Mid 21st Century Experiment

Goal for the Mid 21st Century experiment

The objective of this report was to run an ocean downscaling climate experiment considering the Mid 21st century (Jan 1st 2040 till 31 Dec 2049) to evaluate the climate changes impacts relative to the Early and Late 21st century existing results. The extension to 10 years run (previously planned to 5) was decided to guarantee that the regional ocean model does fully track the shift in the trends coefficient (mainly temperature) of the RCP8.5[6]'s IPCC[7] scenario.

Overall Summary

The regional ocean model settled to Arabian Gulf (hereafter ROM-AG) was initialized and spun up in four stages for the period of 2038-2040 using the same validated configuration fo earlier reports. This is done in order to generate a middle century stable base of climatological results (based on 10 years results, 2040-2049) for direct climate change impacts assessment. Results ofr this mid-century experiment were compared to the early and late 21st century ones. Therefore, the final runs consists of 2 (warm up) + 10 (direct run) years.

Results show also a time asymmetric transient pattern, better perceived in the salinity fields, which basically show diluted water masses up north and along the Arabian Gulf (AG) main canal (Figures 5, 6, 12-14). There is also slightly increase in salinity along the UAE coastal zone. This suggests a new physical mechanism, which is very likely a dynamical disturbance caused by an increase (forced by the ESM[8] results, in the present case the MPI-MR[9] ensemble) in the barotropic signals (Sea Surface Height - SSH), combined with specific meteorological conditions i.e. low (high) precipitation rates at South (North) area.

A secondary, but not less important conclusion is a very high sensitivity of the AG dynamics to relatively small changes in sea level, since these changes were caused exclusively by the Dynamic Sea Level (DSL), which varies in a range of 5-10 cm in the AG area.

Extended trends analysis

The warm up stages are presented in the main body of this report to allow a direct focus in the Mid Century experiment results. The time slice considered to further analyse (mainly trends) is defined between the years 2040 and 2049 period. When reducing analysis (like climatologies) are considered (e.g. means and differences), we have chosen to focus on the first 5 years to avoid any transient effects (e.g the discontinuous change in the ESM atmospheric results after 2045, temperature trends).

[6] RCP8.5 - Representative Concentration Pathways, trajectories adopted by IPCC on its 5th Assessment Report.
[7] IPCC – Intergovernmental Panel on Climate Change
[8] ESM – Earth System Model
[9] MPI-MR – an ESM ensemble from Max Planck Institute (MPI) on its Mixed Resolution experiment (MR)

The extended 10 years run performed mainly to evaluate the SSH increase observed during the experiment is used here (from 2040 till 2049). The model turbulent adjustment responses, after 2045, are also evaluated because it is when the temperature trend index has noticeably changed. The *Early* and *Late* 21st century simulations results are also considered for intercomparison purposes. Figure 1 characterizes these combined experiments, where the area averaged Sea Surface Temperature (SST), Sea Surface Salinity (SSS) and dynamic Sea Surface Height (SSH) trends are shown. In this report, *Early*, *Mid* and *Late* are referred to the periods: 2000-2020, 2040-2049 and 2080-2099, respectively.

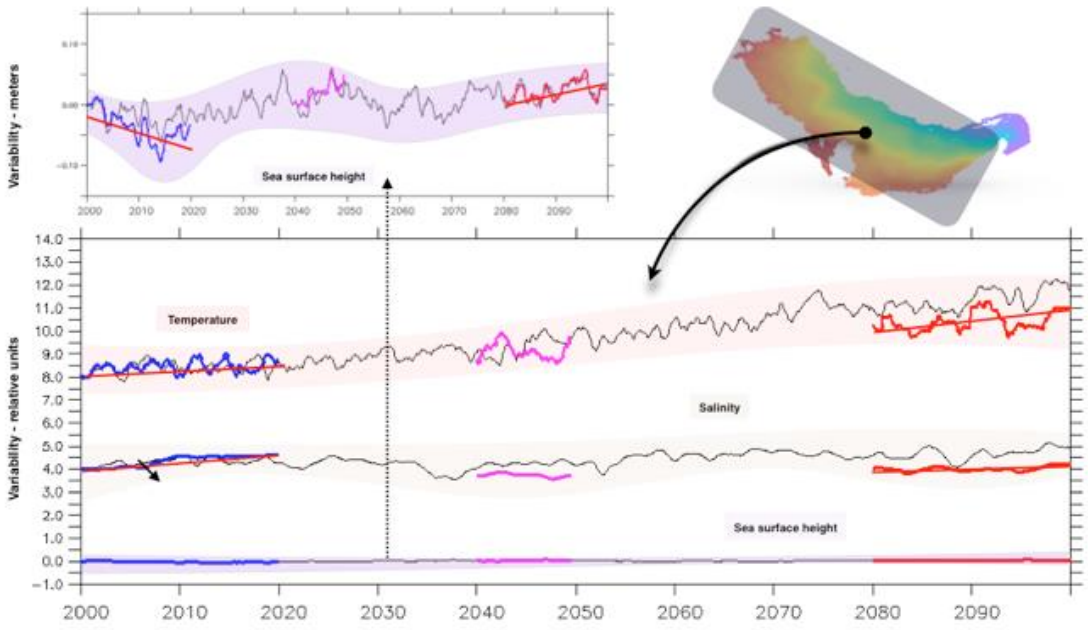

Figure 1: Arabian Gulf averaged timeseries (annually filtered) for SST (degrees C), SSS (practical salinity units, or psu) and dynamic SSH (meters). MPI-MR in black, ROM-AG results in blue (early), purple (mid), late (red) and linear trends in red. Detail (up left) expands the SSH trends. The top right map shows the coverage area.

The trends shown in Figure 1 consider the entire AG surface averages for SST, SSS and SSH. They are computed considering the annual and the area average for the shaded area indicated in the Figure (black arrow). For all the trends presented, the variables have been referenced to the year 2000.

Because of the same reference (year 2000), all trends vary around the y=0 axis. For best viewing in a single axis, arbitrary and fixed values were summed for each one of the variables (y=0; y=4; and y=8) for dynamic SSH, SSS and SST, respectively. The units of the variables and their variability are maintained (less the applied constant displacement). Mathematically, we can represent the statistical treatment of variables as:

$y_i = (x_i - \overline{x}) + c$, Where:

$x_i : variable\ monthly\ timeseries$

$$\overline{x} : variable\ mean\ for\ the\ year\ 2000$$

$$c = \begin{cases} 8, & if\ \ x_i : temperature \\ 4, & if\ \ x_i : salinity \\ 0, & if\ x_i : sea\ level\ height \end{cases}$$

The dynamic processes represented by the ROM-AG at this experiment (mid century) are not linear in time, when compared with the expected changes by the end of the century. Figures 2, 3 and 4 show the trends regionalized for three points of interest, i.e. the coastal region of United Arab Emirate (Figure 2), the Northern Gulf (Kuwait, Figure 3) and at one area centred along the deep channel (deeper zone, Figure 4).

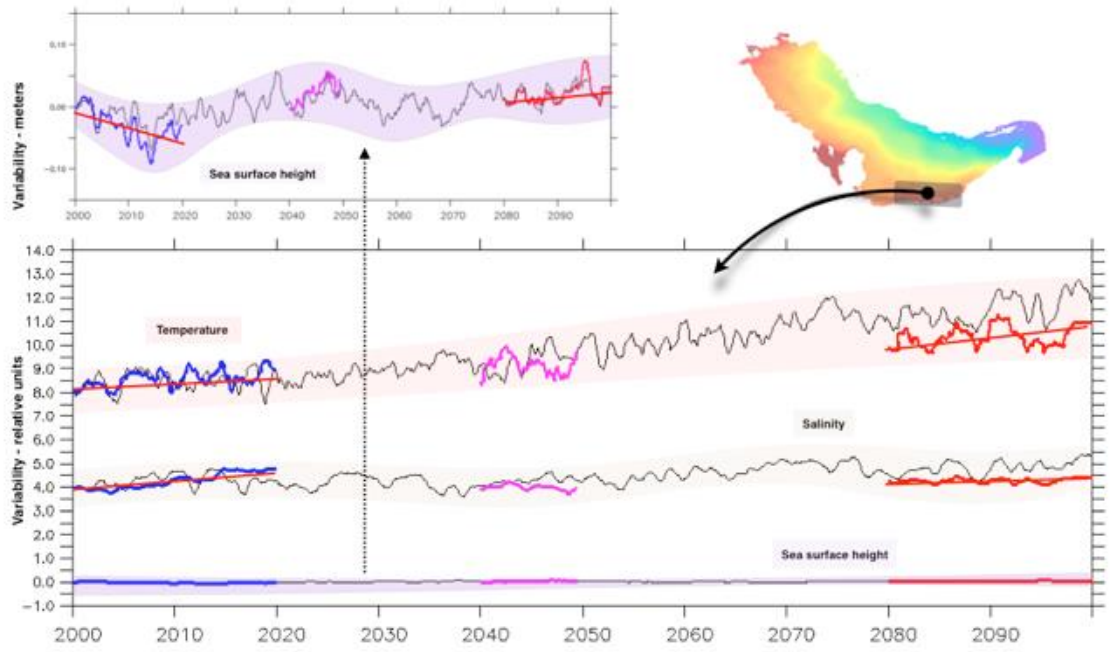

Figure 2: UAE coast area averaged time series (annually filtered) for SST (degrees C), SSS (practical salinity units, or psu) and dynamic SSH (meters). MPI-MR in black, RCM results in blue (early), purple (mid), late (red)

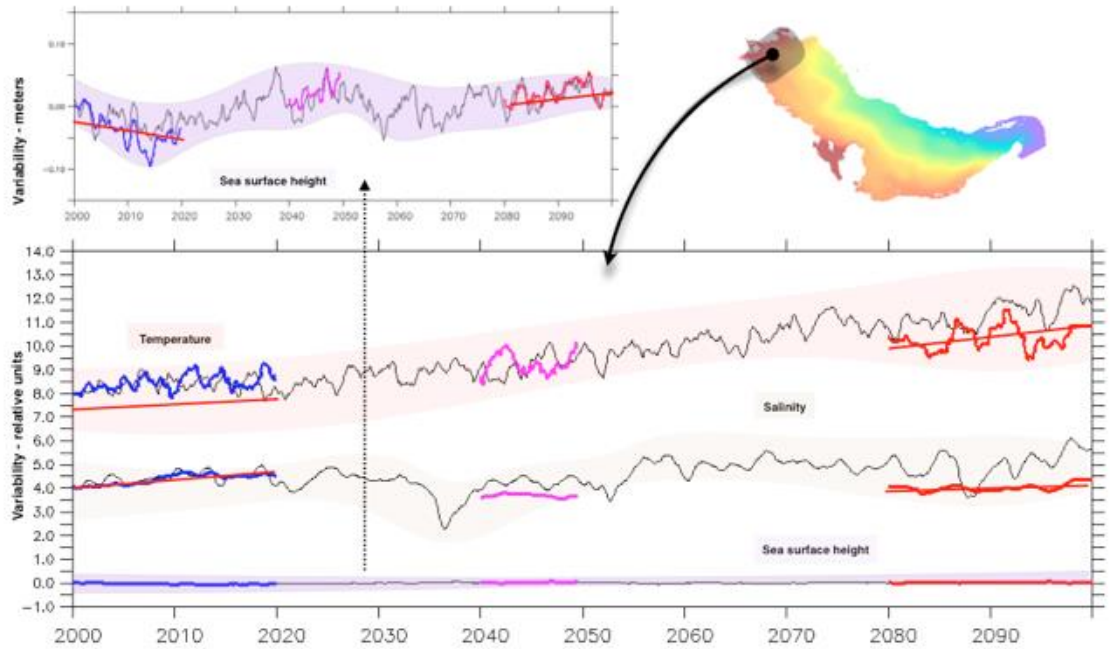

Figure 3: Kuwait coast averaged time series (annually filtered) for SST (degrees C), SSS (practical salinity units, or psu) and dynamic SSH (meters). MPI-MR in black, RCM results in blue (early), purple (mid), late (red) and linear trends in red. Detail (up left) expands the SSH trends. The shaded area in the top right map shows the coverage area.

It is possible to observe in Figures 1 to 4, which refer to different areas of the AG, that there is a consistency (later presented as correlation) between the dynamic processes associated with sea level variation and the averaged salinity levels. Near the Channel entrance into the AG (Figure 4), there is also an obvious similarity between the results of the regional and global models, except for the salinity parameter, which is imposed by the regional model's internal physics.

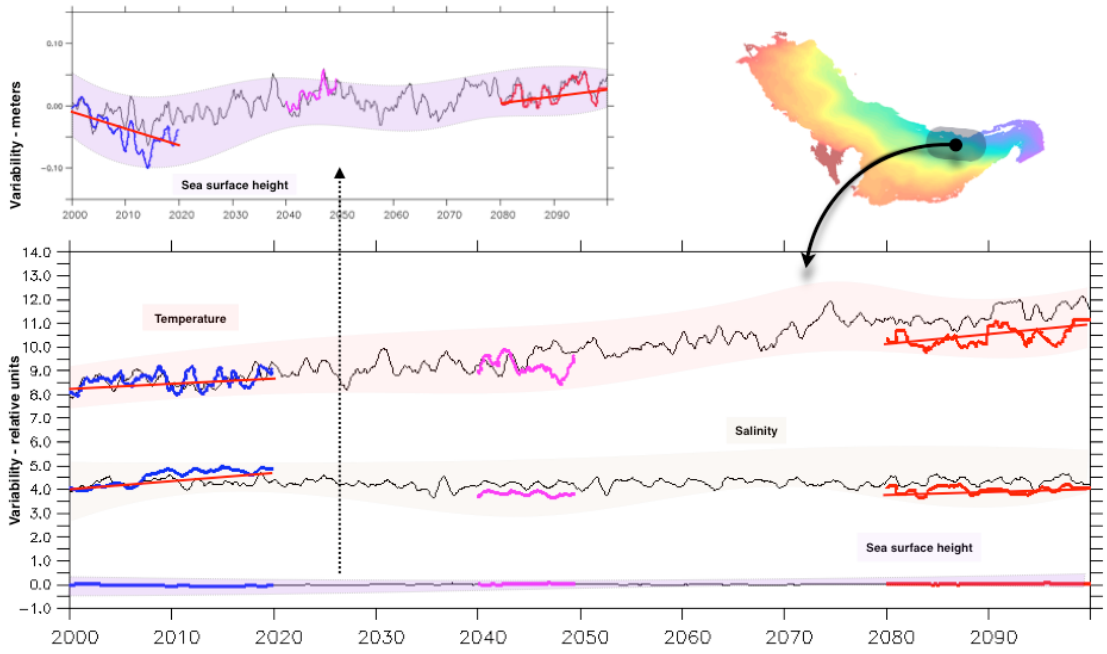

Figure 4: Deep channel area averaged time series (annually filtered) for SST (degrees C), SSS (practical salinity units, or psu) and dynamic SSH (meters). MPI-MR in black, RCM results in blue (early), purple (mid), late (red) and linear trends in red. Detail (up left) expands the SSH trends. The shaded area in the top right map shows the coverage area.

Climatological averages and differences

The averaged results for the variables SST, SSS and SSH are represented in Figure 5 for the Early, Mid and Late 21st century periods. For SST, there is a pattern of gradual warming gradient in space, with the warmest areas in each time slice located in the southern end of the AG and coolest areas located along the northern areas. The same spatial pattern is not evident for salinity and dynamic sea level. The greater uniformity of temperature changes can be explained by the characteristics of its main climate forcing as later discussed.

For SSS, the spatial distribution of average salinity in the mid 21st century period reveals a reduction along the west coast and in the northern part of the AG, when compared to the early 21st century results. Similarly to the Late 21st results, an observed increase of salinity along the coast of the UAE is also observed. This process can be interpreted in dynamical

terms if we consider that the AG has a residual cyclonic circulation (counter clockwise), which tends to accumulate water along the shoreline. Along the east coast and the nearby Hormuz Strait a general freshening occurs in the mid and late 21st century simulations. This freshening is even more pronounced in the mid century results. The mid century DSL is on average smaller then that for the late century period, however the freshening along the east coast is larger, which illustrates the future importance of SST effects in the Gulf circulation.

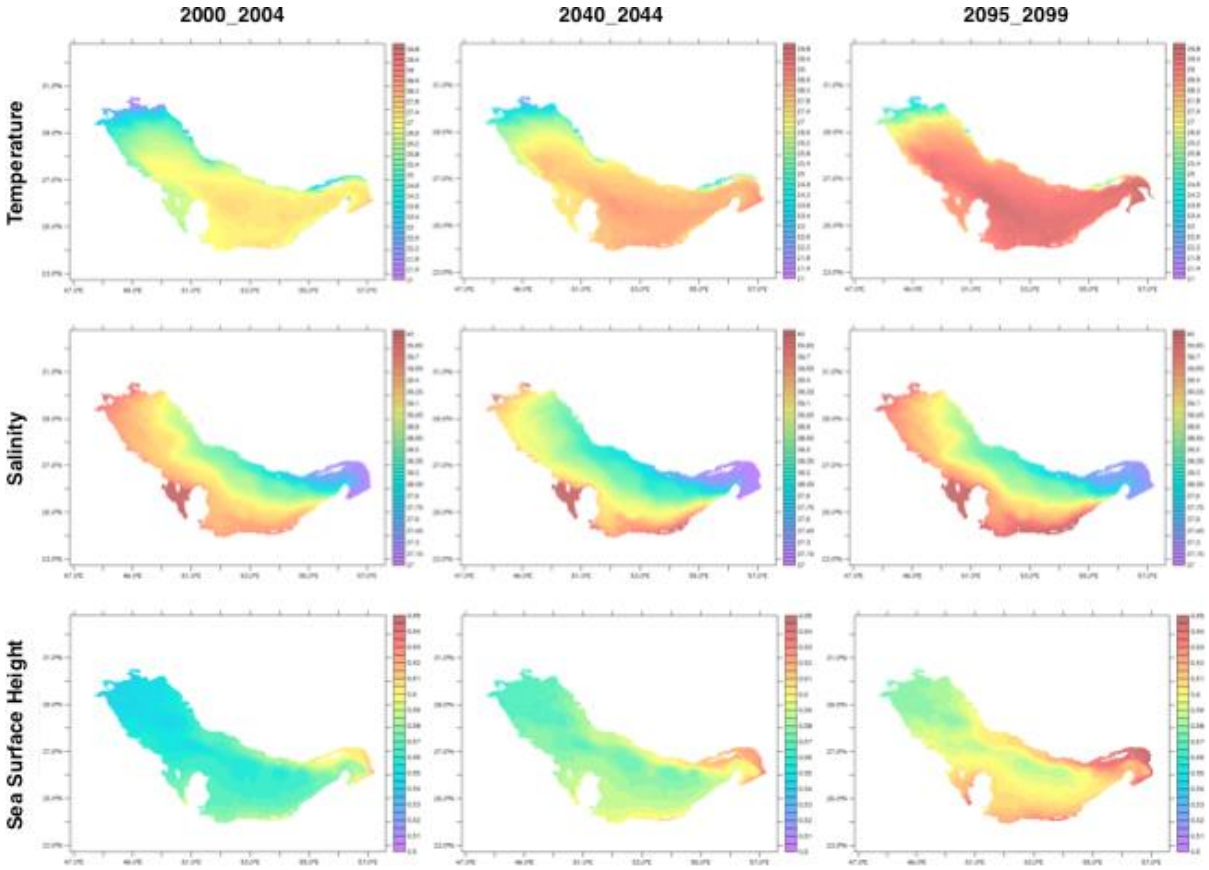

Figure 5: The top set of charts shows results for time averaged SST (degrees Celsius); the middle set shows SSS (primary salinity units, or psu); and the bottom set shows SSH (meters). The left column is the average results for the early 21st experiment (2000-2004 climatology); the middle column is the average for the mid 21st experiment (2040-2044); and the right column is the average for the late 21st experiment (2095-2099).

For SSH, the spatial distribution of average dynamic SSH in the 21st mid-century reveals a barotropic gradient along the coast on both sides of the Gulf. We speculate that the typically coastal-trapped waves, e.g. Kelvin waves (Thompson, 1879) are a very likely dynamical

mechanism that supports such a barotropic gradient[10]. Even though the system own volume conservation can also contribute to these changes.

The patterns are illustrated in Figure 6, which shows differences between the ocean variables in chronological order, later minus earlier. Temperature patterns change evenly throughout the Arabian Gulf, with a clear, continuous warming from early to late 21st century.

[10] We have intentionally referenced here a 19th century classical literature to call the attention to the local Arabian Gulf natural dynamics, which is clearly observed in higher frequency variability (as tides), forming at least 2 anphidromic points in the centre of the gulf. This natural response to forcing fields is also obvious in the previous results (SSH), where minimum changes are observed along the Gulf centre. Not only sea level, but also density fields, will accommodate the forced movement in a "kelvin's like pattern (increasing density and/or sea level along the coastal lines). These effects do have the coastal proximity (trapping) and Coriolis force as the basin mechanisms to the natural system response.
On top of that, and in a much smaller frequency (seasonal) the eastern side inflow energy (by volume conservation) and the Northwesterly winds do contribute in the same direction (anticlockwise) to the residual circulation, forming the pattern observed in the model simulations.

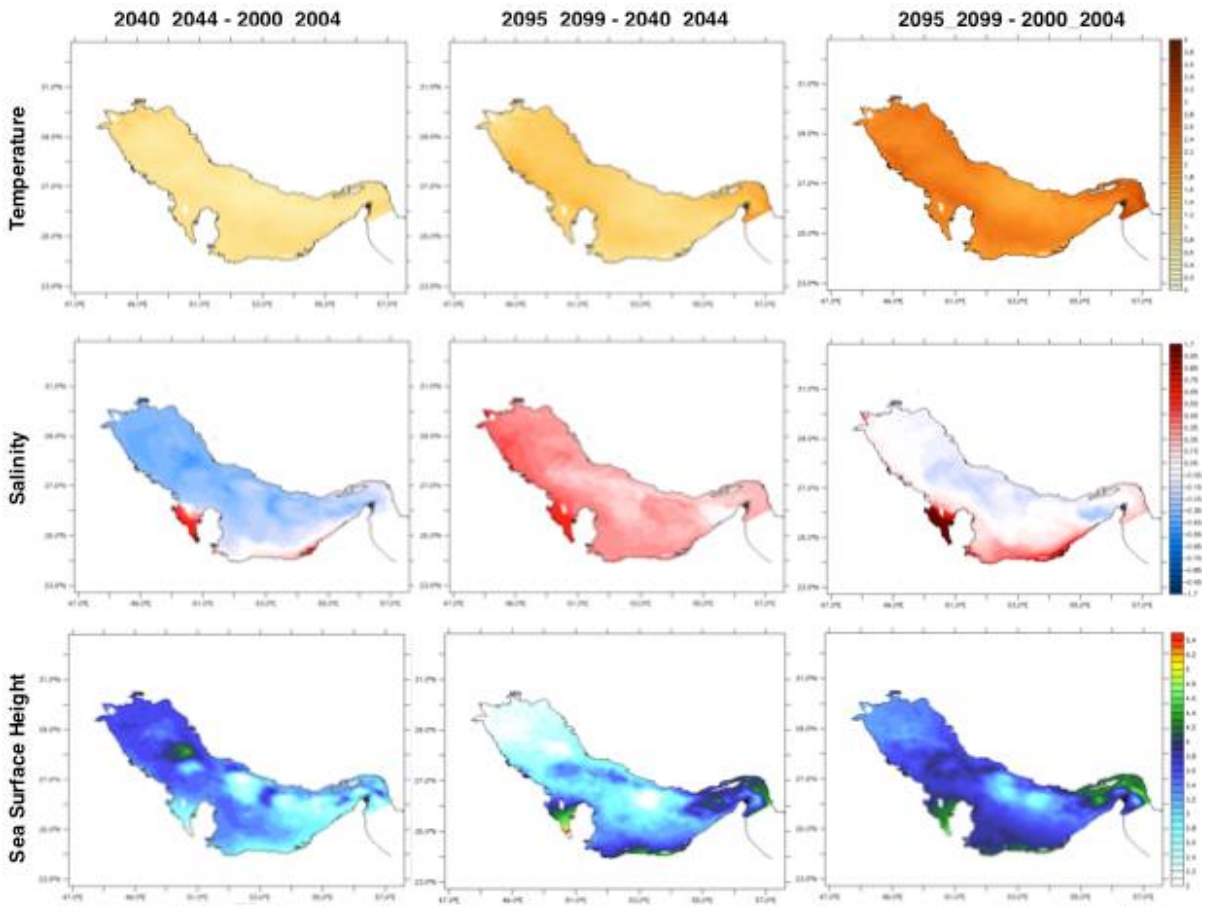

Figure 6: The first line shows results for the SST difference; the second line SSS; and the third line SSH. The first column is the difference for the mid 21st minus early 21st experiments; the second column is the difference for the late 21st minus mid 21st experiments; and the third column is the difference for the late 21st minus early 21st experiments).

Salinity patterns change in a temporally asymmetric manner, with increased levels along the coast (mostly UAE) and freshening (i.e., reduced salinity) along the AG's main channel. An increase in salinity is observed along the southwest coast of the AG (the coastal region of the UAE), consistent with the results of the late 21st century experiment.

Dynamic sea level patterns show relative monotonicity patterns observed in Figure 5 while their differences show asymmetrical long-term climatological patterns along the Gulf. However, because of the SSH higher frequency variability (greater them 0.5 cycle/year), the statistical meaning of the climatology used is likely reduced, apart from the trend, which shows an equivalent level (DSL) for mid and late 21st century periods. This result does have relation with the salinity distribution and will be discussed later on.

Transport and residual circulations impacts

The area-integrated transport along the deep channel (Figure 7A) shows a slight surface flow intensification, which has its source in the sea level increase in the open boundary (Hormuz).

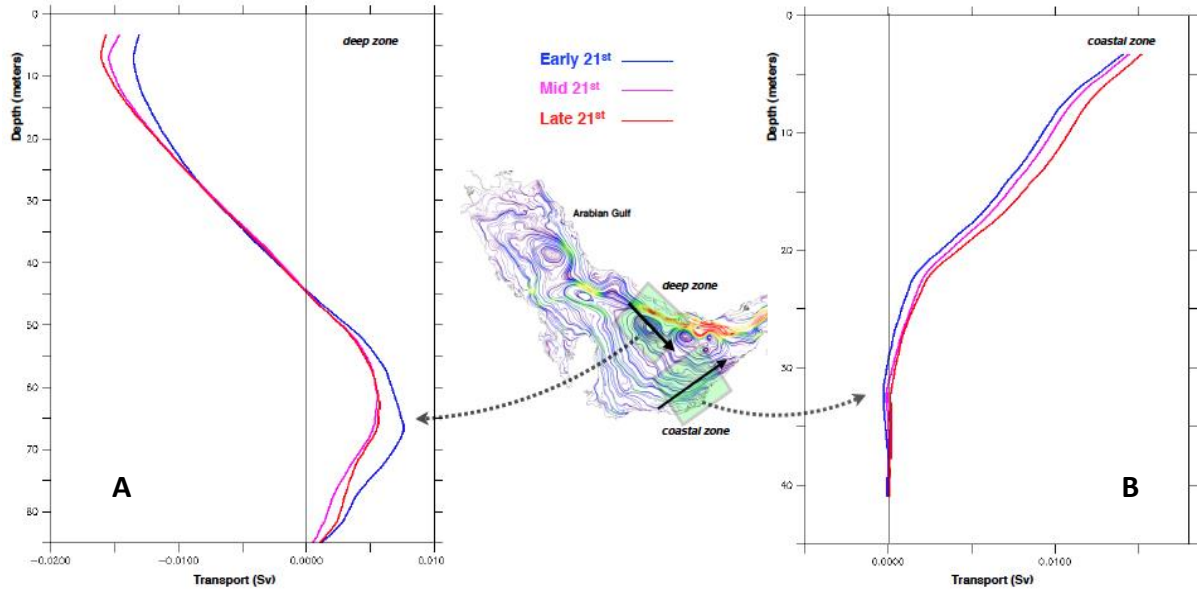

Figure 7: Early (blue), Mid (purple) and Late (red) time averaged climatological net transport along the main axis (black arrows inside the reference areas (green boxes).

These are “fresher" waters from the Arabian Sea. Notice the transport has been rotated, spatially and time (10 yeas) averaged to align with the mainstream direction (boxes axis). In Figure 7a, the reduction of the deep flow of saline water (from the north), for the mid-21st Century experiment, has the same order of magnitude as the 21st late century results.

On the other hand, the transport along the coast has a different behaviour from that observed in the deep channel (Figure 7B). The differences between the experiments point out to a rapid change along the AG channel and a more linear adjustment in the shallow zone (UAE coast).

To understand AG’s transport structure, the residual current (terrain following, surface and bottom) are presented for the three experiments (Early, Mid and Late 21st) in Figure 8. The colour palette in Figure 8 reinforces the current streamlines intensity. The thick black arrows have the same function, but simplifying the circulation structure to better view. Their thickness is also proportional to the local streamlines intensity. It can be noted that the intense flow reproduced for the end of the century (Late 21st experiment) already occurs at the surface in the Mid-Century simulation. At the bottom layers, while the northern effects of the late 21st century increase in temperature are not yet pronounced, the vertical thermodynamic equilibrium still holds, though weakened, i.e. the bottom flow of saline water is still present.

In other words, the effects of the increased temperature in the north of the AG are most noticeable at the end of the century, when there is a disruption of the subsiding saline waters. By the mid century period the temperature has not yet reached its maxima and a weakened, although present, thermodynamic balance does exist.

In summary, experimental results carried out to the middle of the 21st century show and reinforces what has been observed in the results already presented for the late 21st century period. At least two distinct processes are likely operating in the region:

One essentially is a very likely thermodynamic effect, defining the level of vertical mixing (subsidence) in the Gulf scale, Late 21st experiment conclusion,

The other one is predominantly related with the increase of the inflow of low saline waters due to surface gradients (surface elevation), without the extremes effects of the temperature. Thus, carrying a more barotropic mixing larger scale process, and consequently changing the intensity and shape of the cyclonic gyre in the area.

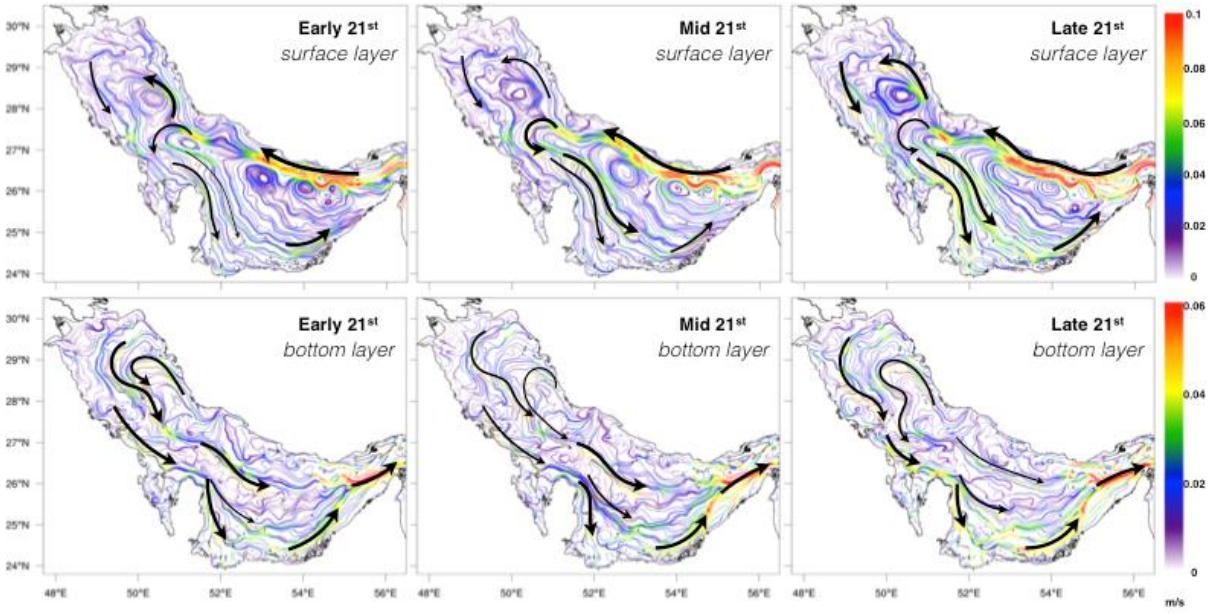

Figure 8: Residual current streamlines at surface and bottom layer (terrain following), early, mid and late 21st century experiments.

Other relevant climate change impacts in the AG

The above results show that the local ocean salinity is the variable with the greatest sensitivity to changes by the mid 21st century. Atmospheric climate change effects, such as air temperature, specific humidity and rainfall, wind, etc., are of course part of the AG balance. However, it is reasonable, because of the magnitude of SSS, to acknowledge that these atmospheric variables alone will not likely be able to generate the rather asymmetric

behaviour observed in the salinity field. To quantify the air-sea changes, some of the most significant meteorological variables that disturb salinity fields are recomposed by area (local average) and presented In Figure 9.

In Figure 9, the total period of the Mid 21st Century simulation (including warm up, 2038 till 2049) is superimposed (black lines and black arrow) in order to provide additional reference. Precipitation is the atmospheric variable that certainly contributes to the freshening observed in mid-century and, should also be considered in the explanation of the observed salinity time asymmetry (greater precipitation in the northern region to the south of the AG).

However, this does not explain the maximum freshening noted in the channel and northern AG. In the same manner, the wind patterns have no significant changes compared to the beginning of the century as can be seen in Figure 10. The current polar histogram is shown for the shallow areas where currents are very sensitive to wind changes. The results shown in Figure 10 are consistent with the shallow water transport profiles that have been previously presented in Figure 7B.

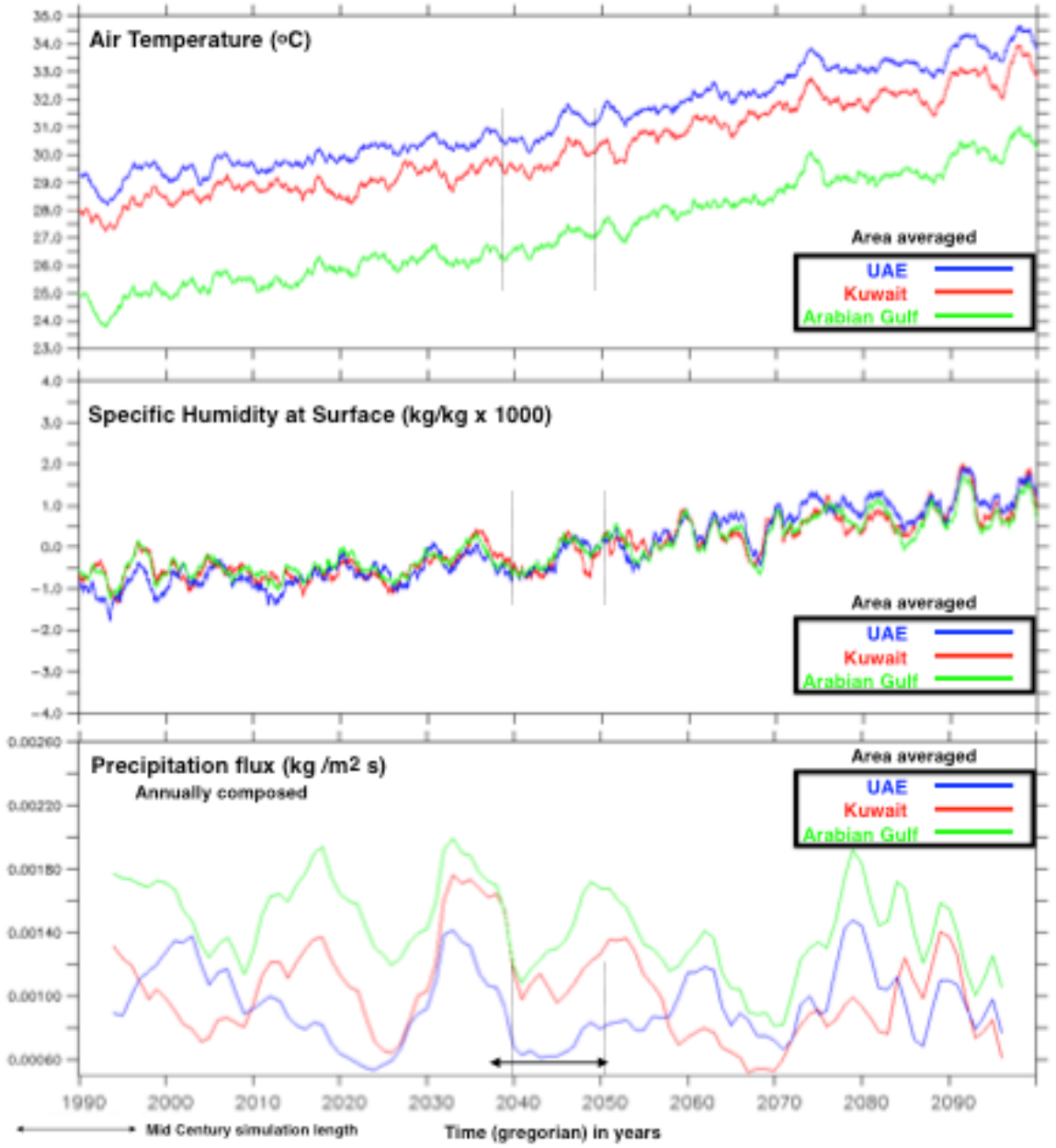

Figure 9: Direct ESM (MPI-MR) atmospheric variables timeseries for the UAE area, Kuwait area and the average for the whole Arabian Gulf.

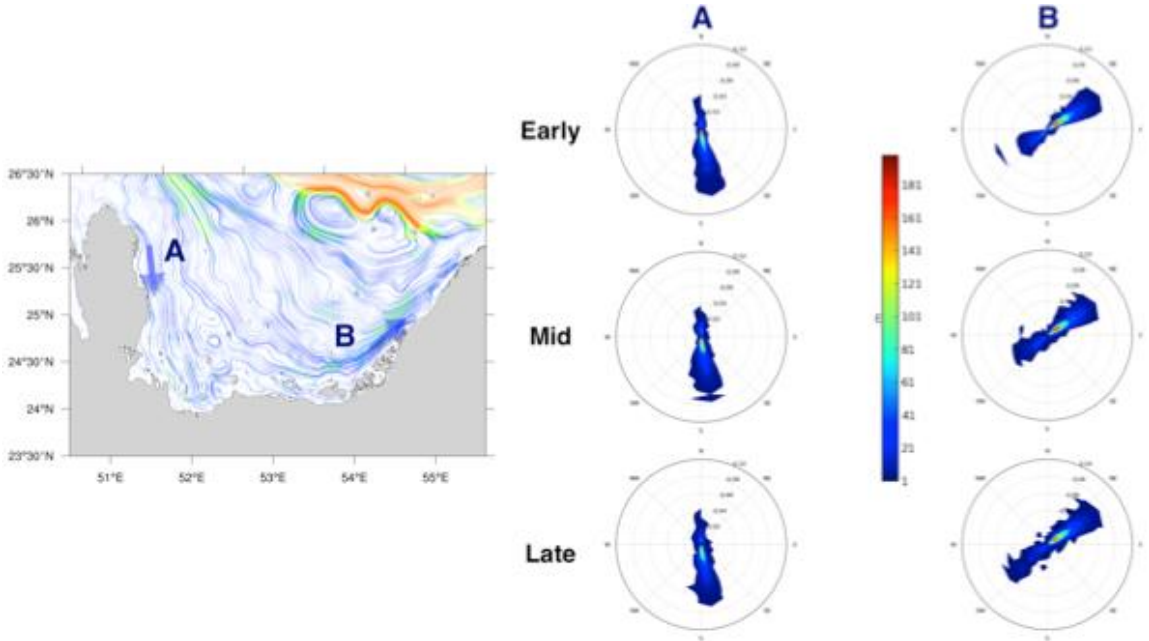

Figure 10: Qatar (A) and UAE (B) coastal jets. The left shows the residual current and the reference areas. The polar histograms on the right show the cumulative frequency of the current at the A and B positions, for the early, mid and late 21st cases.

The Mid Century simulation results show that the effects of low salinity along the eastern AG coast and the unbalance in the cyclonic gyre will cause significant changes in the mixing processes, when small-scale energy cascade are considered as illustrated by the results of the rotational field current for the simulated projections (see Figure 11).

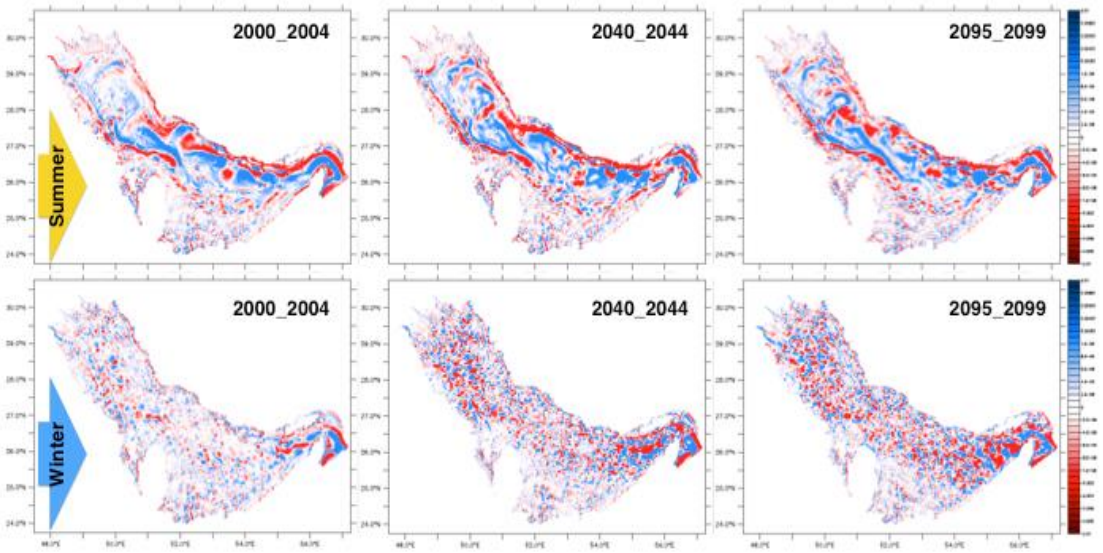

Figure 58: Arabian Gulf vorticity to early, mid and late 21st century. Results were based on climatology. The scale (1/s) is the same for all the vorticity plots.

A visual way to quantify the importance of the southerly fresher water inflow is presented in Figure 12, by assembling the seasonal vertical profiles for the three experiments considered (Early, Mid and Late) in specific regions of the AG (red line).

The purple-green scale zone emphasizes the typical salinity from Arabian Sea that in summer will achieve its maximum inflow in the AG. The dark red to yellow shading scale illustrates the AG internal response. The mid century maximum fresher water inflow trough this vertical

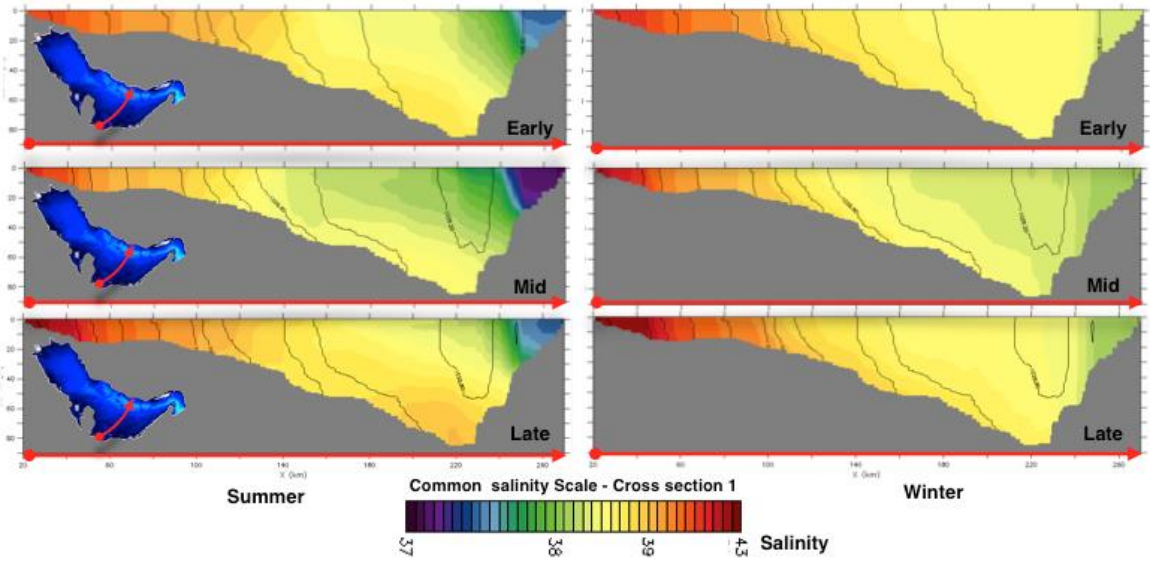

Figure 12: Salinity vertical sections for early, mid and late 21st century climate runs. The left column is the sections for the climatological summer period and the right one for the climatological winter period.

section is evident, and is even larger than the late 21st century results from the ROM-AG. These latter results clearly clarify the source for the along channel and northernmost zones freshening processes.

Conclusions

The mid 21st century results indicate that climate change leads to a general freshening of the AG area. It is also noted in the results that this freshening has a high inverse correlation with the sea surface height changes in the southern boundary (Hormuz strait). The global model forcing (MPI-MR, RCP8.5) does reinforce freshening considering that there is more precipitation projected for the northern areas when compared with the southern part of the Arabian Gulf.

The relationship between the three experiments (i.e., Early, Mid and Late century runs) is shown in Figure 13 where the area averaged, annually filtered dynamic SSH, its maxima and trends coefficients are displayed. It is well defined in the same plot that the maxima dynamic SSH achieved by the mid and late 21st century have the same order. It is also visible that the

trend coefficient in the middle of the century has achieved a relative maximum (compared with other simulated periods). It is also noticeable that this kind of rapid increases (or decrease) in the Dynamic SSH will happen in other periods in the 21st century.

Figure 14 shows the SSS and SSH spatial distribution correlation (annually filtered time series) that complement the above information. It shows the correlation coefficient between the two variables. High inverse correlations are found along the channel and following the main gyres that form the residual cyclonic gyre reproduced to the AG.

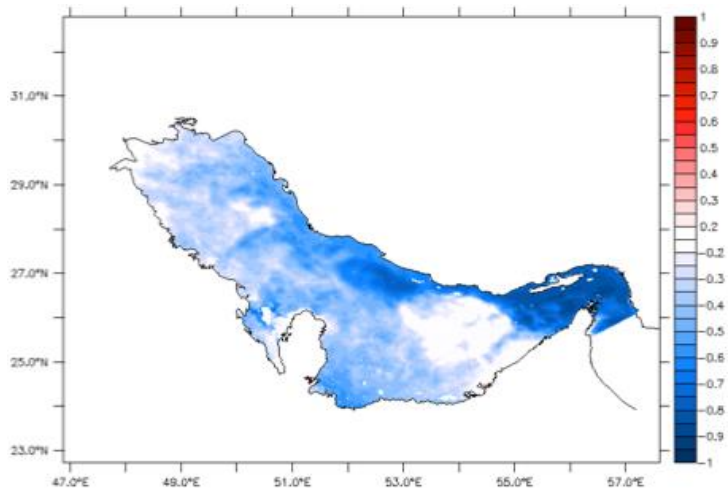

Figure 13: Correlation map between SSH and SSS. The dark blue areas represent the highest correlation (inverse correlated) between these two variables.

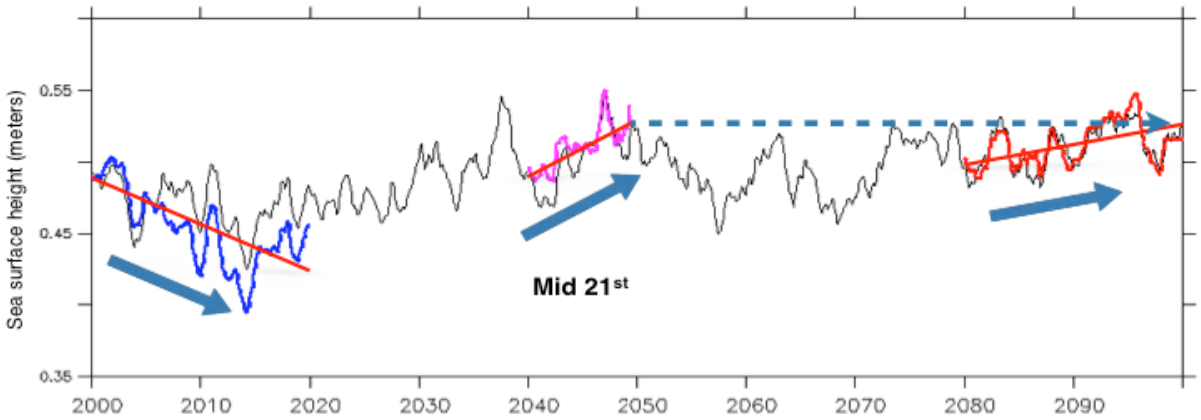

Figure 14: Annual averaged SSH time-series for the AG region. The red lines correspond to the linear trend for each period of simulation.

In summary, a review of the three experiments still point out to a very likely extreme shutdown of the vertical overturning circulation by the end of the century. The mid century run has shown, however, that this process is likely affected by a combination of other oceanic and atmospheric factors, and it is not the only dynamical process that could strongly impact the AG system. The barotropic signal changes observed in this simulation (mid century), depending on its intensity, will induce freshening in the AG, limited by a threshold, defined by the maxima salinity values observed in the surrounding Arabian Sea waters.

It should be noted that the spatial asymmetry of the salinity distribution in the AG (maxima in the UAE and internal bay zones) would tend to remain even in a high freshening situation as the present one. It is likely that the salinity will change, depending on the barotropic (SSH) signal intensity, but because of the morphological (shallow areas) and meteorological conditions, these areas will always be less diluted by the system.

Therefore, the physical process established in the middle of the 21st century shows a dynamic transient due to the variation of dynamic sea level (DSL). The quantification of the partition between this oceanic mechanism and direct atmospheric effects observed in atmospheric forcing (precipitation) is not completely defined but can be completely characterized by the current results.

Possible Future Research Directions

In view of the results that show a significant sea level (DSL) correlation with salinity field, it would be advisable to pursue further research developments, which could enrich the actual knowledge. For example, the expansion of the regional models' integration for longer periods, even longer then 100 years, is a significant topic of interest, in order to explore sea level changes in decadal and inter-decadal time-scales, as observed in the GCM global sea level signals.

Considering the possible relationship observed between rainfall and the AG short-term response dynamics (intra-seasonal and annual periods), it would be quite elucidating to analyze impacts of climate change in the ocean with improved and higher resolution atmospheric forcing.

Finally, concerning the relationship between global sea-level (GSL) rise and the AG dynamics, it should be noted that, even though changes in GSL can be numerically transmitted into the AG, it could not be physically and correctly imposed into the AG through the Hormuz Strait. This is because of the GSL intrinsic dependence on other ocean global variables, such as temperature and salinity. In this research scenario, the inaccuracy of the input baroclinic flows (density ones) will compromise the final results and consequently, their conclusions.

A possible solution, to overcome this issue, would be to use a kind of *telescopic grid approach*. Where telescopic is understood as a stretched grid that is able to still maintain focus on the AG and at the same time consider a larger domain, which could include the Indian Ocean basin or even larger areas. Obviously, further research will be needed in order to establish the limits of this telescopic domain.

AGEDI
مبادرة أبوظبي العالمية للبيانات البيئية
Abu Dhabi Global Environmental Data Initiative

an initiative of

UNEP

هيئة البيئة - أبوظبي
Environment Agency - ABU DHABI

Abu Dhabi Global Environmental Data Initiative (AGEDI)
P.O Box: 45553
Al Mamoura Building A, Murour Road
Abu Dhabi, United Arab Emirates

Phone: +971 (2) 6934 444
Email : info@AGEDI.ae

agedi.org

LNRClimateChange@ead.ae